universitätbonn

Rheinische
Friedrich-Wilhelms-
Universität Bonn

# Analysis of the regulatory function of amino acids on metabolic targets and serotonin production in *Drosophila melanogaster*

Dissertation

zur

Erlangung des Doktorgrades (Dr. rer. nat.)

der

Mathematisch-Naturwissenschaftlichen Fakultät

der

Rheinischen Friedrich-Wilhelms-Universität Bonn

vorgelegt von

**Tatjana Hübner**

aus Zelinograd

Bonn, 2015

Angefertigt mit Genehmigung der Mathematisch-Naturwissenschaftlichen Fakultät der Rheinischen Friedrich-Wilhelms-Universität Bonn

1.Gutachter: Prof. Dr. rer. nat. Michael Pankratz

2.Gutachter: PD Dr. rer. nat. Reinhard Bauer

Tag der Promotion: 09.12.2015

Erscheinungsjahr: 2016

# Table of Contents

# List of Figures

# List of Tables

# List of Abbreviations

| | |
|---|---|
| α | Alpha |
| µ | Micro |
| 4EBP | 4E Binding Protein |
| 5HT | 5- hydroxytryptamin |
| 5HTP | 5-hydroxytryptophan |
| A | Adenosine |
| AA | Amino acid |
| AAT | Amino acid transporter |
| AKH | Adipokinetic hormone |
| GABA | gamma-aminobutyric acid |
| AmpR | Ampicillin resistance |
| AP | Alkaline phosphatase |
| C. elegans | Caenorhabditis elegans |
| cc | corpora cardiaca |
| cDNA | complementary DNA |
| CDS | coding DNA sequence |
| CNS | Central nervous system |
| CTCF | Corrected total cell fluorescence |
| DNA | Deoxyribonucleic acid |
| Ddc | Dopa decarboxylase |
| Dig | Digoxigenin |
| Dilp | Drosophila insulin like peptide |
| DSERT | Drosophila Serotonin Transporter |
| DVMAT | Drosophila Vesicular Monoamine Transporters |
| eIF4E | eukaryotic translation initiation factor 4E |
| EXT | Exterior |
| FKH | Forkhead |
| FOXO | Forkhead Homeobox type O |
| gDNA | genomic DNA |
| InR | Insulin Receptor |
| INT | Interior |
| IPC | Insulin producing cell |
| kb | kilobase |
| l | litre |
| LEL | late lysosomal and endosomal compartment |
| Leu | Leucine |
| Lip | Lipase |
| M | Molar |
| ml | millilitre |
| ns | not significant |
| PAT | Proton assisted amino acid transporter |
| path | pathetic |
| PCR | Polymerase chain reaction |
| PG | Prothoracic gland |
| PI3K | Phosphoinositide 3-kinase |

| | |
|---|---|
| PKA | Protein kinase A |
| POD | Peroxidase |
| PTEN | Phosphatase and tensin homologue |
| Rheb | Ras homolog enriched in brain |
| RNA | Ribonucleic acid |
| RNAi | RNA interference |
| rp | ribosomal protein |
| rpm | revolutions per minute |
| RT | Real Time |
| S6K | S6 Kinase |
| Shi | Shibire |
| SLC | solute carrier |
| sNPF | short Neuropeptide F |
| T | Thymindine |
| TAG | Triacylglyceride |
| TH | Tyrosine hydroxylase |
| TLC | Thin layer chromatography |
| tobi | target of brain insulin |
| TOR | Target of rapamycin |
| Trh | Tryptophan hydroxylase |
| TrpA | Transient receptor potential ion channel |
| TSC/ Tsc | Tuberous sclerosis complex |
| U | Unit |
| UAS | Upstream activating sequence |
| UV | Ultraviolet |
| v-ATPase | vacuolar adenosine triphosphatase |
| Wt | wildtype |

# 1 Introduction

Many organisms have the ability to change their food preference dependent on their nutritional needs suggesting that there have to be internal sensors recording the nutritional situation, status and composition. This information has to be passed to the brain for the adaptation of feeding behaviour and food choice. A lot of these mechanisms have been distinguished for *Drosophila melanogaster* in terms of sugars (Söderberg et al, 2012; Flood et al, 2013, Dus et al, 2011). However, detection mechanisms for single amino acids still remain unclear. Toshima and Tanimura showed in 2011 that flies deficient in amino acid supply change their sensitivity of labellar taste cells to amino acids. In addition, they also revealed that detection pathways for individual amino acids may differ. This suggests that *Drosophila melanogaster* is able to sense its internal amino acid status and availability prior to changing food preference. The ability to sense the amino acid status is important for organismal survival and fitness as amino acid composition and availability in the insect hemolymph changes dependent on nutrition, age and stress (Cônsoli and Vinson, 2002; Hrassnigg et al., 2003). The target of rapamycin (TOR) pathway is involved in sensing the energy status and amino acid availability of the organism. It coordinates growth dependent on nutrient supply. In the brain TOR signalling was shown to change the preference to protein rich food (Vargas et al, 2010; Ribeiro and Dickson, 2010).

The brain as the centre for food choice and behaviour could be the most sensitive sensor for single amino acids as the incoming information of amino acid composition and availability can be directly processed. Apart from TOR pathway, food choice in *Drosophila melanogaster* is also affected by several neurotransmitters like Drosophila insulin like peptides, Drosophila neuropeptide F, Hugin, dopamine, corazonin and serotonin. So far, only for serotonin it is assumed that TOR signalling might be involved in the increase of these neurotransmitters (Vargas et al, 2010). As TOR signalling is dependent on amino acid availability, the presence of certain amino acids might also be important for serotonergic signalling and food choice.

## 1.1 Structure and characterization of amino acids

Amino acids are the building blocks of proteins and precursors of other biologically important molecules like nucleotides and neurotransmitters (Berg et al, 2007; Livingstone and Tempel, 1983). There are twenty-one different proteinogenic amino acids in eukaryotes that are encoded in their sequence for protein synthesis by nucleic acid triplets. All of them are L-



*Drosophila melanogaster* is also termed as fly in this thesis
Serotonin producing neurons are also termed as serotonergic or Trh positive neurons in this thesis

stereoisomers. They show a characteristic structure with two functional groups, the carboxyl group and the amino group that are bound to an alpha carbon. The amino acids differ in their side chain, which is also bound to the alpha carbon (Figure 1.1). Dependent on the properties of the side chain, amino acids are subdivided in polar and nonpolar amino acids (Bettelheim et al, 2010).

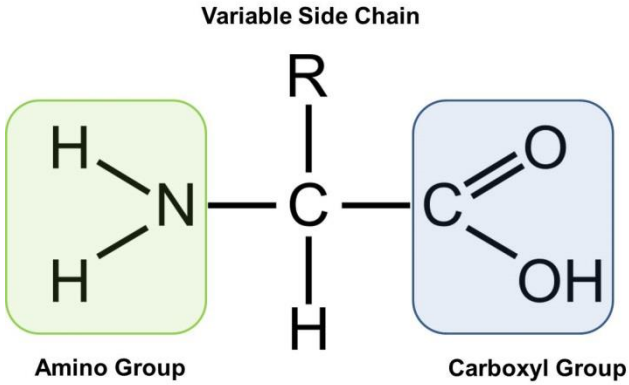


**Figure 1.1 Amino acid structure.**
The figure shows the schematic structure and functional groups of L-amino acids. Modified from Berg et al, 2007

Most amino acids, the nonessential amino acids, can be produced by metazoan organisms on their own. Some amino acids, the essential amino acids, are produced by bacteria, fungi or plants and have to be taken up with the food. Therefore, they are limited in their availability. Whether amino acids are essential or nonessential can differ between species (Costa et al, 2015). In mammals and *Drosophila melanogaster* the amino acids that are essential, are similar (Grandison et al, 2009). Those are isoleucine, leucine, valine, tryptophan, phenylalanine, threonine, lysine, and methionine. Additionally, arginine and histidine are essential for *Drosophila melanogaster* while in mammals they are essential only during development (Yamamoto and Niwa, 1993; Toshima and Tanimura, 2012).

In insects single amino acids can be transported directly into the hemolymph or processed in the epithelial cells of the gut. Peptides have to be cleaved into single amino acids or can be transported directly into the hemolymph as di- and tripeptides. Additionally, peptides could be processed by gut bacteria that use them to produce D-isomers of certain amino acids (Lemaitre and Miguel-Aliaga, 2013; Miguel-Aliaga, 2012). Therefore, the hemolymph amino acid composition might vary dependent on an uptake of the same amino acid composition in the form of single amino acids or peptides. It was shown that the amino acid composition in the insect hemolymph changes dependent on nutrition, age, stress and gender (Cônsoli and Vinson, 2002; Hrassnigg et al., 2003). This condition occurs because the concentration and

composition of single amino acids in *Drosophila melanogaster* is not regulated or kept in a certain homeostasis like the concentration of glucose.

The uptake or transport of certain amino acids into cells is dependent on their availability and ratio compared to other amino acids. This difference in amino acid uptake is due to a low specificity of many amino acid transporters. Most have different affinities for different amino acids. In this respect, some amino acids can inhibit the uptake of others (Christensen, 1977; Diallinas, 2014). The uptake of tryptophan for example is inhibited by other large neutral amino acids, like leucine, isoleucine and valine, as they all are transported by the same transport system (Fernstrom, 1979).

## 1.2 Amino acid transport and signalling

Amino acid transporters with receptor function (transceptors) are abundant in specialized tissues like the *Drosophila melanogaster* fat body (Colombani et al., 2003). Transceptors increase TOR signalling upon protein rich nutrition. Several amino acid transporters with high affinity for certain amino acids were shown to have transceptor function. They mediate the amino acid transport to the TOR pathway and thereby regulate target gene expression and growth. Those transceptors allow a detection of the internal amino acid status of the organism. Impairment in the expression of one of those transceptors affects growth and development (Martin et al, 2000; Colombani et al., 2003; Goberdhan et al, 2005). This effect indicates a highly balanced interplay between amino acid status and organismal growth.

### 1.2.1 The Amino acid transporter family SLC36

A variety of different transporters are responsible for the transport of single amino acids. Dependent on the amino acids they transport, they are classified into neutral, anionic and cationic amino acid transporters. These transporter classes are further subdivided into sodium dependent and sodium independent transporters. Sodium dependent transporters couple their transport to the electrochemical gradient of sodium, while sodium independent transporters couple the amino acid transport to the gradient of other substances. Examples for neutral, sodium independent transporters are the proton assisted amino acid transporters (PAT) of the solute carrier (SLC) 36 family.

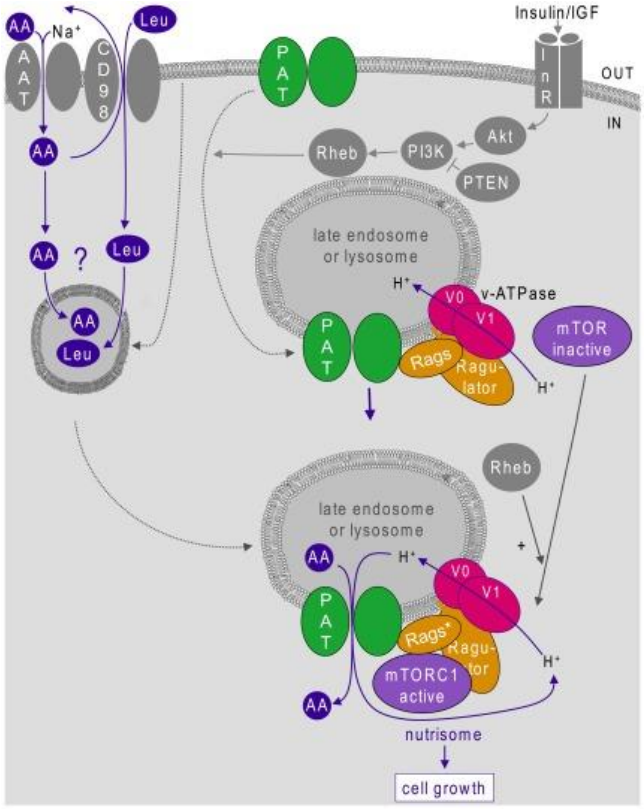


**Figure 1.2 TOR complex interaction with proton assisted amino acid transporters.**
The interaction of the Target of rapamycin complex 1 (mTORC1) with proton assisted amino acid transporters (PATs) and Rag guanosine triphosphatases (Rags) occurs at late lysosomal and endosomal compartments (LELs) upon amino acid (AA) availability. Amino acids like leucine (Leu) are transported into the cell by amino acid transporters (AATs). The Ras homolog enriched in brain (Rheb) as well as the cycling of protons via PATs and the vacuolar adenosine triphosphatase (v-ATPase) activates TORC1. Insulin signalling via the Insulin Receptor (InR) promotes the shuttling of PATs to the LEL membrane. The Insulin Receptor activates the Akt kinase, which phosphorylates the phosphoinositide 3-kinase (PI3K). The Phosphatase and tensin homologue (PTEN) regulates PI3K. PI3K is involved in the activation of Rheb. The figure was composed by Ögmundsdóttir et al in 2012.

The members of this amino acid transporter family link the transport of small neutral amino acids like glycine, alanine and proline with the transport of protons (Hyde et al, 2003; Barker and Ellory, 1989). Thereby, a 1:1 symport of protons and amino acids occurs. In mammals, four different transporters of the SLC36 family, PAT1 to PAT4, are characterized. PAT 1 and PAT4 were shown to activate TOR and to have a growth regulating effect. In cell culture amino acids were shown to stimulate the translocation of TOR to late lysosomal and endosomal compartments. Thereby, PATs are required for an appropriate amino acid dependent TOR translocation. At the lysosomal and endosomal compartments PI3K/Akt/Rheb signalling activates TOR and induces TOR signalling and growth (Figure 1.2). PAT1 is localized to the apical membrane of epithelial cells in the intestines. Here, it is assumed to be involved in the absorption of neutral amino acids after protein digestion. It is also localized to the lysosomes in the neurons of the brain. Until now, it is not known which neurons express

PAT1, neither is the function of the transceptor in the brain explored (Ögmundsdóttir et al, 2012; Boll et al, 2004). Also in *Drosophila* PAT homologs with transceptor function were found.

### 1.2.2 The transceptor Pathetic

In *Drosophila melanogaster* eleven different PAT homologs were identified. The PAT transporter Pathetic (Path) has a high affinity for the small, neutral amino acids alanine and glycine. It has been shown that Pathetic is localized at the plasma membrane and at late lysosomal and endosomal compartments. The transceptor Pathetic activates TOR upon amino acid availability. Like the human PATs it has a growth promoting effect on cellular level. In the brain Path enhances TOR signalling. However, when it is highly overexpressed in the wing it reduces growth of this tissue, as does the overexpression of TOR in the wing. Thereby, the cell size is increased while the total cell number is reduced. It was suggested that in the wing the formation of a TOR containing multiprotein complex is prevented by TOR or Path overexpression during development (Goberdhan et al, 2005; Ögmundsdóttir et al, 2012).
Path also affects overall growth. A reduction of Path expression by mutation or the overexpression of the transporter in the whole animal leads to a reduced growth in *Drosophila melanogaster*. The growth reduction due to the mutation could be rescued partly by Pathetic overexpression in the mutated tissues. These effects reveal that a balanced Pathetic expression is needed for a normal growth (Goberdhan et al, 2005).

## 1.3 Amino acid and TOR signalling pathway in *Drosophila melanogaster*

The target of rapamycin (TOR) signalling pathway is conserved throughout evolution and has the same function and organization in animals and fungi (van Dam et al, 2011). TOR signalling is mediated by the TOR complex 1. Amino acids, the metabolites of proteins, are essential in the activation of this pathway. A depletion in amino acid availability upon food deprivation leads to an inhibition of the TOR pathway und thus to a growth arrest. TOR is affected by amino acid transceptors like Slimfast, Minidiscs and Path. These act as transporters and mediate the amino acid signalling via TOR pathway. Some of those transceptors have a high affinity for certain amino acids and their expression is restricted to different tissues. Thus, they can activate TOR signalling in specific tissues dependent on the amount of the transported target amino acids. Impairment in the expression of one of those transceptors affects growth and development indicating a highly balanced interplay between

amino acid status and organismal growth (Martin et al, 2000; Colombani et al., 2003; Goberdhan et al, 2005; Ögmundsdóttir et al, 2012).

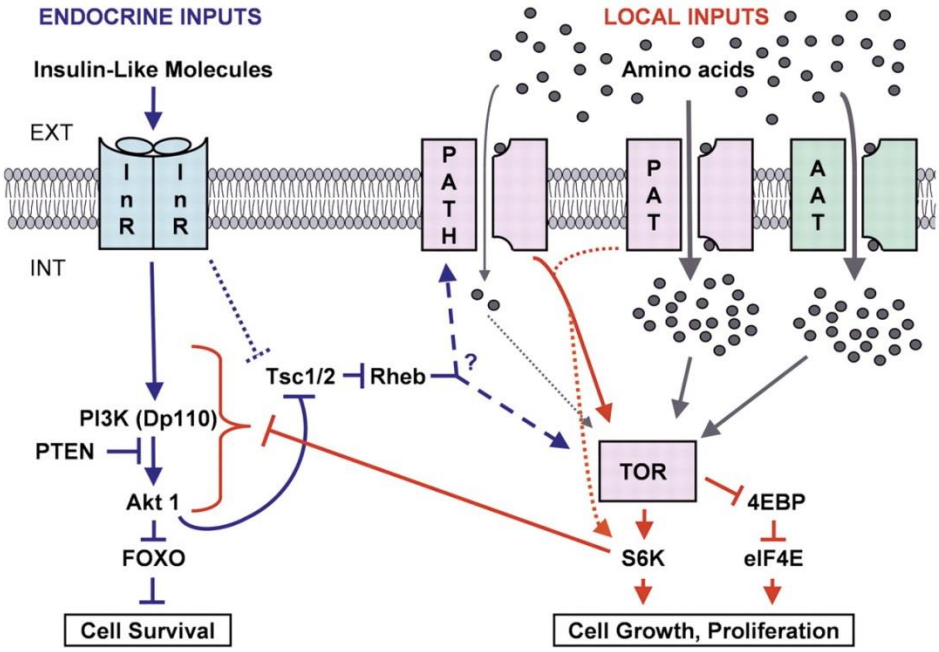


**Figure 1.3 The interaction of Insulin and TOR signalling pathway.**
Cell exterior (EXT). Cell interior (INT). The insulin signalling is mediated by the Insulin receptor (InR). It activates the Phosphoinositide 3-kinase (PI3K). PI3K is regulated and deactivated by the Phosphatase and tensin homologue (PTEN). When active, PI3K phosphorylates phosphoinositides and activates the serine kinase homologue of the retroviral oncogene v-Akt (Akt). Akt inactivates the transcription factor Forkhead Homeobox type O (FOXO) and the complex of Tuberous sclerosis complex 1 (Tsc1) and Tuberous sclerosis complex 2 (Tsc2). Ras homolog enriched in brain (Rheb), an activator of the Target of rapamycin complex 1 (TORC1) is activated when the TSC complex is inactive. It activates the TOR kinase upon amino acid availability, which activates S6 kinase (S6K) and deactivates the 4E binding protein 1 (4E-BP1) which binds the eukaryotic translation initiation factor 4E (eIF4E). The amino acid availability is mediated by amino acid transporters (AAT) and transceptors, like the proton assisted amino acid transporter (PAT) Pathetic (Path). The activation of TOR signalling leads to cell growth and proliferation (Goberdhan et al, 2005).

The amino acid dependent activation of TOR signalling is controlled by small GTPases. Rag GTPases are important for the subcellular localization of the TOR complex, as they direct the complex to the lysosomal compartments. Upon amino acid availability the GTPase Ras homolog enriched in brain (Rheb), which is also localized at the lysosomal surface, activates the TOR kinase function of the complex, when bound to GTP. The complex of Tuberous sclerosis complex 1 (TSC1) and Tuberous sclerosis complex 2 (TSC2) can inhibit TOR signalling by stimulating the GTPase function of Rheb which catalyses the bound GTP and becomes inactive. The TSC complex can be deactivated by phosphorylation through Akt, which means that insulin signalling can activate TOR signalling due to TSC complex phosphorylation (Figure 1.3). The active TOR kinase in turn phosphorylates and activates S6K but deactivates 4EBP this way initiating the transcription and translation of target genes

(Efeyan et al, 2012; Chantranupong et al., 2015). The transcript level of the alpha glucosidase Target of brain insulin was shown to be regulated by amino acids (Hübner, 2010). It is a possible target of TOR signalling (Buch, unpublished data).

### 1.3.1 The alpha glucosidase Tobi is regulated by the amount of protein in the food

The alpha glucosidase Target of brain insulin (Tobi) is a transcriptional target of nutritional protein. *Tobi* is expressed in the gut and the fat body of *Drosophila melanogaster* and is involved in the carbohydrate metabolism. It influences the amount of glycogen in *Drosophila melanogaster*. This influence is promoted by Drosophila insulin like peptide (DILP) and Adipokinetic hormone (AKH) signalling (Figure 1.4). The expression of *tobi* correlates to the ratio of yeast and sugar in the ingested food source. A high amount of yeast in the food leads to a high expression of *tobi* (Buch et al, 2008). Yeast is the optimal food source for *Drosophila melanogaster* in nature. It is rich in nutrients like proteins and amino acids. Single amino acids were shown to increase *tobi* transcription but the mechanism of this regulation is unclear (Hübner, 2010).

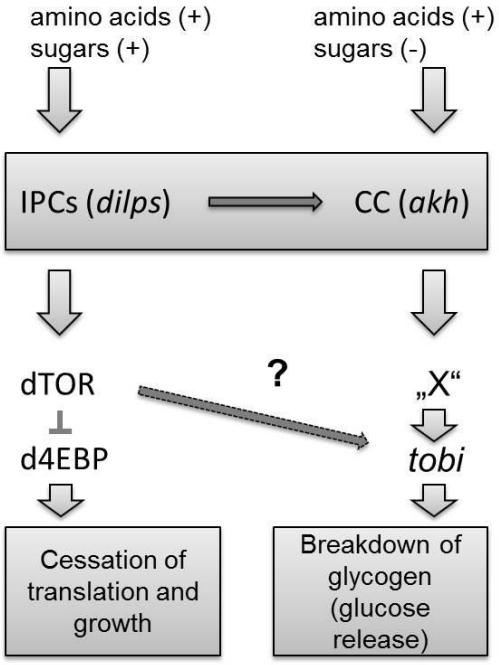


**Figure 1.4 Regulation of the α-glucosidase *tobi* expression.**
*Target of brain insulin* (*Tobi*) expression is regulated by Drosophila insulin like peptides (DILPs/dilps) released by the insulin producing cells (IPCs). A regulation occurs also by the Adipokinetic hormone (AKH/akh) signalling released by the corpora cardiaca (CC). Also a regulation by single amino acids was shown (Hübner, 2010). This regulation might be mediated by Target of rapamycin (TOR) signalling which regulates translation by inactivation of the 4E binding protein (4EBP). The figure was modified from Buch et al, 2008.

As mentioned above, TOR signalling is dependent on amino acid availability. Therefore, it might also be involved in the regulation of *tobi*. Unpublished data by Buch reveal that treatment with the TOR inhibitor rapamycin reduces *tobi* transcript and protein level. This result indicates that *tobi* is a possible target of the TOR pathway.

### 1.3.2 TOR regulates transcription and translation of target genes

TOR is responsible for the regulation of protein synthesis by phosphorylation and inactivation of the 4E binding protein (4EBP). 4E is a translation initiation factor which is bound and inhibited by 4EBP. Additionally to 4EBP, TORC1 phosphorylates the S6 Kinase, which is then activated. S6K phosphorylates the ribosomal S6 protein and enhances the translation of mRNA subsets that encode certain ribosomal proteins and translation elongation factors (Miron et al, 2003; Orlova and Crino, 2010). Thus, the primary goal of TOR is the activation of growth promoting targets. In addition, TOR controls the transcription of genes involved in metabolic pathways. It was shown that TOR regulates the transcription of *4EBP*, *CG6770* and *cabut* via Forkhead (FKH) (Bülow et al, 2010).

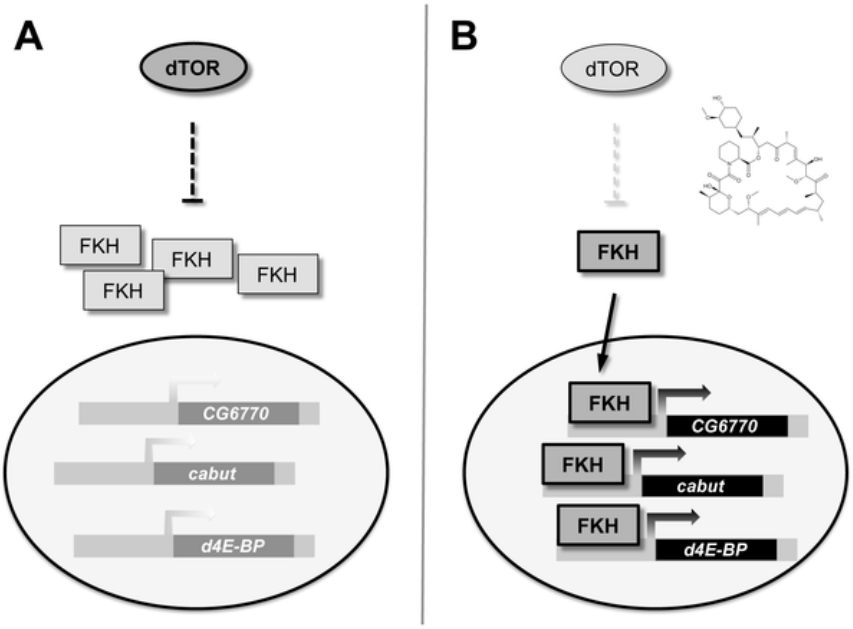


**Figure 1.5 Regulation of transcriptional targets by TOR via Forkhead.**
Forkhead (FKH) acts as a transcription factor when *Drosophila* Target of rapamycin (dTOR) signalling is inhibited. It increases the transcript level of genes like *CG6770*, *cabut* and *Drosophila 4E binding protein* (*d4E-BP*). Figure composed by Bülow et al in 2010.

The transcription factor FKH is activated in *Drosophila* larvae upon amino acid deprivation and reduction of TOR signalling. Active FKH induces the transcription of the above mentioned target genes (Figure 1.5). The TOR pathway also feeds back on the insulin signalling pathway by inactivation of Akt (Kockel et al, 2010). This way TOR signalling

allows a metabolic adaptation regarding the availability of nutrients, like proteins and amino acids. Also a phenotypic adaptation like the alteration of the pigmentation pattern was observed (Shakhmantsir et al, 2013).

### 1.3.3 TOR and nutrient dependent pigmentation of *Drosophila melanogaster*

The nutritional status of an organism leads to an adjustment of metabolism, growth, development, immunity and behaviour to the current nutritional situation (Zhang et al, 2000; Zhang et al, 2005, Wullschleger et al, 2006; Layalle et al, 2008, Araki et al, 2011; Varma et al, 2014). Shakhmantsir et al. also showed in 2013 that the nutritional status during the metamorphosis of *Drosophila melanogaster* is involved in the regulation of cuticle pigmentation of adult flies. Thereby, the pigmentation is coupled to the nutrient sensing mechanisms of the insulin signalling and TOR pathway. Those pathways modulate an existing cuticle pattern as it is also shown for a manipulation by temperature (Gibert et al, 2007). The regulatory mechanism of insulin signalling on pigmentation is not known yet. TOR pathway increases the translation of the enzyme Tyrosine Hydroxylase (TH), which uses the amino acid tyrosine for the production of L-DOPA (Zitserman, 2012). L-DOPA is used by Dopa Decarboxylase (Ddc) to produce dopamine. L-DOPA and dopamine are used in the epidermis to produce different pigments of the cuticle of *Drosophila melanogaster*. An impairment in the function of one of these enzymes leads to an albino phenotype. Up to now the mechanism of Ddc regulation has not been unravelled. TH and Ddc are known to be involved in the neurotransmitter production (Lundell and Hirsh, 1994). The neurotransmitter dopamine is produced by TH and Ddc while Ddc additionally produces serotonin from the precursor 5-hydroxytryptophan. Given that TOR signalling has an impact on an enzyme of the epidermis it is also expected to affect the same enzyme in the central nervous system (CNS) (Wittkopp, 2003; Coleman and Neckameyer, 2004; Coleman and Neckameyer, 2005). This way, TOR signalling might affect neurotransmitter production by regulating the amount of neurotransmitter producing enzymes.

## 1.4 The neurotransmitter serotonin

Serotonin is a signalling molecule that is highly conserved throughout evolution (Andrés et al, 2007; Verlinden et al, 2015). It is produced during a two-step reaction with two different enzymes (Figure 1.6). Its precursor, the amino acid tryptophan, is used by the Tryptophan Hydroxylase (Trh) to produce 5-hydroxytryptophan (5HTP). Afterwards, 5-

hydroxytryptophan is used by Ddc to produce 5- hydroxytryptamin (5HT) or serotonin (Coleman and Neckameyer, 2005; Neckameyer et al, 2007). The amount of transported and available tryptophan in serotonergic neurons determines the amount of produced serotonin. Serotonin is primarily found in the gastrointestinal tract. However, it is also abundant in neurons of the central nervous system.

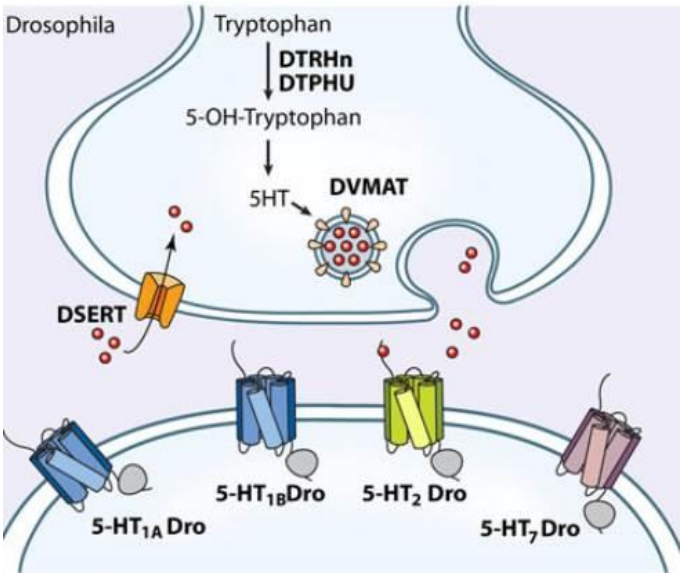


**Figure 1.6 Serotonin production, signalling and reuptake.**
*Drosophila* Tryptophan Hydroxylase (DTRHn/DTPHU) uses tryptophan to produce 5-hydroxytryptophan (5-OH-Tryptophan). 5-OH-Tryptophan is used to produce 5-hydroxytryptamin (5HT) also termed as serotonin. The neurotransmitter is packed into vesicles by Drosophila Vesicular Monoamine Transporters (DVMAT). After depolarization of the synaptic membrane it is released to bind to Drosophila serotonin receptors (5-HT Dro) and to induce receptor specific signalling. The serotonin signalling is terminated by reuptake into the presynapse by the Drosophila Serotonin Transporter (DSERT). The figure was modified from Curran and Chalasani, 2012.

In animals serotonin acts as a neurotransmitter stored in synaptic vesicles. In response to the depolarisation of the synaptic membrane, it is released. The neurotransmitter binds to specific G protein-coupled receptors that are highly expressed in the nervous tissues (Curran and Chalasani, 2012). This way, it affects learning, memory, sleep and behaviour. In *Drosophila melanogaster* four different serotonin receptors are characterized: $5HT_{1A}$, $5HT_{1B}$, $5HT_2$ and $5HT_7$. They promote a tissue dependent effect upon binding serotonin (Curran and Chalasani, 2012; Silva et al, 2014, Verlinden et al, 2015).

The effect of serotonin is terminated by re-uptake of the transmitter into the synapse. The re-uptake is mediated by the serotonin transporter (SERT). After reuptake, the biogenic amine is inactivated enzymatically or repacked into vesicles by monoamine transporters (DVMAT) (Chang et al, 2006; Simon et al, 2008; Giang et al, 2011).

### 1.4.1 Organization and function of the serotonergic clusters

In the brain and the ventral nerve cord of *Drosophila melanogaster* the serotonergic neurons are organized in symmetric, bilateral clusters (Figure 1.7). Their number and projection pattern does not change during larval development.

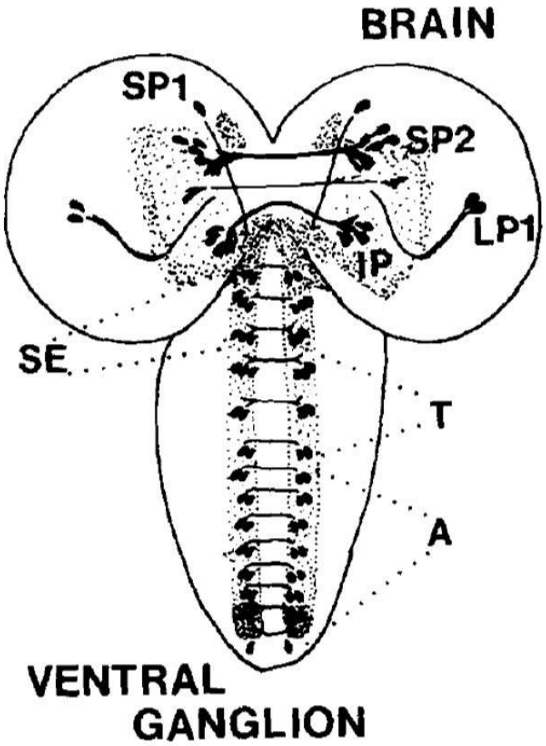


**Figure 1.7 Distribution of the serotonergic clusters in the larval brain.**
Serotonergic clusters of the hemispheres (SP1, SP2, LP1, IP). Subesophageal ganglion clusters (SE). Thoracic ganglion clusters (T). Abdominal ganglion clusters (A). The figure was modified from Vallés and White, 1988.

The clusters SP1, SP2, LP1 and IP are localized in the hemispheres. The SP1 cluster contains one, the SP2 cluster four, the LP1 cluster three to four and the IP cluster two neurons per hemisphere. In the suboesophagial ganglion the clusters SE0 to SE3 are localized. The SE0 cluster contains two to four neurons per side (Huser et al, 2012). It is involved in the developmental timing via projections to the prothoracic gland (PG). This organ is responsible for the production of ecdysone, a hormone important for pupation and metamorphosis in *Drosophila melanogaster* (Shingleton, 2005). The formation of SE0 projections to the PG is dependent on the nutritional condition and seems to be affected by the amount of yeast in the ingested food. Therefore, the development is coupled to the nutritional status of the larva (Shimada-Niwa and Niwa, 2014). The SE2 and SE3 clusters contain three to five neurons per side. In the thoracic ganglion you find the clusters T1 to T3. In the abdominal ganglion the clusters A1 to A9 are localized. Apart from the T1 clusters and the cluster A8 and A9, they all contain two neurons per cluster and side. The T1 cluster contains three neurons on each side

and the clusters A8 and A9 contain just one neuron (Vallés and White, 1988; Huser et al, 2012). Serotonergic neurons project to tissues that are involved in feeding behaviour and neuroendocrine activity (Schoofs et al, 2014; Luo 2012). However, the role in feeding behaviour and metabolism of the single clusters in the brain is not sufficiently analysed up to now (Vallés and White, 1988).

### 1.4.2 The role of serotonin in feeding behaviour and lipid metabolism

Lipids like triacylglycerides (TAG) are an important energy source that enables an organism to survive during long periods of nutrient deprivation. A dysregulation in processes of lipid metabolism like lipid storage or mobilization leads to obesity or severe metabolic diseases. The mechanisms of these processes are conserved between mammals and invertebrates (Trinh and Boulianne, 2013; Arrese and Soulages, 2010). The neurotransmitter serotonin affects fat metabolism and feeding of animals (Srinivasan et al, 2008; Donovan and Tecott, 2013; Jones and Ashrafi, 2009). In mammals injections of serotonergic agonists or serotonin into the medial hypothalamus suppresses appetite. Additionally, serotonin increases energy expenditure, and promotes the reduction of the body fat (Leibowitz, 1989; Leibowitz and Alexander, 1998). In *Drosophila* serotonin regulates feeding via the $5HT_{2A}$ receptor. Thereby, like in mammals, an increased serotonin signalling reduces food intake (Gasque et al, 2013). A knockdown of the $5HT_{1A}$ receptor in the insulin producing cells (IPCs) in *Drosophila* also affects food intake. The receptor knockdown mimics a reduced serotonin signalling but also decreases food intake. Additionally, it diminishes starvation resistance and leads to lowered lipid levels upon starvation (Luo et al, 2012; Luo et al, 2014). This reveals a high complexity in the function of serotonin. Upon knockdown of the $5HT_{1A}$ receptor in the IPC's the Dilp2 level is increased in these cells. Insulin producing cells regulate the glucose and lipid metabolism in *Drosophila* (Kwak et al, 2013). The lowered $5HT_{1A}$ level displays a similar metabolic phenotype as the increase of insulin signalling. Therefore, it is assumed that serotonin signalling in the IPCs is responsible for an inhibitory regulation of these neurosecretory cells. The serotonergic neurons or clusters that innervate the IPCs are not identified yet due to an extensive arborisation (Luo et al, 2012).

Serotonin is also involved in food choice. In mammals, increased serotonin level or increased TOR signalling in the hypothalamus decrease food intake (Leibowitz and Alexander, 1998; Muta et al, 2015). An increase of brain serotonin also enhances the preference to protein rich food. Thereby the intake of carbohydrates is decreased (Leibowitz, 1989). In *Drosophila* serotonin signalling and TOR pathway in the brain are involved in an increased preference to

protein rich food after starvation (Vargas et al, 2010). Vargas et al showed in 2010 that a pan neuronal increase of S6K signalling or increased serotonin production enhances the preference for yeast as food choice in *Drosophila* after a brief phase of starvation. Thereby, active S6K and serotonin were suggested to increase preference for yeast by similar mechanisms. The mechanisms for these processes are not known in detail. Ribeiro and Dickson showed in 2010 that even both decreased and increased TOR/S6K signalling in *Drosophila* neurons stimulate the intake of protein rich food.

## 1.5 Aims of the thesis

The mechanism how organisms sense their amino acid status and how they adapt metabolism and feeding behaviour to their internal nutrient availability is still unclear. In this thesis the adjustment to amino acid availability by nutritional information was analysed on metabolic targets and neurotransmitter production. Therefore, the effect of amino acids and TOR signalling on *tobi* transcription was analysed as an example for a metabolic target. The effect on serotonin production was analysed as an example for a neuronal adjustment. Thereby, the hypothesis that TOR pathway might be involved in the provisioning of nutritional information to the brain was investigated.

# 2 Material

## 2.1 General Materials

### 2.1.1 Consumables

| Consumables | Company |
|---|---|
| Cell strainer | VWR International, Darmstad |
| Cover slips | Roth, Karlsruhe |
| Filter Papers 90mm | Macherey- Nagel, Düren |
| Glass beads 1,25-1,65mm | Roth, Karlsruhe |
| Microscope slides | Roth, Karlsruhe |
| Microseal®`B`seal | Bio-Rad Laboratories, UK |
| Micro tube 2 ml | Sarstedt, Nümbrecht |
| Immobilon®-P | Millipore, Billerica |
| Parafilm | Pechiney Plastic Packaging, Menasha WI |
| PCR Reaction tubes (0,2 ml) | Corning, Schiphol-Rijk, Netherlands |
| Pipet tips | Corning, Schiphol-Rijk, Netherlands |
| Plastic wares | Roth, Karlsruhe; Greiner, Solingen |
| Pre-coated TLC plates | Macherey- Nagel, Düren |
| Reaction tubes (1,5; 2,0 ml) | Eppendorf, Hamburg |
| RealTime PCR 96-well plates | Biozym Sientific, Oldendorf |
| Roti®-Histokitt II | Roth, Karlsruhe |
| Scalpel | Hartenstein, Würzburg |
| Screw cap,white | Sarstedt, Nümbrecht |
| Pre-coated TLC plates | Macherey-Nagel, Düren |

### 2.1.2 Equipment

| Equipment | Type | Company |
|---|---|---|
| Autoklave | Varioklav Dampfsterilisator EP-2 | H+P, Oberschleißheim |

| | | |
|---|---|---|
| Bacteria incubator/shaker | Innova 42 | New Brunswick Scientific, Eppendorf, Hamburg |
| Balances | BL 1500 S, B211 D | Sartorius, Göttingen |
| Binocular | Stemi 2000, SZ40 | Zeiss Olympus, Jena |
| Bunsen burner | Fuego SCS basic | WLD-TEC, Göttingen |
| Centrifuges | 5424, 5810R | Eppendorf, Hamburg |
| Color digital camera | AxioCam MR3 | Carl Zeiss, Jena |
| Confocal Microscope | LSM780 | Zeiss, Jena |
| Foreceps | Dumont #5 | Fine Science Tools, Heidelberg |
| Freezer -20 | G5216 | Liebherr Hausgeräte, Ochsenhausen |
| Freezer -80 | Innova U535 | New Brunswick Scientific, Eppendorf, Hamburg |
| Gel-chamber (elektrophoresis) | PowerPac Basic, 10 - 300 V | Peqlab, Erlangen |
| Gel-documentation | Biozym Alpha Digi Doc Gel Imager | Intas, Göttingen |
| Homogenizer | Precellys | Peqlab, Erlangen |
| Hot plate magnetic stirrer | M82 | Hartenstein, Würzburg |
| Incubator | 3101 | RUMED, Laatzen |
| Microscope | CK40 | Olympus, Hamburg |
| Microscope camera | AxioCam ICc 1 | Zeiss, Jena |
| Microwave | | Panasonic, Hamburg |
| Mini centrifuge | Sprout®HD1000BC | Heathrow Scientific LLC, Illinois, USA |
| PCR-machine | iQ5 Cycler | BioRad, Munich |
| PH meter | HI 221 | Hanna Instruments, Smithfield RI |
| Photometer | NanoDrop Spectrophotometer | Peqlab, Erlangen |
| Pipettes | Pipetman Neo®P2N, P20N,P200N, P1000N | Gilson, Inc. Wi, USA |
| Plate reader | Fluostar Omega | BMG Labtech |
| RealTime PCR- | CFX96 RealTime System | BioRad, Munich |

| | | |
|---|---|---|
| machine | | |
| Rotating disc | Stuart®SB3 | Bibby Scientific Limited, Stone, UK |
| Special accuracy weighing machine | PCB 1000-2 | Kern & Sohn, Balingen-Frommern |
| Thermomixer | Thermomixer comfort | Eppendorf, Hamburg |
| Vacuum concentrator | Savant Speed-Vac SPD 111 V | Thermo Fisher Scientific, Oberhausen |
| Voltage source | PowerPac Basic | BioRad, Munich |
| Vortexer | Vortex Genie2 | Scientific Industries, New York, USA |
| Water bath | 1002 | GFL, Burgwedel |

## 2.2 Chemicals and solutions

| Name | Abbreviation | Company |
|---|---|---|
| Acetic acid | | Roth, Karlsruhe |
| Agar-agar, Kobe I | Agar | Roth, Karlsruhe |
| Agarose | | Roth, Karlsruhe |
| Ampicillin sodiumsalt | Amp | Carl Roth, Karlsruhe |
| Apple juice | | Lidl Dienstleistung, Neckarsulm |
| Brewer's yeast | | Gewürzmühle Brecht, Eggenstein |
| 5-Bromo-4-chloro-3-indolyl-phosphate | X-Phos | Roche, Penzberg |
| 5-Bromo-4-chloro-3-indolyl-β-D-galactopyranoside | X-Gal | Carl Roth, Karlsruhe |
| Chloroform | | Merck, Darmstadt |
| Copper sulphate | | Roth, Karlsruhe |
| Cornmeal | | Broicher Mühle, Bedor |
| Diethylether | | Roth, Karlsruhe |
| Diethylpyrocarbonate | DEPC | Sigma-Aldrich, Steinheim |
| Dimethyl sulfoxide | DMSO | Sigma-Aldrich, Steinheim |
| Disodium hydrogen phosphate | $Na_2HPO_4$ | Roth, Karlsruhe |
| Dry yeast | | Lidl, Neckarsulm |
| Ethylene glycol bis(β-aminoethyl)-ether) tetraacetic acid | EGTA | Roth, Karlsruhe |

| | | |
|---|---|---|
| Erioglaucine | | Acros Organics, Geel (Belgium) |
| Ethanol | | Roth, Karlsruhe |
| Ethylendiamintetraacetic acid | EDTA | Carl Roth, Karlsruhe |
| Fiberagar | | Gewürzmühle Brecht, Eggenstein |
| Formaldehyde 37% | | Carl Roth, Karlsruhe |
| Formamide | | Sigma-Aldrich, Steinheim |
| Glycine, p.a. | | Sigma-Aldrich, Taufkirchen |
| Goat serum | | Life Technologies, Darmstadt |
| Heparin | | Carl Roth, Karlsruhe |
| Herring-sperm single strand-DNA | ssDNA | Sigma-Aldrich, Steinheim |
| Hepes | | Roth, Karlsruhe |
| Isopropanol, 2-Propanol | | Roth, Karlsruhe |
| Kanamycin sulphate | | Carl Roth, Karlsruhe |
| LB-broth | | Carl Roth, Karlsruhe |
| Levamisole-hydrochloride | Levamisole | AppliChem, Darmstadt |
| Lithium chloride | LiCl | Roth, Karlsruhe |
| Magnesium chloride Solution | | Bioline, Luckenwalde |
| Magnesium sulphate | $MgSO_4$ | Roth, Karlsruhe |
| Meat Peptone | | Roth, Karlsruhe |
| Methanol | MetOH | Roth, Karlsruhe |
| Methyl-4-hydroxybenzoate | Methylparaben | Sigma-Aldrich, Taufkirchen |
| Mowiol40-88 | | Sigma-Aldrich, Steinheim |
| 3-(N-Morpholino)propane sulfonic acid | MOPS | Roth, Karlsruhe |
| n-Heptan | | Roth, Karlsruhe |
| Nitroblue-tetrazoliumchloride | NBT | Roche, Penzberg |
| Oligonukleotides for PCR | | Erofins, Ebersberg |
| Peptone ex casein | | Roth, Karlsruhe |
| Peptone ex fish | | Roth, Karlsruhe |
| Peptone ex gelatine | | Roth, Karlsruhe |
| Phosphoric acid | | Roth, Karlsruhe |
| 2-Propanol/Isopropanol | | Roth, Karlsruhe |
| Protector RNase Inhibitor | | Roche, Mannheim |
| Rapamycin | | Roth, Karlsruhe |
| Saccharose | | Roth, Karlsruhe |

| | | |
|---|---|---|
| Sodium acetate, p.A. | NaAc | AppliChem, Darmstadt |
| Sodium chlorate | NaClO | Roth, Karlsruhe |
| Sordium chloride | NaCl | Roth, Karlsruhe |
| Sodium dihydrogen phosphate | $NaH_2PO_4$ | Roth, Karlsruhe |
| Sodium-dodecyl-sulphate | SDS | Roth, Karlsruhe |
| Soy peptone | | Roth, Karlsruhe |
| Sugar beet syrup | | Grafschafter Krautfabrik, Meckenheim |
| Tris(hydroxymethyl)-aminomethane | Tris/Tris-Base | Roth, Karlsruhe |
| Tween20 | | Roth, Karlsruhe |
| Yeast | | Edeka, Bonn |
| Yeast autolysate | | Sigma-Aldrich, Steinheim |
| Yeast extract (yeast peptone) | | Roth, Karlsruhe |

## 2.3 Buffers und Media

The concentration factor for solutions, which were made as concentrated stocks, is indicated. For the production of buffers and solutions double distilled water (aqua bidest) was used, otherwise the use of other solvents is noted.

| Name | Zusammensetzung |
|---|---|
| Amino acid agar | 2% Agar (w/v), 7.5% saccharose (w/v), 0.3% methyl paraben(w/v), 2.1% EtOH (v/v), Eriogaucine solution (1:100) and 1 g of yeast or fish amino acid mixture |
| Ampicillin (1000x) | 50 mg/ml |
| AP-buffer | 100 mM Tris pH 9.5, 50 mM $MgCl_2$, 100 mM NaCl, 0.1% Tween20, 50 mM levamisole |
| Apple juice agar | 2.1% (w/v) agar, 25% (v/v) apple juice, 2.5% (w/v) saccharose, 10 mM methylparaben, 1% (v/v) EtOH |
| Erioglaucine solution | 50 mg/ml |
| Flyfood (18 l) | 15 l $H_2O$, 248 g brewer's yeast, 1223 g cornmeal, 130 g fiberagar, 1.5 l, 300 ml 10% methylparaben (solved in 100 % ethanol) |

| | |
|---|---|
| Fix1 solution | 100 mM Hepes, 2 mM $MgSO_4$, 1 mM EGTA; pH was adjuted to 6.9 |
| Glycine agar | 2.5% Agar (w/v), 16% saccharose (w/v), 4% autolysed yeast, 0.3% methyl paraben(w/v), 2.1% EtOH (v/v), erioglaucine solution (1:100) and 1 M, 200 mM or 20 mM glycine |
| Hybe | 50% (v/v) formamide, 5 x SSC, 200 µg/ml ssDNA, 100 µg/ml tRNA, 25 µg/ml heparin, pH 5.0 |
| HybeB | 50% (v/v) formamide, 5 x SSC |
| Hydrogen peroxide agar | 2.5% Agar (w/v), 16% saccharose (w/v), 4% autolysed yeast, 0.3% methyl paraben(w/v), 2.1% EtOH (v/v), erioglaucine solution (1:100) and 5%, 1% or 0.1% hydrogen peroxide |
| LB-agar | 10 g LB broth powder, 6 g agar, 400 ml ddH2O |
| LB-ampicillin agar | LB agar with 50 µg/ml ampicillin |
| LB-ampicillin medium | LB-medium with 50 µg/ml ampicillin |
| LB-kanamycin agar | LB agar with 50 µg/ml kanamycin |
| LB-medium | 10 g LB-Medium-powder solved in 400 ml $ddH_2O$ |
| LB-kanamycin medium | LB-medium with 50 µg/ml kanamycin |
| Lysis buffer | 100 mM TrisHCl pH 7.5, 100 mM EDTA, 100 mM NaCl, 0.5% SDS |
| Metyl paraben solution | 10% methylparaben in 70% ethanol |
| MOPS-buffer (20 x) | 400 mM MOPS, 100 mM NaAc, 10 mM EDTA, pH 7.0 |
| Mowiol | 12 ml Glycerine, 9.6 g Mowiol40-88, 24 ml $H_2O$, 48 ml 0.2M TrisHCl, pH 8.5 |
| Neutralization buffer | 3 M Potassium acetate |
| PBS 10x | 2 g KCl, 2 g $KH_2PO_4$, 11.5 g $Na_2HPO_4$, 80 g NaCl filled up to 1 litre of $ddH_2O$; pH adjusted to 7.4 with HCl oder NaOH, buffer was sterile filtered |
| PBS agar | 300 ml aqua bidest, 100 ml 1xPBS, 8.5 g agar, 0.6 g methylparabene solved in 4 ml ethanol |
| 0.1 PBT | 0.1% (v/v) Tween20 in PBS |
| 0.5 PBT | 0.5% (v/v) Tween20 in PBS |

| | |
|---|---|
| Peptone agar | 2% Agar (w/v), 7.5% saccharose (w/v), 0.3% methylparaben (w/v), 2.1% EtOH (v/v), Eriogaucine solution (1:100) and 1 g of peptone |
| Rapamycin solution | 2 mM Rapamycin solved in ethanol |
| Resuspension buffer | 25 mM Tris, 10 mM EDTA, 100 µg/ml RNAse A |
| SOC | 20 g Tryptone, 5 g yeast extract, 0.5 g NaCl, 10 ml 0.25 M KCl, 5 ml 2 M $MgCl_2$, 20 ml 1 M glucose; filled up to 1 l with $ddH_2O$; pH 7.0 adjusted with NaOH; autoklaved |
| Solution A (SolA) | 100 mM TrisHCl pH 7.5, 100 mM EDTA, 100 mM NaCl, 0.5% SDS |
| SSC 20x | 3 M NaCl, 300 mM Trinatriumcitrat pH 7.0 |
| Sugar agar | 2% Agar (w/v), 7.5% saccharose (w/v), 0.3% methylparaben (w/v), 2.1% EtOH (v/v), |
| TAE 50x | 242 g Tris, 27.5 g Borsäure, 20 ml 0.5M EDTA pH 8.0; filled up to 1 l with $ddH_2O$ |
| Water agar | 300 ml $ddH_2O$, 8.5 g agar-agar |
| Yeast paste | 42 g yeast, 6 ml 1xPBS-buffer |

## 2.4 Enzymes

| Name | Abbreviation | Company |
|---|---|---|
| Mango Taq™ DNA- | Taq | Bioline, Luckenwalde |
| KOD Hot Start DNA | KOD | Novagen® Merck KGaA, Darmstad |
| Proteinase K | | Sigma-Aldrich, Taufkirchen |
| Restriction endonucleases | | NEB, Frankfurt |
| SP6 RNA Polymerase | SP6 | Roche, Mannheim |
| T7 RNA Polymerase | T7 | Roche, Mannheim |

## 2.5 Standards and Kits

| Name | Company |
|---|---|
| Pierce™ BCA Protein Assay | Life Technologies, Darmstadt |
| DIG RNA labeling Mix | Roche Diagnostics, Mannheim |
| dNTP Set 100mM | Life Technologies, Darmstadt |

| | |
|---|---|
| Gateway® LR Clonase™II Enzyme Mix | Invitrogen, Carlsbad |
| Gene Ruler DNA Ladder Mix | Fermentas, Heidelberg |
| NucleoSpin® Extract II Kit | Macherey-Nagel, Düren |
| PCR Grade Nucleotide Mix | Roche Diagnostics, Mannheim |
| Precellys- Keramik- Kit; 1,4 mm tubes | PeqLab, Erlangen |
| Qiagen Plasmid Maxi Kit | Qiagen, Hilden |
| Quantitect cDNA Synthesis Kit | Quiagen, Hilden |
| Rapid DNA Dephos & Ligation Kit | Roche Diagnostics, Mannheim |
| RNAse ZAP | Sigma-Aldrich, Taufkirchen |
| SensiMixTM SYBR No-ROX kit | Bioline, Luckenwalde |
| TOPO™TA Cloning® Kit | Invitrogen, Carlsbad |
| TriFast total RNA Isolation | PeqLab, Erlangen |
| TSA™Plus Fluorescein System | PerkinElmer, Boston |

## 2.6 Oligonucleotides

### 2.6.1 Primers for conventional PCR

| Name | Gen | Sequence (5'→3') | Company |
|---|---|---|---|
| actin5cF2 | act | GAGCGCGGTTACTCTTTCAC | Metabion, Martinsried |
| actin5cR2 | act | ACATCTGCTGGAAGGTGGAC | Metabion, Martinsried |

### 2.6.2 Primers for quantitative Real Time PCR

| Gene | Primer | Sequence (5'→3') | Company |
|---|---|---|---|
| Actin | actfwd | GATCTGGCTGGTCGCGATT | Metabion, Martinsried |
| | actrev | GGCCATCTCCTGCTCAAAGTC | |
| Dopa decarboxylase | ddc (fwd) | TTTCATTTGCCCCGAGTATC | Eurofins, Hamburg |
| | ddc (rev) | TCACCAGCATCCATTTGTGT | |
| Insulin receptor | InR (fwd) | CGACGATTAGGCAAACGACT | Metabion, Martinsried |
| | InR (rev) | AAGAATCGTGAAGGCGGTTA | |
| Lipase3 | lip3-sy F1 | TGAGTACGGCAGCTACTTCCC | Metabion, Martinsried |
| | lip3-sy R1 | TCAACTTGCGGACATCGCT | |
| Pathetic | path (fwd) | CACCATTTTCACCGCCTTTA | Eurofins, Hamburg |

| | | | |
|---|---|---|---|
| | path (rev) | TCCGCATTTTACCAACACG | |
| Ribosomal protein 49 | rp49 (fwd) | TCCTACCAGCTTCAAGATGAC | Metabion, Martinsried |
| | rp49 (rev) | CACGTTGTGCACCAGCAACT | |
| Serotonin transporter | SerT2L | GCCAAACAACGAGGACGA | Eurofins, Hamburg |
| | SerT2R | CACGGAGACCACCAGAATG | |
| Synaptobrevin | SybL | ACAATGCAGCCCAGAAGAAG | Eurofins, Hamburg |
| | SybR | TCCACGTTCACACGCATAAT | |
| Synaptotagmin 4 | Syt4L | GGTGGATGGTAATGGGTTGA | Eurofins, Hamburg |
| | Syt4R | AATGGTCACACTTCCGTTGG | |
| Syntaxin 18 | Syx18L | CTTCACAAGCAAATGGCAAC | Eurofins, Hamburg |
| | Syx18R | TCCTCGTCTTCATCCCAGTC | |
| Syntaxin 5 | Syx5L | GGCAAGAACATAGCCAGCAC | Eurofins, Hamburg |
| | Syx5R | GCGGTCTGTCATCAAATAAGC | |
| Target of brain insulin | tobi (fwd) | GTAGCGGCATTCGGAGAC | Metabion, Martinsried |
| | tobi (rev) | CATCCCCATTCGGAGTCCTT | |
| Tryptophane hydroxylase | trh (fwd) | GGTGGTGGTCAGGATAATGG | Eurofins, Hamburg |
| | trh (rev) | TGGTTACGCAGGGTGAAAAT | |

### 2.6.3 Primers for cloning

| Generegion | Primer | Sequence (5'→3') | Company |
|---|---|---|---|
| Pathetic promoter region 1.473 kb | pathcons Ifwd | TATCTCGAGTTAATTGCTCCTT CTTTCTCTGAAGTGC | Eurofins, Hamburg |
| Pathetic promoter region 1.473 kb | pathcons Irev | TTGGTACCAATATAAGTATTAA ACGCCCCGCTATC | Eurofins, Hamburg |
| Pathetic promoter region 4.818 kb | pathcons IIfwd | GAGCTCGAGGCCTTCACCCAGT AAAGAACAGAAAAA | Eurofins, Hamburg |
| Pathetic promoter region 4.818 kb | pathcons IIrev | CTCGGTACCTTTATATTTAAGC AGGGACTGTGTTTCTCA | Eurofins, Hamburg |

### 2.6.4 Primers for RNA probe production

| Gene | Primer | Sequence (5'→3') | Company |
|---|---|---|---|
| Pathetic | pathinsituFWD | TTGGTAAAATGCGGACACAA | Eurofins, Hamburg |
| | pathinsituREV | GCAGATTCAGGGTGATGCTC | Eurofins, Hamburg |

## 2.7 RNA Probes

| Target RNA | RNA Probe | Length [bp] | Source |
|---|---|---|---|
| *Pathetic* | *path* sense | 649 | T. Hübner |
| | *path* antisense | 649 | T. Hübner |
| *Dopa decarboxylase* | *ddc* sense | 701 | R. Bader |
| | *ddc* antisense | 701 | R. Bader |

## 2.8 Plasmids

| Plasmid | Plasmid source |
|---|---|
| pBPGUw | Addgene, Cambridge |
| pBPGw | Addgene, Cambridge |
| pentry4 | Invitrogen, Carlsbad |
| pCR®II-TOPO® | Invitrogen, Carlsbad |
| pCR®II-TOPO®pathconsI | T. Hübner |
| pCR®II-TOPO®pathconsII | T. Hübner |
| pentry4-pathconsI | T. Hübner |
| pentry4-pathconsII | T. Hübner |
| pBPGw pathconsI | T. Hübner |
| pBPGw pathconsII | T. Hübner |
| pBPGUw pathconsI | T. Hübner |
| pBPGUw pathconsII | T. Hübner |

## 2.9 Software/ Server- services

| Bezeichnung | Version | Company/Website |
|---|---|---|
| Adobe Photoshop CS5 Extended | 12.0.4x64 | Adobe Systems, Munich |
| AxioVision LE | AxioVs40 V 4.8.1.0 | Carl Zeiss, Jena |
| Biorad CFX manager | 2.0 | Biorad, Hercules (USA) |
| Excel | Microsoft®Office Excel ®2007 | Microsoft Corporation, USA |
| Fiji | | http://fiji.sc/Fiji |
| Flybase | FB2010_06 | National Human Genome Research Institute at the U.S. National Institutes of Health |
| GraphPad Prism | 6.0 | GraphPad Software, Inc. |
| NanoDrop ND-1000 | V 3.5.2 | peqLab, Erlangen |
| NCBI | | National Center for Biotechnology Information, U.S. National Library of Medicine |
| Primer 3 | 0.4.0 | Whitehead Institute for Biomedical Research, |
| SerialCloner | 2.6.1 | http://www.serialbasics.com |

## 2.10 Antibodies

### 2.10.1 Primary antibodies

| Antibody | Antigene | Source | Concentration | Company |
|---|---|---|---|---|
| α-Dig AP | Anti-Digoxigenin- | Sheep | 1:1000 | Roche, Mannheim |
| α-Dig POD | Anti-Digoxigenin-POD | Sheep | 1:1000 | Roche, Mannheim |
| α-Elav | embryonic lethal abnormal vision | Rat | 1:500 | Developmental Studies Hybridoma Bank, Iowa City |
| α-Repo | Reversed polarity protein | Mouse | 1:500 | Developmental Studies Hybridoma Bank, Iowa City |
| α-Serotonin | Serotonin | Rabbit | 1:1000 | Sigma-Aldrich, Taufkirchen |
| α-Trh | Tryptophane hydroxylase | Guinea pig | 1:500 | Life Technologies, Darmstadt |
| FITC | Green fluorescent protein | goat | 1:500 | Abcam, Cambridge |

### 2.10.2 Secondary antibodies

| Antibody | Source | Dilution | Company |
|---|---|---|---|
| α -rabbit Alexa 488 | Goat | 1:500 | Life Technologies, Darmstadt |
| α –guinea pig Alexa 568 | Goat | 1:500 | Life Technologies, Darmstadt |
| α –mouse Alexa 633 | Goat | 1:500 | Life Technologies, Darmstadt |
| α –rat Alexa 633 | Goat | 1:500 | Life Technologies, Darmstadt |

## 2.11 Bacterial strains

| Target RNA | Genotype |
|---|---|
| Top10 (E. coli) | See manufacturers data of TOPO$^{TM}$TA Cloning® Kit |
| One Shot® OmniMAX™ 2 T1$^{R}$ Chemically competent E.coli | See manufacturers data of Life Technologies, Darmstadt |

## 2.12 Fly lines

| Fly line | Genotype | Source |
|---|---|---|
| UAS-Tsc1;UAS-Tsc2 | w; UAS-TSC1,UAS-TSC2 | Tapon, N., Charlestown |
| UAS-Cam2.1 | w1118; P{w[+mC]=UAS-Cameleon.2.1} | Thum, A., Fribourg |
| UAS-Rheb | w[*]; P{w[+mC]=UAS-Rheb.Pa}2 | Saucedo, LJ., Seattle |
| UAS-Path | y1 w67c23; P{GSV6}pathGS13857/TM3, Sb1 | Goberdhan, D.C.,Oxford |
| Path-Gal4(2.2) | w1118;P{path1.4-Gal4}attP2 | Hübner, T., Bonn |
| UAS-GFP.nls | w[1118]; P{w[+mC]=UAS-GFP.nls}14 | Bloomington Drosophila Stock Center, Indiana |
| UAS-Shibire | w*; P{UAS-shits1.K}3 | Bloomington Drosophila Stock Center, Indiana |
| UAS-TrpA | w*; P{UAS-TrpA1(B).K}attP16 | Bloomington Drosophila Stock Center, Indiana |
| Cg-Gal4 | w[1118]; P{w[+mC]=Cg-GAL4.A}2 | Bloomington Drosophila Stock Center, Indiana |
| OregonR-S | wt | Pankratz, Bonn |

# 3 Methods

## 3.1 Fly keeping

### 3.1.1 Rearing conditions

Fly lines were reared at 18°C in plastic vials containing standard fly food. The flies were transferred to fresh food every four weeks. Virgins or male flies were collected for crosses upon paralysation by carbon dioxide. For egg collections flies were transferred into cages placed on apple juice agar plates. Yeast paste was applied to the middle of the plate as protein source. Flies were kept in an incubator at 25°C two days prior to the actual egg collections for experimental use. In the incubator an air humidity of 60% and a night and day cycle of twelve hours of light and dark was maintained. Egg collections were performed for four hours. For *in situ* hybridization of embryos, eggs were collected overnight. The collections were kept in the incubator until the required age for the experimental procedures was reached. If needed additional yeast paste was added.

### 3.1.2 Feeding experiments

Feeding experiments were performed to examine the effect of certain food components like sugar, amino acids or peptides on gene expression. The focus was set on the analysis of the nutritional regulation via amino acids. Therefore, flies were fed with different food sources. These flies were then used for the identification of transcriptional targets of amino acids and amino acid signalling via TOR pathway.

#### 3.1.2.1 Rapamycin feeding

Rapamycin is an antibiotic and an inhibitor of the Target of rapamycin (TOR) kinase (Ballou and Lin, 2008). It was used to deactivate TOR signalling in the larval organism by ingestion with the food. Therefore, rapamycin yeast paste was prepared using 10 g of yeast with 200 µl of rapamycin solution and 1.8 ml of water. For control larvae yeast paste with ethanol instead of a rapamycin-ethanol solution was used. It was fed to 72+/-2 hour old third instar larvae for 24 hours. The brains of those larvae were used for real time PCR analysis.

#### 3.1.2.2 Sugar and yeast feeding

Sugar feeding activates insulin signalling but deactivates TOR signalling due to amino acid deprivation. Yeast feeding activates TOR signalling. These food sources were used to

determine whether *pathetic*, *tryptophane hydroxylase* and *dopa decarboxylase* are transcriptional targets of TOR signalling pathway. For sugar feeding sugar agar plates and for yeast feeding PBS agar plates were prepared the day before. Yeast paste was added to the PBS agar plates and fifty 74+/-2 hours old OregonR-S wiltype larvae were kept feeding on each of the different food sources for 24 hours in the incubator. Brains of these third instar larvae were dissected and the tissue was prepared for Real time PCR analysis.

#### 3.1.2.3 Peptone, amino acid, glycine and hydrogen peroxide feeding

The feeding experiments, for analysis of *tobi* regulation, were performed with adult male and female flies. Fresh food was prepared one day before transferring the flies to the new food source. Therefore, agar master batches were prepared. For the master batches, first agar was heated with double distilled water until solved. Then it was cooled down to 60°C and methyl paraben (10% solved in 70% ethanol), erioglaucine (1:100) and sugar was added. The agar mix was filled up to the final volume and kept in a water bath at 60°C. Batches containing 2% agar and 7.5% sugar were used for the peptone mixes. For glycine and hydrogen peroxide feeding, batches with 4% autolysed yeast, 16% sugar and 2.5% agar were used. The different food mixes were prepared by adding 4 ml of the corresponding master batch to 1 g of peptone, 1 ml of a glycine (5M, 1M and 0.1M and) or 1 ml of a hydrogen peroxide solution (25%,5%,1%). Yeast extract was used as yeast peptone. The ingredients were mixed on a magnetic stirrer directly in the food vial. Male and female OregonR-S wildtype flies were separated a few days after eclosion kept on standard flyfood for five to seven days and 30 to 35 flies were transferred to the prepared food mixes for two days. Feeding was controlled by the blue dye erioglaucine. Flies with the strongest gut staining were used for Real time PCR analysis.

### 3.1.3 Starvation assays

Starvation assays were performed to analyse whether TOR manipulation in serotonergic neurons lead to a diminished starvation resistance.

#### 3.1.3.1 Starvation of third instars larvae

For starvation experiments twenty 72+/-2 hours old third instar larvae were starved in vials containing 20 ml of PBS agar. The amount of pupated larvae was counted after six days and the amount of adult flies after fourteen days.

#### 3.1.3.2 Starvation of adult flies

For starvation experiments on adult flies, twenty male flies were used five to seven days after eclosion. They were paralysed by carbon dioxide and separated from the female flies. Then they were incubated for one day at 25°C in vials with PBS agar and yeast paste for recovery. Thereafter, they were starved in vials containing just 20 ml of PBS agar. The amount of surviving flies was counted every twenty four hours as long as flies were alive. Dead flies were removed daily.

### 3.1.4 Gal4/UAS system

The Gal4/UAS system is a binary expression system derived from *Saccharomyces cerevisiae*. The yeast transcription factor Gal4 can be expressed under the control of a promotor of interest to limit its expression to certain cells or tissues. It binds to the yeast UAS promoter and can activate expression of a transgene of interest downstream of UAS (Figure 3.1). This way, it allows a targeted gene expression of transgenes of interest.

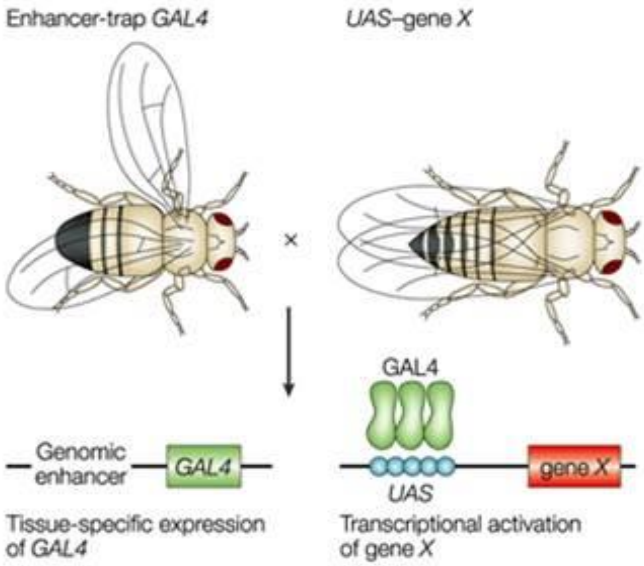


**Figure 3.1 Scheme of the Gal4-UAS system.**
The driver line expresses Gal4 under control of a genomic enhancer. The reporter line comprises a gene of interest under control of an upstream activating sequence (UAS). A cross of these lines results in the activation of the gene of interest in the Gal4 expressing cells of the offspring. The figure was modified from Johnston, 2002

*Drosophila melanogaster* fly lines are produced to carry these two components separately. Therefore, the Gal4 driver line and the UAS effector line need to be crossed to activate the system in the offspring (Duffy, 2002; del Valle Rodríguez et al, 2011). In this thesis, the Gal4-UAS system was used to manipulate the TOR signalling pathway and the neurotransmitter release or to label cells. TOR signalling was downregulated in the serotonin producing neurons by using the driver line Trh-Gal4 for crosses with UAS-TSC1;UAS-TSC2.

An upregulation of TOR signalling was achieved by crossing Trh-Gal4 with UAS-Rheb or UAS-Path. As control Trh-Gal4 was crossed with the wildtype strain (Wt) OregonR-S. Trh-Gal4 expresses the transcription factor Gal4 in Tryptophane hydroxylase positive cells. These cells are also termed as serotonergic or serotonin producing neurons or clusters in this thesis. The Tryptophane hydroxylase is involved in the serotonin production and is expressed in serotonergic neurons. Path, Rheb and the TSC1;TSC2 complex are involved in the amino acid signalling of the TOR pathway (Figure 3.2).

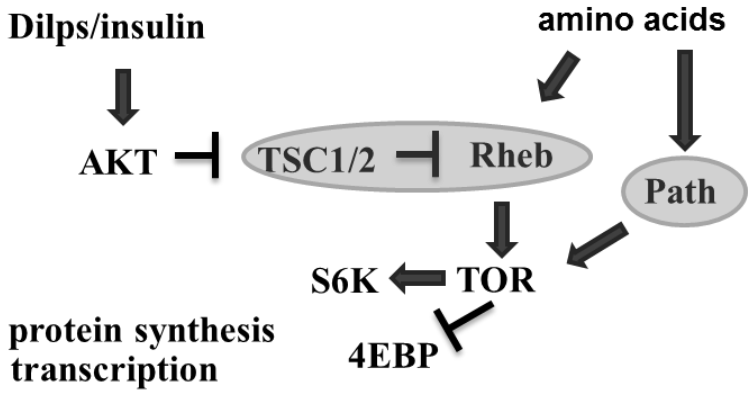


**Figure 3.2 Scheme of the TOR signalling pathway.**
The overexpression of Tuberous sclerosis complex 1 (TSC1) and Tuberous sclerosis complex 2 (TSC2) via the Gal4/UAS system was used to inhibit Target of Rapamycine (TOR) signalling. The overexpression of Ras homolog enriched in brain (Rheb*)* and Pathetic (Path) via Gal4/UAS system activated the TOR pathway. (S6K) S6 kinase. (4EBP) 4E binding protein. (Dilps) Drosophila insulin like peptides. (Akt) Homologue of the retroviral oncogene v-Akt.

For analysis of the Pathetic expression pattern, Pathetic-Gal4 flies were crossed with the GFP -reporter line UAS-GFP.nls. This way, the cells, where Gal4 is expressed under the control of the *pathetic* promoter, were marked with a fluorescent signal.

The Gal4-UAS system was also used for the targeted manipulation of neurotransmitter release from serotonergic neurons. Therefor, Trh-Gal4 was crossed to UAS-TrpA or UAS-Shibire $^{ts1}$ to overexpress the transient receptor potential ion channel TrpA or the dynamin Shibire $^{ts1}$. TrpA is a temperature sensitive cation channel that increases the cation influx upon temperatures above 25°C. This way, it depolarizes the cells in which it is expressed upon a restrictive temperature. In neurons it leads to an increased neurotransmitter release (Pulver et al, 2009). Therefore, overexpression of TrpA was used to induce an increased serotonin signalling at 32°C. Overexpression of Shibire$^{ts1}$ in contrary was used to inhibit serotonin release. Shibire (Shi) is a dynamin. Dynamins are responsible for synaptic vesicle recycling. The semidominant mutated allele shi$^{ts1}$ is defective in synaptic vesicle reuptake at temperatures above 29°C. This way, it inhibits neurotransmitter release reversibly (Kitamoto, 2001).

## 3.2 Molecular biological Methods

### 3.2.1 Spectrophotometric measurement of RNA and DNA content

The RNA or DNA content of a probe was measured by a Peqlab NanoDrop Spectrophotometer. The measurement device was normalized to 1.2 µl of the same double distilled water sample that was used to solve the nucleic acid.

The RNA or DNA content in 1.2 µl of a probe was determined in ng/µl by measurement of the absorption at 260 nm. The calculation of the nucleic acid concentration was performed using the Nanodrop software. Also possible contaminations by phenol or proteins were determined by the Nonadrop software. Therefore, the absorption ratio of 260 nm / 280 nm was determined. In case of RNA measurement, the ratio of an uncontaminated probe was expected to be about 2. Otherwise, a contamination with protein, phenol or genomic DNA was assumed. In case of DNA measurement, a ratio of about 1.8 was expected in probes without contaminations.

### 3.2.2 Agarose gel electrophoresis of RNA and DNA probes

Agarose gel electrophoresis was used to separate nucleic acids according to their molecular size. After enzymatic digestion for extraction and purification of amplified fragments and for analysis of a successful PCR or RNA probe, production samples were separated by this method. Therefor 1% agarose gels were used. Agarose was microwaved in 1x TAE buffer until it was solved completely. The heated agarose solution was cooled down to 60°C. The fluorescent reagent Syber-Safe, which intercalates in nucleic acid structures, was added in a dilution of 1:10000 while the gel was still fluid. The gel was poured into a cast. Combs were added to create wells for gel loading. Combs were removed after the gel had set. The cast containing the gel was placed in a chamber with 1x TAE buffer. A 5- fold loading buffer was diluted 1:5 with the DNA probes and the samples were loaded into the wells. Also a DNA marker that allowed estimating the molecular weight of the analysed fragments was loaded and run with the probes. Separation was performed at 80-120 V dependent on gel size. The DNA fragments were visualized by stimulation of the florescent reagent and documented by a gel detection system. When RNA probes were analysed for degradation and correct size 1x MOPS buffer was used instead of TAE buffer. The electrophoresis chamber, the combs and the cast were treated with an RNase decontamination solution (RNase ZAP) and rinsed with double distilled water to prevent RNA degradation by RNases. For loading RNase free loading buffer was used.

## 3.2.3 Isolation and purification of nucleic acids

### 3.2.3.1 Phenol chloroform extraction

Phenol chloroform extraction is used to separate components of homogenized cells and tissues like RNA, DNA and proteins due to their different properties of solubility. This way, it allows purification and further analysis of those components. For this thesis, phenol chloroform extraction was used to purify RNA of *Dorsophila melanogaster* tissues. Extraction was performed on three third instar larvae, four adult *Drosophila melanogaster* males or, in case of *tobi* expression analysis, 30 adult heads. Tissues were shock frozen by liquid nitrogen and homogenized with 700 µl TriFast in disposable Precellys polypropylene tubes. Therefor a peqlab Precellys 24 homogenizer was used. The tissue was broken open by ceramic pearls in the tubes while shaking three times at 5500 rpm (revolutions per minute) with 20 seconds of breaks in between. The homogenate was kept at room temperature for five minutes. Phase separation was performed by shaking the homogenate for 15 seconds with 140 µl chloroform. The mixture was kept at room temperature for three minutes to reach a separation of the different phases. Afterwards, it was centrifuged for five minutes at 12000 g and 4°C. After phase separation 350 µl of the aqueous phase was vortexed with 350 µl isopropanol in a new 1.5 ml tube. The samples were precipitated for at least 20 minutes at minus 20°C and centrifuged for ten minutes at 12000 g and 4°C. The whole supernatant was removed carefully. The remaining pellet was washed with 1 ml of 70% ethanol and centrifuged for further 10 minutes at 12000 g and 4°C. The supernatant was discarded completely. The RNA pellet was dissolved immediately in 10-200 µl water, dependent on pellet size.

### 3.2.3.2 Isolation of DNA fragments from agarose gels

After agarose gel electrophoresis, fragments of interest were detected by UV light and cut out of the gel precisely with a scalpel. This step occurred as fast as possible to prevent DNA damage by radiation. The purification of the fragment was performed using the NucleoSpin® Extract II Kit according to the manufacturer's instructions. The elution step was performed with 15-30 µl of aqua bidest, which was prewarmed to 70°C. DNA content was measured and the probes were stored at -20°C.

### 3.2.3.3 Isolation of genomic DNA

Genomic DNA was isolated from adult *Drosophila melanogaster* ovaries. Therefor female flies were paralyzed by carbon dioxide, killed and dissected in PBS. Two pairs of ovaries were transferred into a 1.5 ml tube. They were homogenized for two minutes with a pestle in

50 µl of solution A. Two microliter of Proteinase K was introduced to lyse the cells for thirty minutes at 37°C. The Proteinase function was stopped by heating the lysate up to 95°C for five minutes. Cell components were spun down and the solved DNA in the supernatant was used for further processes.

#### 3.2.3.4 Isolation of Plasmid DNA

After cloning and amplification of the vector of interest, the correct insertion and orientation of the inserted fragment was tested. Therefore, first an alkaline lysis of the bacteria cells was performed. Before lysis 1.5 ml of each bacteria culture was transferred into 1.5 ml Eppendorf tubes and centrifuged for one minute at 13000 rpm. The supernatant was discarded and 200 µl of resuspension buffer was added to the bacteria to solve them evenly. The plasmids were isolated by breaking the protein-lipid bilayer of the cell membranes using 200 µl of lysis buffer containing the detergent SDS and sodium hydrate. The alkaline solution was neutralized by a neutralization buffer containing potassium acetate. Thereby, proteins and genomic DNA were precipitated while the smaller plasmid DNA remained in solution. The bacteria cell residues were removed by centrifugation for ten minutes at 13000 rpm. The supernatant containing the plasmid DNA was transferred carefully into a new 1.5 ml Eppendorf tube. It was vortexed with 500 µl isopropanol for precipitation. After centrifugation for ten minutes at 13000 rpm, the supernatant was discarded. The pellet that contained the precipitated plasmid DNA was washed with 500 µl of 70% ethanol. Then, it was centrifuged at 13000 rpm for five minutes. The supernatant was discarded and the pellet was dried for ten minutes at room temperature. The dried pellet was resuspended with 50 µl of water and used for digestion and analysis by agarose gel electrophoresis.

For further cloning procedures or for RNA sense and antisense probe synthesis, greater amounts of plasmid DNA were isolated. Therefor midicultures of 50 ml were prepared. For plasmid isolation, the Qiagen Plasmid Maxi Kit was used mostly according to the manufacturer's specifications. During precipitation with isopropanol, centrifugation was performed for 90 minutes at 4000 rpm instead of 30 minutes at 15000 rpm and during the washing step with ethanol, centrifugation was performed for fifteen minutes at 4000 rmp instead of five minutes at 15000 rpm.

### 3.2.4 Reverse transcription of RNA

For the reverse transcription of RNA to cDNA, template RNA was thawed on ice. Wipeout buffer, gDNA, QuantiTect RT buffer, RT Primer Mix and RNase free water were thawed at

room temperature. Each solution was vortexed, centrifuged briefly to collect residual liquid droplets and stored on ice.

Template RNA of 0.5 µg per sample was transferred into 0.2 ml Corning Thermowell Gold PCR tubes and filled up to 6 µl with RNase free water. For the elimination of genomic DNA 1µl of Wipeout buffer was added into each sample. The probes were vortexed and incubated at 42°C for 2 minutes. After incubation, the samples were transferred on ice immediately. A mix of 2 µl of QuantiTect RT Buffer, 0.5 µl RT Primer mix and 0.5 µl QuantiTect Reverse Transcriptase was added to each prepared template RNA mix. For each sample another mix with water instead of Reverse Transcriptase was used to examine samples for DNA contamination. The mixtures were vortexed and kept on ice. If more than one reaction was set up, a volume of master mix 10% greater than required for the total number of reactions was prepared. Samples containing the reverse transcriptase mix were incubated for 20 minutes at 42°C for the reverse transcription reaction. Samples containing the control mix were treated the same way. After cDNA synthesis, the probes were incubated at 95°C for 5 minutes to inactivate the QuantiTect Reverse Transcriptase. The cDNA mix was filled up to 100 µl with double distilled water. It was used for further analysis by quantitative Real time polymerase chain reaction.

## 3.2.5 Cloning of DNA fragments

### 3.2.5.1 TOPO TA Cloning of DNA fragments

TOPO TA Cloning was used for direct onestep insertion of PCR products with 3’ adenosine (A)-overhangs into a plasmid vector. The pCR®II-TOPO® vector is a commercially available vector. It contains covalently bound Topoisomerases I at the terminals which keep the vector linearized. It also features single thymindine (T) overhangs. PCR fragments containing a 3’A-overhang interact with the T-overhangs and ligate to the vector. Thereby, the Topoisomerases are released and the vector forms a circularized structure. The circularized vector can be used for transformation into bacteria cells.

Amplified fragments were introduced into the pCR®II- TOPO ® vector using 1 µl of vector with 2 µl of fragment DNA and 3 µl of water. The reaction required a time interval of five minutes at room temperature. Transformation was performed on One Shot® TOP10 competent cells according to the TOPO TA Cloning Kit protocol for One Shot chemical transformation. Finally, of each transformation 100 to 150 µl were spread on prewarmed LB-ampicillin agar plates with X-Gal for blue-white screen and incubated overnight.

The blue white screen is based on a disruption of the beta galactosidase sequence due to a successful fragment insertion into the vector. A successful fragment insertion resulted in colonies unable to utilize the X-Gal. Colonies that incorporated a vector with the fragment of interest remained white while colonies without insert in the vector showed a blue staining due to X-Gal utilization. Five to ten white colonies were picked for further analysis. TOPO cloning was used to amplify a fragment of interest in a high amount for in vitro transcription and also for Gateway cloning.

#### 3.2.5.2 Gateway cloning of DNA fragments

Gateway cloning is based on the mechanism of a site specific recombination due to attachment sites in the entry (attL) and the destination vector (attR). Thereby, an expression vector with attB sides containing the fragment or gene of interest is generated. The entry clones were purified by midipreperation and used for Gateway cloning according to the instructions provided with the Gateway® LR Clonase™ II Enzyme Mix. For transformation with the expression clone One Shot® OmniMAX™ 2 T1 Phage-Resistant cells were used and plated on LB-ampicillin agar plates. Successfully transformed colonies were reared in 50 ml of LB-ampicillin medium overnight shaking at 37°C.

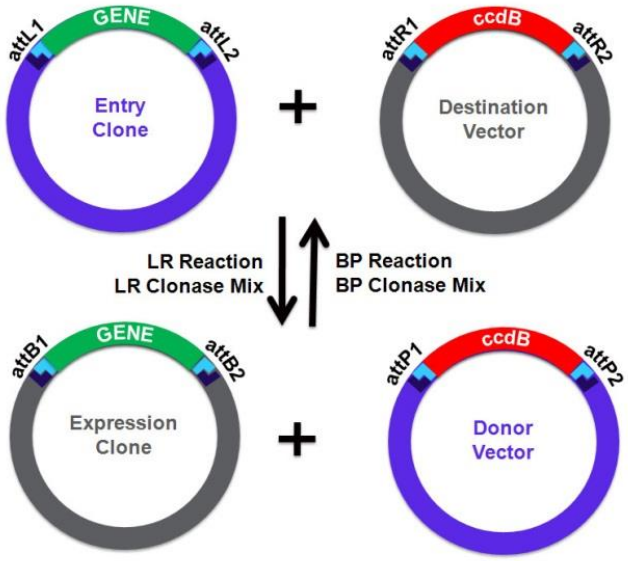


**Figure 3.3 LR reaction during gateway cloning.**
The gene or fragment of interest is introduced into the destination vector by an LR reaction of the destination vector attR sides with the entry clone attL sides. Thereby an expression clone with attB sides and a donor vector with attP sides are formed. The attB sides of the expression clone flank the fragment of interest. It can be used for a BP reaction. The figure was modified from intechopen.com

The Gateway vectors were purified by midipreperation and analysed for insertion of the correct insert by digestion and sequencing. They were sent to BestGene for the production of transformant flies after preparing them according to the requirements of the company.

## 3.2.6 PCR techniques

### 3.2.6.1 Polymerase chain reaction

Polymerase chain reaction was used to amplify inserts for cloning or as control for a correctly performed reverse transcriptase reaction. For reaction 5 µl of cDNA or diluted gDNA were vortexed with 20 µl of a PCR- mix containing 1 µM of the primerpair mix of interest, 0.2 mM of Invitrogen dNTP mix, 1x Bioline Reaction Buffer, 1.5 mM Bioline $MgCl_2$ and 0.625 U of Bioline Mango Taq DNA Polymerase. Before placing the probes into the PCR cycler, they were vortexed and spun down. As control for reverse transcriptase reaction actin5c primers were used. For the PCR run the cDNA-PCR mix was initially denatured for 5 minutes at 95°C. Afterwards 22 cycles of 30 seconds for denaturation at 95°C, 30 seconds for primer annealing at 56° C and 30 seconds for DNA stand extension at 72°C followed the initial denaturation. The reaction was terminated with a final extension step for 5 minutes at 72°C (Table 3.1). The samples were kept at 12°C before using them for gel electrophoresis. For insert amplification used for cloning, annealing, extension steps and cycle number were modified dependent on primer properties, amplicon size and amplification efficiency.

**Table 3.1 PCR- programm for primer elongation by MangoTaq DNA Polymerase**

| PCR –programm: | | |
|---|---|---|
| 1. Predenaturation | 95 °C | 3:00 min |
| 2. Denaturation | 95 °C | 0:30 min |
| 3. Annealing | 56°C | 0:30 min |
| 4. Elongation | 72°C | 0:30 min |
| Step 2 to 4 was repeated 22 times | | |
| 5. Final elongation | 72°C | 3:00 min |
| 6. PCR stop | 12°C | Infinite |

Insert amplification for the production of transformant flies was performed with KOD Hot Start DNA Polymerase. Thereby, the instructions of the KOD Hot Start DNA polymerase protocol of Novagen were followed. The total reaction volume was reduced to 25 µl. As template 0.2 µl of gDNA was used. The PCR programm was adjusted as follows:

**Table 3.2 PCR- programm for primer elongation by KOD Hot Start DNA Polymerase**

| PCR –programm: | | |
|---|---|---|
| 1. Predenaturation | 95 °C | 3:00 min |
| 2. Denaturation | 95 °C | 0:20 min |
| 3. Annealing | 57°C | 0:10 min |
| 4. Elongation | 72°C | 1:12 min |
| Step 1 to 4 were repeated 5 times, then step 2-4 were repeated 30 times | | |
| 5. PCR stop | 12°C | infinite |

#### 3.2.6.2 Real Time PCR

Real Time PCR was performed to identify expression changes in *Drosophila melanogaster*. Thereby, amino acid and TOR target genes were analysed upon different food conditions or upon TOR signalling manipulation. For expression analysis in third instar larvae cDNA of three larvae, three larval guts or cuticles with attached epidermis or 30 larval brains were used. For expression analysis in adult flies three whole male flies or 30 male or female heads were used.

Primer pairs for Real Time PCR were designed to amplify 50-150 base pair fragments of the gene of interest. Therefor a GC content of 40 to 60% and the optimal annealing temperature of 60 °C were choosen. For primer design the Primer 3 Plus program was used. To ensure an appropriate primer quality, a primer test was performed. The PCR reactions were set up as duplicates to detect pipetting errors. Therefor two different master mixes were prepared (Table 3.3 and Table 3.4).

**Table 3.3 Real Time PCR Mastermix 1**

| **Compound** | **Volume per sample** |
|---|---|
| Template cDNA | 1µl |
| Aqua bidest | 5.75 µl |
| Final volume | 6.75 |

**Table 3.4 Real Time PCR Mastermix 2**

| **Compound** | **Volume per sample** |
|---|---|
| 2x Sybr Green | 7.5µl |
| Primermix forward/reverse | 0.75 µl |
| Final volume | 8.25 |

If a high volume of master mixes for numerous reactions was needed, 10% additional master mix was prepared to prevent a deficit. For each PCR reaction 6.75 µl of master mix 1 and 8.25 µl of master mix 2 was pipetted into a well of a Realtime-PCR 96 well plate. The plate was sealed accurately to prevent evaporation. The PCR reactions were performed by a Biorad RealTime maschine using a PCR programm adjusted as follows.

**Table 3.5 Quantitative RealTime PCR- programm**

| step | temperature | Time |
|---|---|---|
| 1. Predenaturation | 95°C | 10:00 min. |
| 2. Denaturation | 95°C | 0:10 min. |
| 3. Annealing | 60°C | 0:10 min. |
| 4. Elongation | 72°C | 0:30 min. |
| Step 2 to 4 were repeated 39 times | | |

The amplification was recorded due to fluorescence of Sybr Green, a dye that intercalates between double stranded DNA. Therefore, the fluorescence increased proportional to the amount of amplified fragments and could be measured by the Real time cycler.

During RNA-extraction and cDNA synthesis inconsistencies can occur. To compensate possible irregularities, the housekeeping genes ribosomal protein 49 (rp49) or rp49 and actin were used as internal controls during Real time PCR. Reactions with primers for these genes were prepared as duplicates for every tested sample. Values obtained for the housekeeping genes were used for normalization. Control conditions were set to 1. The data was calculated using the Biorad software.

#### 3.2.6.3 Analysis of primer quality

Primer pairs that do not bind correctly to the target sequence, that contain contaminations or form dimers falsify the results. Therefore, a primer test was performed before using a primer pair for experiments. For a primer test a Real time PCR was performed. Therefor mastermixes with undiluted cDNA and dilutions of 1:5, 1:25, 1:125 and 1:625 of the same cDNA were prepared and used as previously described for Real time PCR with the primer mix of interest. Also a Sybr Geen/ primer mix duplicate with water instead of cDNA was pipetted. This way the primer mix was tested for contaminations. Contaminations could be assumed if an increase of fluorescence occurred without an included template. Additionally to the normal Real time PCR program a melt curve analysis was included at the end of a run. For melt curve analysis denaturation was performed for ten seconds at 95°C. Then temperature was increased

every five seconds by 0.5°C increments beginning at 55 °C and ending at 95°C. Fluorescence changes were documented in a melt curve. This way the appearance of primer dimers or mispriming incidents were analysed. Those were revealed by more than one peak in the melt curve. Primer efficiencies were determined using the Biorad software. Primers with efficiencies above 80% were taken for transcript analysis.

### 3.2.7 Generation of the Path-Gal4 constructs and the Path-Gal4 transgenic flies

Primer pair sequences flanking a 1.473 or a 4.818 kb of the putative *pathetic* promoter region were chosen using the ApE-A Plasmid Editor. Restriction sides for the endonucleases XhoI (forward primer) and KpnI (reverse primer) respectively were added into the primer sequences for a later insertion into the Gateway vector. The primers were ordered at Eurofins. The fragments of interest were amplified by KOD Hot Start PCR for a higher amplification quality. A further amplification was reached by cloning the fragments into a TOPO vector. This construct was used for transformation into One Shot TOP10 cells according to the manufacturer's instructions. Thereafter, the fragment was cut out of the vector by enzymatic digestion with NEB endonucleases XhoI and KpnI. It was purified by gel electrophoresis and gel elution. The pentry4 vector was also cut with XhoI and KpnI on each side of the dual selection cassette. Cutting vector and fragment with the same enzymes assured a directed insertion of the fragment in the planned orientation. The vector was dephosphorylated to prevent circularization and ligated with the fragment in a ratio of 1:2. The construct was used for the transformation of TOP10 cells according to the manufacturer's instructions.

These entry clones were used to generate an expression clone (Figure 3.4). Therefor a recombination reaction between the entry clone and the Gateway® destination vector pPGW or pBPGUW was performed (Figure 3.3). The pentry constructs were purified by midipreperation and used in the LR-reaction of the Gateway® LR Clonase™ II Enzyme Mix according to manufacturer's instructions. Successfully produced expression vectors were prepared according to the requirements of BestGene and sent to this company for the production of transformant flies. Transformant flies with the inserted 4.818 kb promoter fragment were not viable. Therefore, further experiments were performed on flies containing the 1.473 bp promoter fragment in front of the Gal4 coding DNA sequence (CDS).

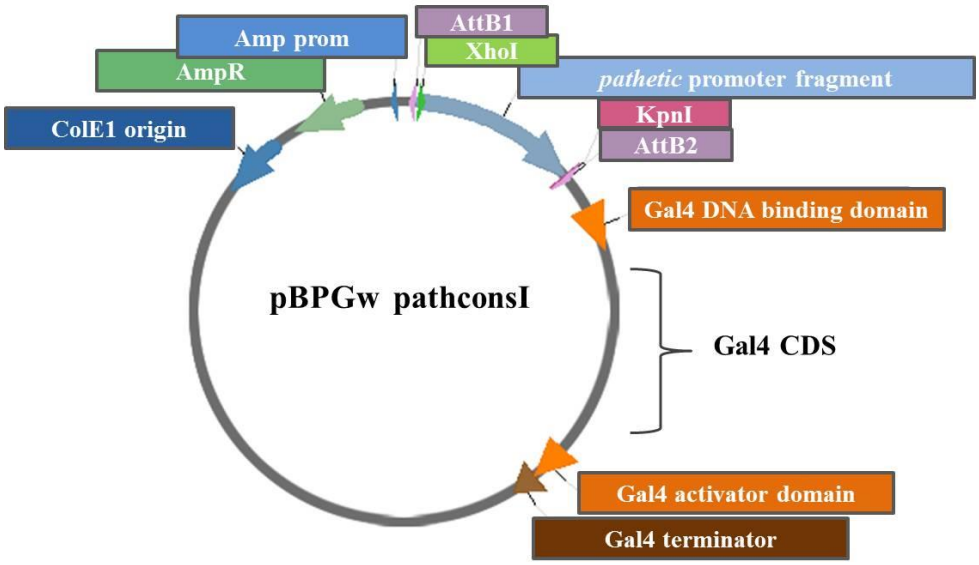


**Figure 3.4 pBPGW pathetic promoter construct I.**
The expression vector contains the Gal4 coding DNA sequence (CDS) under control of a pathetic promoter fragment. After LR Clonase reaction the fragment is flanked by attachment (attB) sides. ColE1 codes the origin of replication for amplification in E.coli bacteria. The vector enables bacteria to grow in ampicillin medium due to an ampicillin resistance (AmpR) gene. Further vector maps are shown in the appendix.

#### 3.2.7.1 3'-Desoxyadenosine-Overhang Post Amplification

The Desoxyadenosine (A) overhang amplification was needed for later cloning procedures. The KOD polymerase does not add A overhangs to the PCR fragments after amplification like the Taq polymerase. Thus, they had to be inserted after KOD Hot Start PCR by a prolongation reaction. Therefor 1000 ng of the DNA fragment of interest was used for the reaction with dATP. The Taq Polymerase catalysed the reaction due to its terminal transferase activity that adds a single A to the 3'end of an amplified fragment. Therefore, 1x Taq buffer, 0.2 mM dATP, 0.625U Taq polymerase and an optimal temperature of 72°C were needed for a 20 minute process to complete the overhang production. The fragments with 3'desoxyadenosine were used for TOPO TA Cloning.

#### 3.2.7.2 Dephoshorylation and Ligation

Dephoshorylation and ligation were performed using the Rapid DNA Dephos & Ligation Kit of Roche according to the manual. For dephosphorylation 1 µg vector was used. For ligation vector and insert were used in a ratio of 1:2. The ligated construct was used for transformation into TOP10 E. coli.

#### 3.2.7.3 Enzymatic digestion

Enzymatic digestion was used to analyse for a successful incorporation of a DNA fragment into a vector and for its orientation in the vector. It was also used to prepare vectors and

corresponding fragments for ligation or to linearize a construct for in vitro transcription. Therefor NEB restriction endonucleases and optimal NEB buffers were used according to the manufacturer's instructions. Suitable restriction enzymes were chosen after DNA sequence and restriction site analysis of the DNA fragment of interest. Therefore, the Serial cloner software was used. To analyse for successful fragment incorporation and for its orientation, total volumes of 30 µl were prepared. For extraction of fragments after gel electrophoresis 100 µl reactions were used. Digestion was performed for 1-2 hour at 37°C. Around 2-5 U of enzyme were used for digestion of 1 µg of DNA. The digested DNA was mixed with loading buffer and separated on a gel for analysis or extraction.

#### 3.2.7.4 Sequencing

DNA was prepared according to the requirements of 4base lab and sequenced by this company. The sequence was analysed using the Serial Cloner software. Sequence data for the DNA fragments of interest were provided by flybase.org and the vector sequence was provided by the corresponding company.

### 3.2.8 Immunochistochemical stainings

#### 3.2.8.1 Dissection and fixation of tissues for staining

Tissues were dissected under the binocular microscope in a dissection dish with PBS**.** The degradation of tissue after dissection was prevented by fixation in a 1.5 ml tube upon rotation on a rotation disc. Therefor 4% formaldehyde in 0.5% PBT was used. Afterwards, formaldehyde was removed and washed away by inverting the brains in 0.5% PBT twice for 5 minutes, twice for 15 minutes and twice for 30 minutes. For storage the tissues were dehydrated. Therefor they were inverted for ten minutes in 30% methanol and 70% methanol. Probes were stored over night at -20°C in 100% methanol. The tissues were used for histochemical and fluorescence *in situ* hybridization and for antibody staining. They were stored not longer than two weeks before use.

#### 3.2.8.2 *In situ* hybridization

*In situ* hybridization was performed to detect transcript availability of certain genes of interest in *Drosophila melanogaster* tissues. Therefor RNA sense and antisense probes were produced. For the expression analysis in embryos and larvae different protocols were used. That way, optimal staining results of the different tissues were ensured.

The RNA probes were produced following the instructions of the Bio RNA labelling kit of Roche. Tissues stained by histochemical *in situ* hybridization were embedded into Roti®-

Histokitt II medium and analysed using a transmitted light microscope. Tissues stained following the fluorescence *in situ* hybridization protocol provided by Perkin Elmer were embedded in Mowiol and analysed using a confocal laser scanning microscope.

#### 3.2.8.3 Production of the RNA sense and antisense probes

A 649 base pair (bp) fragment of the gene *pathetic* was amplified by PCR using larval cDNA as template. Therefor a PCR with 30 cycles, a primer annealing temperature of 60°C and an elongation interval of 60 seconds was performed. Otherwise, the same settings as described in Table 3.1 were used. The fragment was detected by agarose gel electrophoresis. It was cut out and purified by gel elution. The purified fragment was used for cloning into the pCRII®-TOPO® -vector. For amplification of the vector it was introduced into E.coli TOP10 cells. The transformation was analysed by a blue white screen. The incorporation of the correct insert was examined by minipreparation and digestion of the extracted plasmid DNA by EcoRI. E.coli cultures, producing a fragment of the correct size were reared in midicultures. After midipreperation, the fragments were analysed for their orientation in the vector by digestion with EcoRV and sequencing. The construct was linearized by SpeI. Therefor 10 µg of the vector and 2 µl of the enzyme were used. Linearized construct was separated from circularized construct by agarose gel electrophoresis. For elution the NucleoSpin® Extract II Kit was used according to the manufacturers' advice.

RNA probes for the analysis of the *pathetic* transcription pattern were produced following the manufacturers' instructions (Dig/Fluo/Bio RNA labelling Kit, Roche). After RNA probe production the RNA was dissolved in 50 µl DEPC water and 150 µl of Hybe. The probe was tested for degradation and correct size by agarose gel electrophoresis using MOPS buffer. RNA probes were stored in the freezer at -20°C.

#### 3.2.8.4 Dot blot

A proper incorporation of digoxigenin was tested by dot blot analysis. The intensity of the staining reaction allows determining the sensitivity of the anti digoxigenin alkaline phosphatase coupled antibody (α-Dig-AP) to the RNA probe. Therefor a dilution series for the RNA probe of interest was performed. Dilutions with DEPC water of 1:1, 1:10, 1:50 and 1:100 were used to dot 1 µl of different RNA probe concentrations on a nitrocellulose membrane. The membrane was placed in a 2 ml tube. During the following steps the probes were treated being inverted on a rotation disc. Before adding new buffers previous were discarded. Hybe was added for thirty minutes of prehybridization and was first washed away with HybeB for five minutes. Then, it was washed three times with 0.5% PBT for five

minutes. The antibody staining was performed using α-Dig-AP antibody (1:1000) in PBT with 5% goat serum. Unspecific binding sides were blocked with 5% goat serum in PBT for ten minutes. After treatment with the antibody, the unbound antibody was washed away with PBT three times for five minutes. Then, the membrane was washed five minutes with AP buffer. It was stained with 4.5 µl NBT and 3.5 µl XPhos in 1 ml of AP buffer for two to three minutes. The staining was stopped by washing once for five and once for ten minutes with PBT. Finally the membrane was dried and the staining intensity of the different dilutions was analysed. The antibody dilution with the best intensity and lowest background staining was used for histochemical *in situ* hybridization.

#### 3.2.8.5 Histochemical *in situ* hybridization of embryonal tissues

Embryos from overnight egg collections, not older than sixteen hours, were transferred into a cell strainer and rinsed in water. Thereafter, they were incubated in 50% of sodium hypochlorite from three to five minutes until dechorionation. Dechorionation was indicated by an agglutination of the embryos. The hypochlorite solution was washed away by rinsing the tissue tree times with water. In a glass vessel 4 ml of Fix1 solution was mixed with 5 ml of n-heptane and the embryos were released from the cell strainer into the interphase of this mixture. The embryonal vitelline membrane was removed by adding 500 µl of formaldehyde and shaking the sealed vessel for thirty minutes by a shaking device. The lower phase was then discarded, filled with methanol and the vessel was sealed and shaken vigorously. Embryos that sediment to the vessel ground were transferred into a 1.5 ml Eppendorf tube with a glass pipet. They were washed in methanol three times for five minutes inverting on a rotation disc before they were stored at -20°C overnight in methanol.

The Hybe and HybeB solutions were preheated to 65°C in a water bath, while embryos were rinsed twice and washed twice for five minutes in 1 ml of 0.5% PBT. To increase the permeability of the embryonal tissues, 2 µl of Proteinase K in 1 ml of PBT was added to the embryos. The membrane proteins were digested for one minute upon rotation and the probes were left to sink down for another minute. Then the proteinase was removed by rinsing the tissue twice with PBT. The embryos were then postfixated with 4% formaldehyde in PBT for twenty minutes on the rotation disc. The formaldehyde was removed by rinsing and washing the tissue twice. Then, embryos were transferred stepwise into the preheated Hybe solution rinsing them in 250 µl PBT with 250 µl Hybe B, then in 500 µl HybeB, afterwards in 250 µl of Hybe B and 250 µl Hybe and finally in 500 µl Hybe. Thereafter, embryos were incubated in 500 µl Hybe for one hour at 65°C. The Hybe solution was mostly discarded and 5 µl of *pathetic* RNA antisense or sense probe were added and incubated with the embryos overnight

at 65°C. After hybridization, the RNA probe was first washed away by adding 500 µl of Hybe, wich was replaced by 500 µl of fresh Hybe for fifteen minutes of post hybridization. This way, the unspecific binding of the RNA probe was minimized. The tissue was then transferred stepwise into 0.5% PBT. Therefore, 500 µl of HybeB was added to the Hybe solutuion without discarding it. After fifteen minutes the mixture was replaced by 500 µl of HybeB and after another fifteen minutes 500 µl of PBT was added. All the following washing and incubation steps were performed inverting the tissue on a rotation disc at room temperature. The residual HybeB solution was washed away rinsing it twice, washing it twice for fifteen minutes and once for twenty minutes with 1 ml of PBT. Anti-digoxigenin-AP coupled antibody in PBT was added to the tissue in a dilution of 1:1000 and was incubated for one hour. The unspecific bound antibody was washed away by rinsing the embryos twice and washing them with PBT once for five minutes, once for twenty minutes and once for thirty minutes. Embryos were prepared for staining by rinsing and incubating them for five minutes in 1 ml of AP buffer. For staining they were transferred into a dissection dish. The staining was performed in the dark by adding 1 ml of the staining solution containing 4.5 µl NBT and 3.5 µl X-Phos in AP buffer. When the staining reaction reached an appropriate intensity it was stopped rinsing the embryos in PBT and washing them once for twenty minutes. The embryos were then dehydrated for five minutes in 30% ethanol, five minutes in 70% ethanol and five minutes in 100% ethanol. They were embedded in Roti®-Histokitt II.

#### 3.2.8.6 Histochemical *in situ* hybridization of larval tissues

For *in situ* hybridization brains of wildtype OregonR-S larvae were dissected and fixated as described previously. In methanol stored brains were transferred stepwise back into PBT. Therefore, they were inverted for five minutes in 70% and then in 30% of methanol. Then washing steps with 0.5 PBT, twice for fifteen, twice for thirty and once for sixty minutes were performed. The following steps were carried out in a water bath at 65°C. The tissues were transferred stepwise into Hybe solution by first mixing them carefully in 250 µl HybeB with 250 µl 0.5% PBT, then in 500 µl HybeB and afterwards in 250 µl HybeB with 250µl of Hybe. The tissue was washed in 500 µl of Hybe to remove residual HybeB and prehybridized in 250 µl Hybe for one hour. After prehybridization, most of the Hybe solution was discarded. A volume of 5 µl of a RNA antisense probe was added. For a control staining a RNA sense probe was used. The hybridization occurred over night at 65°C.

Unbound RNA probes were mostly washed away by Hybe. After that, 500 µl of fresh Hybe solution was added for posthybridization at 65°C for one hour. Then the tissues were transferred stepwise back into PBT. Therefore, it was first carefully mixed in 250 µl of Hybe

with 250 µl of HybeB, then in 500 µl of HybeB, and afterwards in 250 µl of HybeB with 250 µl of PBT. Then washing steps at room temperature in PBT were performed twice for fifteen minutes, twice for thirty minutes and once for one hour. Binding sides of proteins that could be bound unspecific by the alkaline phosphatase coupled antibody were blocked by inverting the tissues in PBT with 5% of goat serum for one hour. Then the alkaline phosphatase (AP) coupled antibody against digoxigenin was added 1:1000 to the tissue in PBT with 5% of goat serum. Probes were inverted at 4°C overnight on a rotation disc to bind the digoxigenin coupled RNA probes. Unspecifically bound antibody was removed by washing the tissue in 0.5 PBT twice for fifteen minutes and twice for thirty minutes. Thereafter, the probes were incubated in AP-buffer for ten minutes and transferred into dissection dishes. The staining was performed in the dark at room temperature. Therefore, 1 ml AP buffer with 3.5 µl X-Phos and 4.5 µl NBT buffer were added to the tissue. As soon as appropriate color intensity was reached, the staining reaction was stopped. Therefor the staining solution was discarded and the tissues were washed in PBT twice for fifteen, twice for thirty minutes and once for one hour. The probes were dehydrated by inverting them for five minutes in 30% ethanol, five minutes in 70% ethanol and five minutes in 100% ethanol. The tissue was embedded in Roti®-Histokitt II on a slide and fixed with a cover glass. Stainings were analysed after at least one day.

#### 3.2.8.7 Fluorescence *in situ* hybridization of larval brains

Florescence *in situ* hybridization (FISH) increases the staining intensity of RNA probes by a fluorescence signal. It was used to compare the *dopa decarboxylase* RNA availability in the larval brain upon upregulation and downregulation of TOR signalling. The *ddc* RNA probes were provided by Rüdiger Bader. The staining was performed according to the protocol provided by the TSA™-Plus Fluorescein System of Perkin Elemer™.

Brains were prepared and hybridized with the RNA probe as described for the histochemical *in situ* hybridization. Instead of an anti-digoxigenin alkaline phosphatase coupled antibody, a horseradish peroxidase (POD) coupled antibody was used 1:1000. After washing the antibody treated tissue, the PBT was discarded and remaining PBT was removed by letting the brains sink down in 150 µl of Tyra solution. Then, brains were incubated in 400 µl of Tyra solution for ten minutes. The staining reaction was performed in the dark by adding 500 µl of Tyra with 4 µl of Tyramide, the substrate of the horseradish peroxidase. After reaction, the tissue was washed in 0.5% PBT twice for fifteen minutes, twice for thirty minutes and once for one hour in the dark. The brains were embedded in Mowiol on a slide and fixed with a cover glass. They were dried for at least two days in the dark before staining analysis.

#### 3.2.8.8 Antibody staining of larval brains

Antibody staining was used to visualize the Path-Gal4 expression pattern and to identify its colocalization with different cell types of the brain. Furthermore, it was used to determine the amount of serotonin and the serotonin producing enzyme Tryptophan hydroxylase by the intensity of the fluorescence signal.

Therefor, brains of third instar *Drosophila melanogaster* larvae were dissected in PBS and fixated as previously described. All of the following steps were performed inverting the tubes by a rotation disc. Before using the brains for antibody stainings, they were transferred from methanol into 0.5 % PBT by inverting them in 70% and 30% methanol for 10 minutes. The residual methanol was washed away by inverting the brains in PBT twice for 15 minutes, twice for thirty minutes and once for one hour. After washing, the probes were rotated with 0.5% goat serum in 0.5 PBT for one hour to block the antigens of the tissue. This way, unspecific binding of the primary antibody of interest was reduced. The blocked probes were incubated with the primary antibody in 5% goat serum over night at 4°C. At the next day, the brains in the antibody solution were incubated for another hour at room temperature. The unbound or unspecific bound primary antibody was washed away by 0.5% PBT twice for five, fifteen and thirty minutes and once for an hour. Tissues were blocked again for one hour in 0.5 PBT with 5% goat serum. Brains were then incubated with the secondary antibody overnight in 0.5 PBT with 5 % goat serum at 4°C. The secondary antibody was used in a dilution of 1:500 and the tubes were wrapped with aluminium foil to keep them in the dark and to protect the fluorophore from decay. The secondary antibody was washed away the next day by 0.5% PBT twice for fifteen minutes, for one hour and once for two hours and also over night at 4°C on a rotation disc. The tissue was embedded in Mowiol and fixed by a cover glass on a slide. They were dried for at least two days, before analysing the stainings by a confocal laser scanning microscope,

### 3.2.9 Quantitative fluorescence analysis of Trh and Serotonin antibody staining

Differences in the amount of Tryptophan hydroxylase or serotonin upon TOR signalling manipulation in serotonergic neurons were analysed. Therefor, antibody stainings were performed and the fluorescent signals of the different serotonergic clusters in the brain were measured. Stainings were performed on 96+/-2 hour old third instar larvae of the crosses Trh-Gal4>Wt, Trh-Gal4>UAS-TSC1; UAS-TSC2, Trh-Gal4>UAS-Rheb and Trh-Gal4>UAS-Path that were reared on yeast paste. Their brains were treated with α-Trh-antibody (1:500) and α-serotonin-antibody (1:1000). The brains were scanned at least two days after

embedding using a confocal microscope with a 25x objective and a 0.7 magnification. Parameters for laser intensity, aperture, master gain and stack dimensions were always equal. The adjustments and recording of the brain stacks was performed and controlled using the Zen software. The fluorescence signal of Trh and serotonin in the serotonergic clusters was measured via Fiji software. Fluorescence quantification was modified from Géminard et al in 2009. Thereby, the maximum intensity instead of summed intensity was used for measurements. The cluster area was included in the calculations to prevent position effects.

The LSM files containing the brain scans were opened in Fiji [File→Open...] and a Z-stack was produced [Image→Stacks→Z-Project...] containing the maximal intensity signals of all slices (Max Intensity). Each cluster was marked individually using the freehand selection tool. The marked area, the mean gray value of the area and the integrated density were measured [Analyse→Measure]. Around each cluster three background areas were marked and measured as a mean background signal. The data for *Area; Mean; IntDen* was extracted from the results window and transferred to Exel.

As cells or neurons could have been scanned in different positions dependent on how the brains were embedded, the measured area differed between different brain clusters. Thus, a smaller area resulted in a higher mean signal distribution while a larger area resulted in a lower signal distribution though the total amount of signal was the same. To prevent such position effects, the marked area was included into the calculation as published by Nagarajan et al in 2014 and Madeira et al in 2015. For each cluster, the corrected total cell fluorescence (CTCF) was calculated.

***CTCF= Integrated Density - (Area of the selected cluster x Mean fluorescence of background readings)***

Cluster CTCF of brains with manipulated TOR signalling in the serotonergic neurons was compared to a control without TOR manipulation (Trh>Wt) by unpaired two tailed Student's t- test with Welch correction. For statistical tests the GraphPad Prism software was used.

## 3.2.10 Analysis of the triacylglyceride level in third instar larvae

#### 3.2.10.1 Thin layer chromatography

Thin layer chromatography (TLC) was used to analyse the triacylglyceride (TAG) level of larvae with activated and deactivated TOR signalling pathway in serotonergic neurons. The TAG level was determined upon yeast feeding but also upon starvation to detect differences in fat metabolism. Three larvae of the crosses Trh-Gal4>Wt, Trh-Gal4>UAS-TSC1;UAS-

TSC2, Trh-Gal4>UAS-Rheb and Trh-Gal4>UAS-Path were shock frozen by liquid nitrogen. Probes were homogenized in 150 µl double distilled water. To ensure an analysis of equal probe sizes, a protein measurement was performed. Therefor, the BCA kit was used according to the instructions of the corresponding manual.

For thin layer chromatography, lysates with the same amount of protein were used in a volume of 100 µl. They were vortexed with 375 µl of a chloroform/methanol (1:2) mixture. Then 125µl chloroform and the same amount of water was added and vortexed with the lysate mixture. The emulsion was centrifuged for phase separation. The lower phase was transferred into a new tube. The purified lipids were dried in a speedvac centrifuge at 45°C for around 40 minutes. Meanwhile 100 ml of a running solvent (70:30:1 n-hexane: diethylether: acetic acid) was prepared in a glass chamber. A lid was placed on the chamber to keep the vapours back. A HPTLC Silica gel 60 plate was marked with 0.5 cm spacers between 0.5 cm lanes for probe application using a pencil. Also 1.5 cm space to the bottom and to the sides was left.

The dried lipids were dissolved in 10 µl of a chloroform/methanol mix (1:1) and distributed carefully on the prepared lanes of the silica gel plate. Triacylglycerides, cholesterolester, or olive oil standards were used. Then the silica gel plate was placed into the prepared running solvent in the glass chamber for lipid separation. The plate was removed and dried at room temperature after migration had finished. Meanwhile, a bath of 10% copper sulphate and 8% phosphoric acid in aqua bidest was prepared. The dried silica plate was added carefully into the bath for around 30 seconds until bands were visible. It was dried standing for one hour. To visualize the separated lipids, the plate was placed into an oven preheated to 180°C on top and bottom heating for around 5 minutes. Before scanning and analysing the bands of the different feeding and TOR signalling conditions, the plate was left to cool down.

#### 3.2.10.2 Measurement of the protein concentration in lysates by BCA-Assay

Protein measurement of tissue lysates was performed using the BCA kit according to the instructions of the corresponding manual. Triplets of water controls, the standards and the probes were pipetted to the kit reagents in a total volume of 10 µl into a 96 well culture plate. Of each homogenized sample 2 µl were used for protein measurement and filled up to 5 µl with double distilled water. The standards were used in a seven step dilution series of 1:2 with double distilled water. The culture plate was incubated for 25 minutes at 37°C for colour reaction. For the colorimetric determination of the protein concentration a plate reader was used. Plotting and application of the standard curve and the calculation of the protein concentration in the probes was performed with Microsoft Exel.

#### 3.2.10.3 Analysis of TAG band intensity

The scanned silica gel plate, containing the separated TAG bands, was analysed by Fiji software. Therefor the bands were marked with the Rectangle tool [shortcut key: Strg1] using the same selection parameters [shortcut key: Strg2] for all bands. The relative weight of the grey value was determined in the selections using the wand tracing tool. For each selection, the threshold was set at the background grey value. The resulting grey value data was transferred to GraphPad Prism for further analysis.

## 3.3 Statistical analysis

Statistical tests were performed using the GraphPad Prism software.

### 3.3.1 Unpaired two tailed Students t-test

An unpaired two tailed Student's t- test was used to compare the means of two independent groups with equal variances and samples that are normal distributed. The unpaired t-method tests the null hypothesis that the means of these groups are equal. The alternative hypothesis suggests a difference of the group means. The t-test is used to determine a p-value. The null hypothesis is rejected in favour of the alternative hypothesis if the determined p-value is below the threshold of 0.5 for a statistical significance. Not significant: $p \geq 0.5$. Significant: $p < 0.05$; *. Very significant: $p < 0.01$; **. Extremely significant: $p < 0.001$;***. Extremely significant: $p < 0.0001$;****. If unequal variances were assumed, a Welch's correction was performed additionally (GraphPad Statistics Guide).

### 3.3.2 Log rank test

The logrank test was used to compare two groups of survival curves. It tests the null hypothesis that the survival times of these groups are equal. The alternative hypothesis suggests a difference of the survival times. The null hypothesis is rejected in favour of the alternative hypothesis if the determined p-value is below the threshold of 0.5 for a statistical significance (Goel et al, 2010). Not significant: $p \geq 0.5$. Significant: $p < 0.05$; *. Very significant: $p < 0.01$; **. Extremely significant: $p < 0.001$;***. For calculation medians of repeated survival experiments were used.

# 4 Results

## 4.1 Analysis of the amino acid dependent regulation of *tobi* expression

The nutrient dependent regulation of α-glucosidases in *Drosophila melanogaster* was previously investigated in the context of a diploma thesis (Hübner, 2010). The focus was on the transcriptional regulation of the α-glucosidase *tobi* by amino acids. This investigation was based on previous results by Buch et al. in 2008. Those showed a regulation of *tobi*, which was dependent on the amount of protein ingested with the food. It remained unclear whether proteins or their building blocks, the peptides or amino acids, were responsible for this effect. Results gained from the diploma thesis indicated that the ingestion of single amino acids induced *tobi* transcription. Though the impact was very low compared to the effect caused by the ingestion of yeast. Upon yeast feeding also a gender specific regulation of *tobi* transcript level was observed. Thereby, females showed a higher transcript level of *tobi* in the head compared to male flies. Some amino acids also showed a down regulating effect on *tobi* transcript level when used in higher concentrations. It was assumed that this effect was due to intoxication caused by amino acid imbalance (Hübner, 2010).

The amino acid composition of the hemolymph is dependent on nutrition, gender and age (Cônsoli and Vinson, 2002; Hrassnigg et al., 2003). Therefore, it was suggested that the amino acid composition in the hemolymph might be responsible for the observed effects on *tobi* transcription. The transport of single amino acids and peptides was assumed to be involved in the regulation of target genes like *tobi*. To confirm that the composition and transport of amino acids is important for a high induction of *tobi* expression, further experiments were performed for this thesis.

### 4.1.1 Analysis of *tobi* regulation by nutritional amino acid composition

In nature *Drosophila melanogaster* feeds on yeast that grows on rotten fruits (Becher et al, 2012; Begg and Robertson, 1948). Yeast is a protein source with an amino acid composition different from other protein rich food sources. It contains a high amount of essential amino acids (Csonka, 1935). Extracts or peptones of protein sources contain mostly peptides and single amino acids. They differ in their amino acid composition dependent on their protein source (See Appendix Table 8.2). To demonstrate that the transcript level of *tobi* is dependent

on the amino acid composition of the food, flies were fed on food sources with different amino acid compositions. Therefore food with extracts or peptones of different protein sources was used. The expression of *tobi* was analysed in head fat bodies of adult flies. For analysis the whole heads were used.

A *tobi* expression in the female head

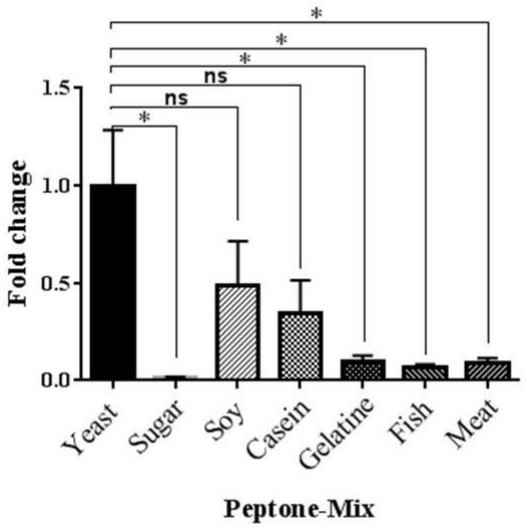


B t-test

*tobi* expression in the female head

| Yeast vs. | p-value |
|---|---|
| **Sugar** | p=0.0259; * |
| **Soy** | p=0.2003; ns |
| **Casein** | p=0.0922; ns |
| **Gelatine** | p=0.0340; * |
| **Fish** | p=0.0305; * |
| **Meat** | p=0.0326; * |

**Figure 4.1 *Tobi* expression analysis upon feeding different peptone mixes**
*Tobi* expression was analysed in the head fat body of female adults. Therefore, whole heads were used. Data was normalized to the yeast condition. *Tobi* expression upon yeast peptone feeding was compared to the *tobi* expression upon feeding on the other peptone mixes. The highest expression was observed upon yeast peptone feeding. (A). Unpaired 2-tailed Student's t-test with Welch correction was used to analyse the data for significant differences (B). N=5. Not significant (ns): $p>0.5$; *: $p\leq0.05$. The Error bars represent the standard error of the mean (SEM). Significant differences were obtained for sugar and gelatine, fish and meat peptone feeding.

In Figure 4.1 it is shown that *tobi* expression in the head of female fruit flies is highest, when a yeast peptone mix is offered to the flies as food source. Peptone mixes of fish, meat or gelatine are no food sources for *Drosophila melanogaster* in nature. Feeding of those peptones led to a very low *tobi* expression. Also soy and casein peptone showed the tendency to induce *tobi* transcription less than yeast peptone in every experiment. Feeding on a sugar agar mix without amino acids and peptides led to a reduction of *tobi* expression compared to the other food sources. Accordingly, upon amino acid deficit *tobi* transcript level is low and upon optimal amino acid availability it is increased. Hübner showed in 2010 that upon yeast feeding *tobi* expression level is highly increased in female flies while the increase in male flies is moderate. It was assumed that amino acid compositions in male and female fly hemolymph differ due to the different demands of the genders. These differences might lead to a dissimilar regulation of target genes. Further feeding experiments were performed to determine whether different amino acid sources affect *tobi* transcription gender dependent.

### 4.1.2 Analysis of *tobi* expression level in male and female flies upon feeding on different amino acid sources

The metabolic needs of male and female flies are different. Therefore, also the food preference and consumption might differ. Female flies have a high need in protein because of egg production while male flies have a higher need in sugars as they spend more energy for the search for females, for courtship and aggression behaviour towards rivals (Magwere et al, 2003; Yuan et al, 2014). Due to the difference in the requirement of the sexes, the amino acid composition in the hemolymph might be different upon feeding on the same food.

A *tobi* expression in the adult head

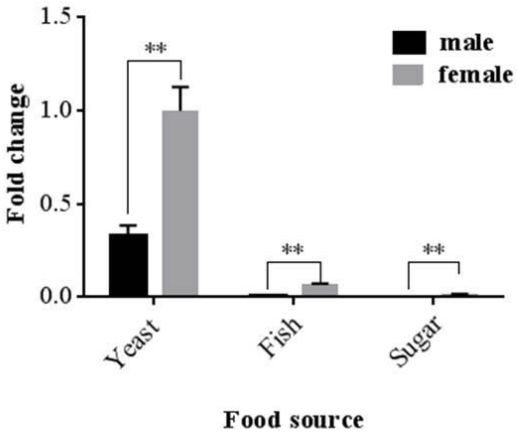


B

t-test

*tobi* expression in the adult head

| Male vs. female | p-value |
|---|---|
| **Yeast** | p=0.0039; ** |
| **Sugar** | p=0.0043; ** |
| **Fish** | p=0.0013; ** |

C *tobi* expression in the adult head

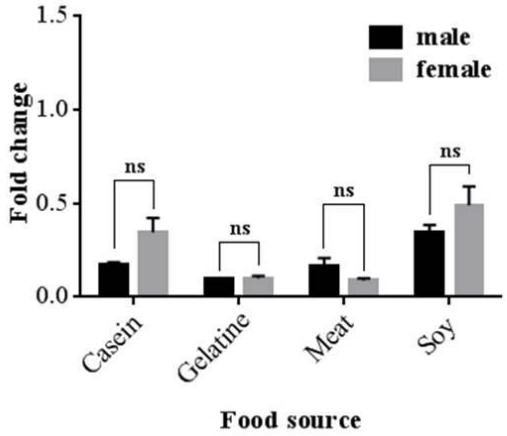


D

t-test

*tobi* expression in the adult head

| Male vs. female | p-value |
|---|---|
| **Casein** | p=0.0791; ns |
| **Gelatine** | p=0.7098; ns |
| **Meat** | p=0.1937; ns |
| **Soy** | p=0.2379; ns |

**Figure 4.2 Differences of *tobi* expression in the head of male and female flies.**
Adult OregonR-S flies were kept on a peptone or sugar mix for two days. *Tobi* expression was compared in the heads of male and female flies. Data was normalized to the yeast condition of females. Unpaired 2-tailed Student's t-test with Welch correction was used to analyse the data for significant differences. Significant differences were obtained for yeast peptone, fish peptone and sugar feeding (A, B). Feeding with other food sources did not result in a significant difference of *tobi* expression in male and female flies (C, D). N=5. Not significant (ns): $p>0.05$;*: $p\leq0.05$.; **: $p\leq0.01$. The error bars represent the standard error of the mean (SEM).

This might lead to a dissimilar nutritional status and a different regulation of target genes like *tobi* (Hübner, 2010). It was not identified yet whether the gender dependent difference of the *tobi* expression is due to the internal composition of amino acids. Therefore, male and female flies were fed with peptone mixes of protein sources with different amino acid compositions. Gender specific differences were identified upon feeding on certain food sources. It could be shown that female and male flies induce *tobi* expression differently upon feeding on a yeast peptone, sugar or fish peptone mix. Females showed a higher *tobi* induction than males feeding on these food sources while other amino acid sources could not induce a gender specific difference in the expression (Figure 4.2). It was unclear whether the amino acid or the peptide compositions in yeast peptone and fish peptone were responsible for a higher *tobi* expression in the female fly. Therefore, *tobi* expression in the adult head was analysed upon feeding on yeast peptone, fish peptone and their corresponding single amino acid mixes.

### 4.1.3 Analysis of peptide and single amino acid composition dependent *tobi* regulation

The peptone mixes contain not just single amino acids but also peptides. Peptides or the same amount and composition in terms of single amino acids are taken up by different transport mechanisms (Matthews, 1987; Webb 1990). Therefore, there might be a difference in the final hemolymph amino acid composition dependent on the ratio of peptides and single amino acids in the food. To determine whether such a difference occurred and affected *tobi* expression, the effect of certain peptone food mixes was compared to the effect of their corresponding single amino acid food mixes. For comparison yeast peptone and fish peptone were chosen. Both of these extracts were able to induce a sexual dimorphism in *tobi* expression while other peptones could not trigger such an effect (Figure 4.2 A).

The *tobi* transcript level, upon feeding on yeast peptone and the corresponding amino acid mix, differed exceedingly. The expression of *tobi* was highest upon feeding the flies with a yeast peptone mix while a single amino acid mix with the same composition could not trigger the transcript level the same way. Fish peptone and the corresponding amino acid mix showed no significant difference on the induction of *tobi* transcription in females (Figure 4.3 A, B). Nevertheless, in male heads the amino acid mix triggered a higher *tobi* transcription than the fish peptone mix. This way, it was shown that the availability and composition of peptides are involved in the high induction of *tobi* expression by yeast peptone (Figure 4.3). Additionally, it was shown that the gender dependant *tobi* expression differs upon the same amino acid and peptide compositions.

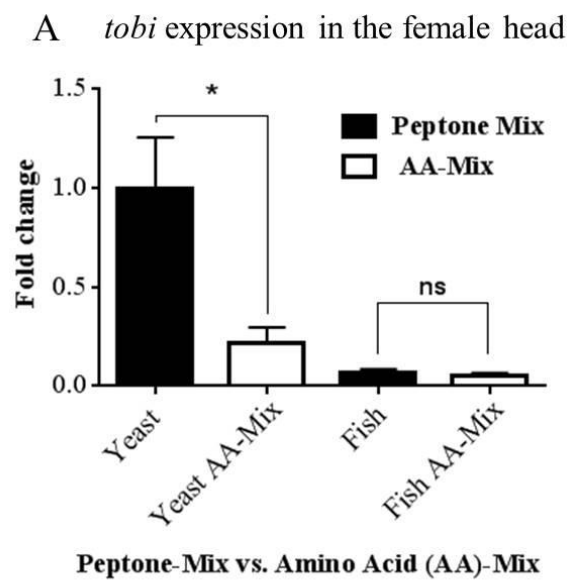


B

t-test

*tobi* expression in the female head

| | p-value |
|---|---|
| **Yeast vs. Yeast AA-Mix** | p=0.0497; * |
| **Fish vs. Fish AA-Mix** | p=0.6382; ns |

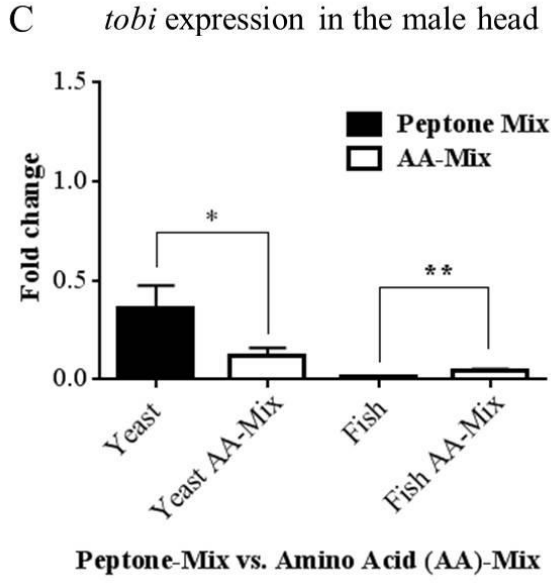


D

t-test

*tobi* expression in the male head

| | p-value |
|---|---|
| **Yeast vs. Yeast AA-Mix** | p=0.0172; * |
| **Fish vs. Fish AA-Mix** | p=0.0064; ** |

**Figure 4.3 *Tobi* expression analysis upon feeding a peptone mix or the corresponding single amino acids.**

Adult OregonR-S flies were kept on a peptone or amino acid (AA) mix for two days. *Tobi* expression was analysed in the heads of females (A, B) and males (C,D). *Tobi* expression upon yeast and fish peptone feeding was compared to *tobi* expression upon feeding on the corresponding amino acid mixes. Data was normalized to the female yeast peptone sample. Unpaired 2-tailed Student's t-test with Welch correction was used to analyse the data for significant differences. (A, B) N=5. (C, D) N=4. Not significant (ns): $p>0.05$; *: $p\leq0.05$; **:$p\leq0.01$. The error bars represent the standard error of the mean (SEM).

It is uncertain whether peptides are able to signal and provide nutritional information on their own. They affect the internal amino acid composition and the concentration of single amino acids after uptake into the hemolymph. Hübner showed in 2010 that single amino acids are able to induce *tobi* transcription. It was assumed that a composition of single amino acids triggers amino acid signalling and target gene expression. Also the amount of certain amino acids in the food could be involved in the regulation. It was not shown yet whether single

amino acids can induce *tobi* expression dependent on their amount in the food. Therefore, it was examined whether single amino acids can induce *tobi* expression concentration dependent. Additionally, gender dependent expression differences were analysed. It was of interest whether the dimorphism discovered for yeast peptone, fish peptone and upon amino acid starvation could be induced by a single amino acid.

### 4.1.4 The single amino acid glycine affects *tobi* expression in a concentration dependent manner

In a screen for amino acids with an inducing effect on *tobi* transcript level the amino acid glycine has been identified as a possible effector (Hübner, 2010). This inducing effect was analysed further by using different concentrations of glycine in an agar mix that was offered as food source to the flies.

A *tobi* expression in the adult head

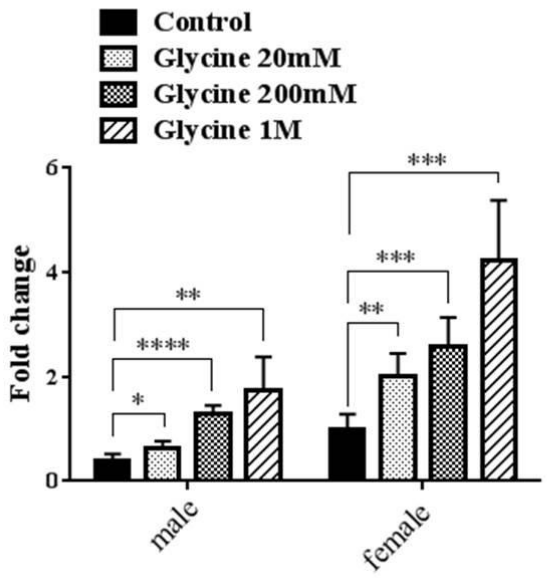


B t-test

*tobi* expression in the adult head

| Control vs. glycine | p-value (males) | p-value (females) |
|---|---|---|
| 20mM | p=0.0104; * | p=0.0012; ** |
| 200mM | p<0.0001; **** | p=0.0005; *** |
| 1M | p=0.0030; ** | p=0.0007; *** |

| Male vs. female | p-value |
|---|---|
| Control | p=0.0021; ** |
| 20mM | p=0.0003; *** |
| 200mM | p=0.0021; ** |
| 1M | p=0.0017; ** |

**Figure 4.4 *Tobi* expression analysis upon feeding food mixes containing different concentrations of the single amino acid glycine.**
Adult OregonR-S flies were kept on an agar food mix with glycine concentrations of 20 mM, 200 mM and 1 M. Control flies were fed with an agar mix without glycine. Expression was analysed in the heads of male and female flies. Data was normalized to to the female control sample. *Tobi* expression upon glycine feeding was compared to the *tobi* expression upon feeding on a food mix without glycine. Also the expression in male and female flies was compared upon the different food conditions (B). Unpaired 2-tailed Student's t-test with Welch correction was used to analyse the data for significant differences. N=6; *:p≤0.05; **: p≤0.01; ***: p≤0.001; ****: p≤0.0001. The Error bars represent the standard error of the mean (SEM).

The expression of *tobi* was analysed in the head of male and female flies to compare the gender specific induction by glycine. It was expected that *tobi* transcript level is induced by high glycine levels and that the induction would differ in its intensity between male and female flies. The results show as expected that an induction of *tobi* expression occurs upon glycine feeding. The induction in the female head fat body is stronger than in the male head fat body but the *tobi* level of the control flies is also higher in females than in males. A significant difference to the control could be determined for the different glycine concentrations. Hence, the ingested glycine concentration in the food induces the transcriptional target *tobi* in male and female flies.

### 4.1.5 *Tobi* induction by glycine is not due to a side effect by stress

In a screen for amino acids that are able to induce *tobi* expression a concentration dependent effect was observed. Many amino acids increase *tobi* transcript level when used in low concentrations while high concentrations decreased it. It was assumed that this effect was caused by stress (Hübner, 2010). Nutritional stress is induced not only upon starvation but also upon an imbalance of nutrients which leads to intoxication (Kolss et al, 2009; Suraweera et al, 2012). An overload of a nutritional component leads to an increased degradation of this component and to the accumulation of toxic metabolites (Dilger and Baker, 2008; Wu, 2009; Heinrichsen et al, 2013). The feeding of single amino acids might cause nutritional stress due to an amino acid imbalance in the hemolymph. The elimination of toxic metabolites is energy-intensive (Rydström, 2006; Castañeda et al, 2009). This might involve the need to release additional glucose from glycogen stores. The release could be mediated by the glucosidase Tobi which was shown to play a role in the glycogen breakdown (Buch et al, 2008). Therefore, the induction of *tobi* expression upon increasing glycine concentration might be due to a higher energy requirement. To control whether intoxication stress has caused an induction of *tobi* expression, male and female flies were fed with different concentrations of hydrogen peroxide. This reagent is widely used to induce oxidative stress (Courgeon et al, 1988; Mocali et al, 1995; Chen et al 2007; Slack et al, 2010; Kumsta et al, 2011).

A *tobi* expression in the adult head

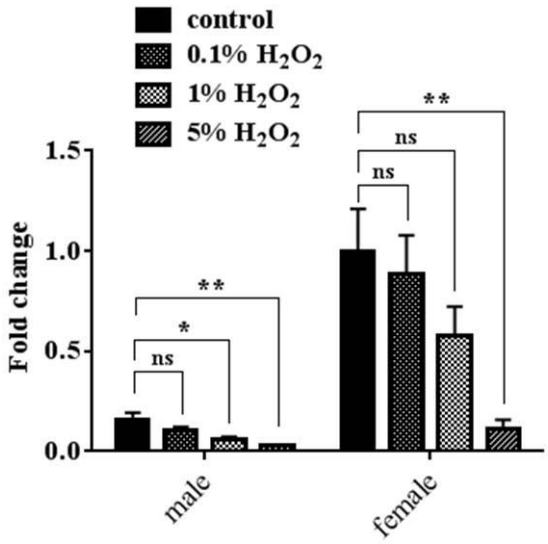


B

t-test

*tobi* expression in the adult head

| Control vs. $H_2O_2$ | p-value (males) | p-value (females) |
|---|---|---|
| **0.1% $H_2O_2$** | p=0.1565; ns | p=0.697 ; ns |
| **0.5% $H_2O_2$** | p=0.0205; * | p=0.1263; ns |
| **5% $H_2O_2$** | p=0.0054; ** | p=0.0052; ** |

**Figure 4.5 *Tobi* expression analysis upon feeding food mixes containing different percentages of the stressor hydrogen peroxide ($H_2O_2$).**
Adult OregonR-S flies were kept on an agar food mix with hydrogen peroxide percentages of 0.1%, 1% and 5%. Control flies were fed with an agar mix without hydrogen peroxide. Data was normalized to the female control sample. Expression was analysed in the heads of male and female flies. *Tobi* expression upon hydrogen peroxide feeding was compared to the *tobi* expression upon feeding a food mix without hydrogen peroxide. Unpaired 2-tailed Student's t-test with Welch correction was used to analyse the data for significant differences. N=7; not significant (ns): $p>0.5$; *: $p\leq0.05$; **: $p\leq0.01$. The Error bars represent the standard error of the mean (SEM).

The results show that the effect of intoxication by hydrogen peroxide leads to a concentration dependent decrease of *tobi* transcript level in male and female flies (Figure 4.5). This effect is opposite to the observed regulation caused by glycine (Figure 4.4).

To identify whether the decrease of *tobi* expression upon oxidative stress might be due to a regulatory effect on glycine transporter transcript level, the transcription of the transporter Pathetic upon hydrogen peroxide feeding was analysed. It was expected that also *pathetic* level is downregulated upon nutritional stress.

A *path* expression in the adult head

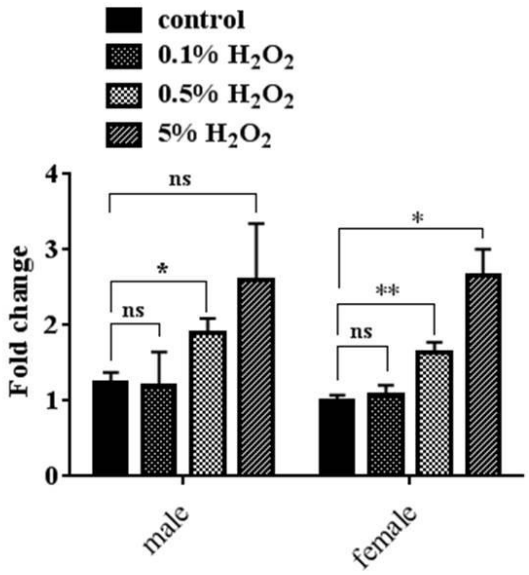


B

t-test

*path* expression in the adult head

| Control vs. $H_2O_2$ | p-value (males) | p-value (females) |
|---|---|---|
| **0.1% $H_2O_2$** | p=0.9119; ns | p=0.6069; ns |
| **0.5% $H_2O_2$** | p=0.0423; * | p=0.0076; ** |
| **5% $H_2O_2$** | p=0.1698; ns | p=0.0161; * |

**Figure 4.6 *Pathetic* expression upon feeding food mixes containing different percentages of the stressor hydrogen peroxide ($H_2O_2$).**
Adult OregonR-S flies were kept on an agar food mix with hydrogen peroxide percentages of 0.1%, 1% and 5%. Control flies were fed with an agar mix without hydrogen peroxide. Expression was analysed in the heads of male and female flies. Data was normalized to the female control sample. *Pathetic* expression upon hydrogen peroxide feeding was compared to the *pathetic* expression upon feeding a food mix without hydrogen peroxide. Unpaired 2-tailed Student's t-test with Welch correction was used to analyse the data for significant differences. N=4; not significant (ns): $p>0.5$; *: $p\leq0.05$; **: $p\leq0.01$. The Error bars represent the standard error of the mean (SEM)

Figure 4.6 shows that *pathetic* is increased upon a rise of hydrogen peroxide in the food while *tobi* transcript is decreased upon the same conditions (Figure 4.5). How *pathetic* transcript level affects *tobi* transcription was analysed further.

## 4.2 Analysis of transceptor function and effect on *tobi* expression

*Tobi* expression is regulated by single amino acids, like glycine. Also the TOR pathway was shown to be involved in its regulation (Buch, unpublished data; Figure 8.4 and Figure 8.5). Glycine might affect *tobi* expression by inducing TOR signalling in *tobi* expressing tissues via transceptors. Transceptors transport amino acids and pass the information of the translocation to signalling pathways like TOR. Therefore, they act as receptors and transporters alike. The expression of transceptors is limited to certain tissues where they induce growth by induction of TOR signalling. Such transporters with receptor function show also an affinity for certain single amino acids (Martin et al, 2000; Colombani et al., 2003; Goberdhan et al, 2005). Accordingly, they are specialized to detect the availability of single amino acids and provide

the cell with nutritional information. The transceptor Pathetic was shown to transport glycine and to signal the transport of this amino acid via the TOR pathway (Goberdhan et al, 2005). Therefore, this transceptor might be involved in the regulation of *tobi* transcript level.

### 4.2.1 Overexpression of the transceptor Pathetic affects *tobi* expression

The transporter Pathetic was shown to have transceptor function and to signal nutritional information via TOR pathway. It has a high affinity for the transport of the small neutral amino acids alanine and glycine (Goberdhan et al, 2005). Therefore, Pathetic seemed to be a potent candidate for the analysis of *tobi* regulation by glycine.

A *path* expression in the larva

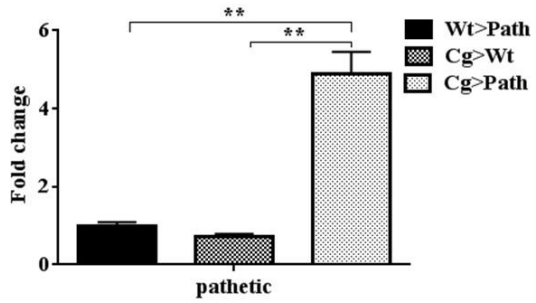


B *cbt* expression in the larva

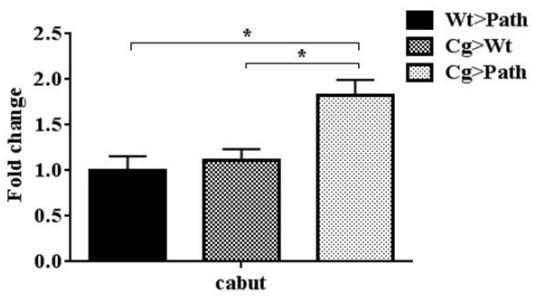


C *tobi* expression in the larva

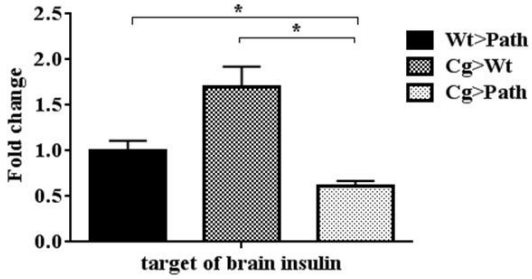


D t-test

Gene expression in the larva

| Cg-Gal4> UAS-Path vs. | *path* | *cbt* | *tobi* |
|---|---|---|---|
| Wt> UAS-Path | p=0.0053; ** | p=0.0129; * | p=0.0327; * |
| Cg-Gal4> Wt | p=0.0045; ** | p=0.0186; * | p=0.0151; * |

**Figure 4.7. Analysis of *tobi* expression in the larva upon upregulation of *pathetic* in the larval fat body.**
Third instar larvae with Pathetic overexpression in the fat body (Cg-Gal4>UAS-Path) and controls without Pathetic overexpression (Cg-Gal4>Wt; Wt>UAS-Path) were fed with *tobi* expression inducing yeast. Expression was analysed in the whole larva. Data was normalized to the Wt>UAS-Path control sample. (A) *Pathetic* (*path*), (B) *cabut* (*cbt*) and (C) *target of brain insulin* (*tobi*) transcript level upon Pathetic overexpression was compared to the expression of the two controls. Unpaired 2-tailed Student's t-test with Welch correction was used to analyse the data for significant differences (D). N=4; *: $p \leq 0.05$; **: $p \leq 0.01$. The Error bars represent the standard error of the mean (SEM).

Pathetic was overexpressed in the larval fat body. Therefore, the Gal4- UAS system was used. The fat body specific driver line Cg-Gal4 was crossed to the effector line UAS-Path to cause a high ectopic *pathetic* expression in the target tissue of the progeny. The expression of *tobi*

was analysed in whole larvae. For control of TOR activity also the expression of *cabut* was documented. *Cabut* is a transcriptional target of Forkhead. The transcription factor Forkhead is active when TOR signalling is downregulated (Bülow et al, 2010). As a result, *cabut* transcript level should be lowered upon a high TOR signalling.

The results show that *tobi* expression is not induced upon Pathetic overexpression in the fat body as expected. In the contrary, it is down regulated compared to the controls. Also *cabut* the marker of Forkhead activity is downregulated and indicates that TOR signalling is lower upon *pathetic* overexpression in the fat body. This way, an effect of Pathetic on TOR signalling and *tobi* expression could be shown.

## 4.3 Analysis of *pathetic* regulation and expression pattern

During early embryonic stages *pathetic* expression is ubiquitously strong. It is still expressed almost in all tissues during development but in later embryonic stages a high transcript level is observed in specialized tissues like the muscle primordia, midgut, proventriculus and salivary glands. In the larva *pathetic* was shown to be expressed in developing tissues like the imaginal discs (Goberdhan et al, 2005).

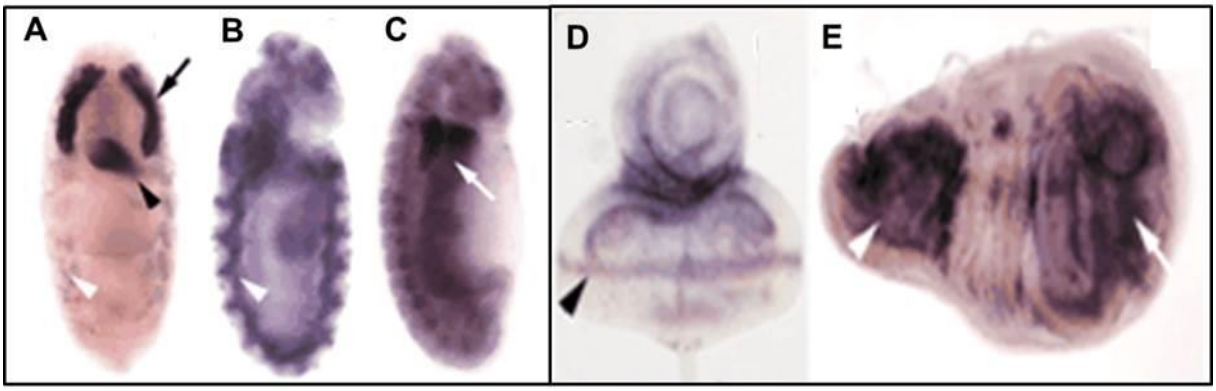


**Figure 4.8 *Pathetic* expression pattern.**
*In situ* hybridization of embryos **(A-C**) and larval imaginal discs **(D-E)** . **(A)** embryonal stage 11, **(B)** stage 13, **(C)** stage 16. High *pathetic* mRNA levels in embryos were found in the muscle primordia (white arrowhead), the proventriculus (black arrowhead), the midgut (white arrow) and the salivary glands (black arrow). **(D)** larval wing imaginal disc, **(E)** larval eye antennal disc. In larvae high mRNA levels were observed in the pouch (arrow) and hinge (arrowhead) regions of the developing wing and at the morphogenetic furrow (arrowhead) in the eye. Modified from Goberdhan et al, 2005

Flyatlas Anatomical Expression Data (http://flybase.org/reports/FBgn0036007.html) for larval tissues illustrates a low expression level of *pathetic* in the tracheae and the malphigian tubules and a moderate expression in the carcass, the midgut, the hindgut and the fatbody. A very high expression level was determined for the salivary glands and especially for the central nervous system.

Transporters and transceptors are involved in the promotion of cell growth and proliferation in developing tissues but in the brain they might affect behaviour as it was shown for the transporters genderblind and white (Grosjean et al, 2008; Zhang and Odenwald, 1995). It is assumed that they are involved in the release of factors modulating behaviour, metabolism and growth of the organism.

Specialized neuronal clusters of the central nervous system, like the insulin producing cells (IPCs), are modulators of behaviour, metabolism and growth. IPCs release Drosophila insulin like peptides (Dilp) to induce insulin signalling in target tissues (Ikeya et al, 2002; Arquier et al, 2008; Zhao and Campos, 2012). Neurotransmitters like octopamine, gamma-aminobutyric acid (GABA), short neuropeptide F (sNPF), corazonin, tachykinin-related peptide and serotonin and also factors released by fat cells collaborate to adjust the release of Drosophila insulin like peptides to the environmental changes and the organismal requirements (Ruaud and Thummel, 2008; Géminard et al, 2009; Nässel et al, 2013). The transceptor Pathetic might be involved in this adjustment by providing the brain with nutritional information.

The transcription pattern and regulation of *pathetic* in the brain has not been analysed yet. To reveal its role in brain function, brain structures in which it is abundant and regulators that affect its expression had to be identified. Therefore, in this thesis the expression pattern and regulation of *pathetic* was analysed by quantitative Real Time Polymerase Chain Reaction (RT-PCR) and antibody staining.

### 4.3.1 Analysis of *pathetic* regulation in the brain by TOR pathway

Several feedback mechanisms were described in the regulation of growth promoting pathways like the TOR and the insulin signalling pathway (Dunlop and Tee, 2009; Kockel et al, 2010; Ivanov et al, 2013). Insulin signalling is induced when insulin binds to its receptor in the target tissues. It provides information about the availability of sugar in the ingested food. During development, it couples this nutritional information to the growth of the organism. However, it also feeds back on the transcript level of the own receptor. In this way, uncontrolled growth is prevented (Shingleton et al, 2005; Puig and Tjian, 2005). TOR signalling couples growth to the availability of amino acids. It is activated via amino acid transport by Pathetic (Goberdhan et al, 2005). This way, it might regulate the transcription and translation of target genes in Pathetic expressing tissues. It was not shown yet whether *pathetic* expression in the brain is regulated by TOR signalling via a feedback mechanism. Hence, *pathetic* transcription was analysed upon rapamycin feeding and sugar and yeast feeding. Rapamycin feeding and amino acid deprivation by sugar feeding supresses TOR

signalling. In larvae, kept under these conditions, a regulation of *pathetic* upon a direct effect of TOR was expected.

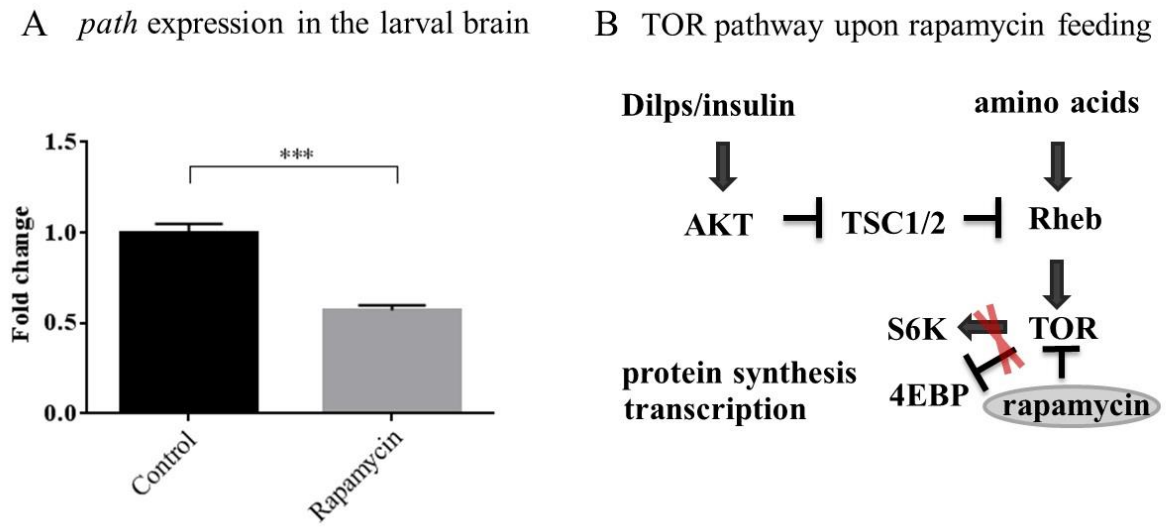


**Figure 4.9 Analysis of *pathetic* expression in the brain of Oregon R-S third instar larvae upon rapamycin feeding.**
Early third instar larvae were fed with yeast containing rapamycin for 24 hours. The control larvae were fed with yeast without rapamycin. Expression was analysed in the larval brain. Data was normalized to the control sample. (A) *Pathetic* (*path*) transcript level upon yeast feeding was compared to the expression upon feeding on yeast with rapamycin. (B) Scheme of rapamycin effect on Target of rapamycin (TOR) pathway. Tuberous sclerosis complex 1 (TSC1).Tuberous sclerosis complex 2 (TSC2). Ras homolog enriched in brain (Rheb). (S6K) S6 kinase. (4EBP) 4E binding protein. (Dilps) Drosophila insulin like peptides. (Akt) Homologue of the retroviral oncogene v-Akt. Unpaired 2-tailed Student's t-test with Welch correction was used to analyse the data for significant differences. N=5; p=0.0002; ***: p≤0,001. The error bars represent the standard error of the mean (SEM).

The rapamycin feeding is downregulating the *pathetic* expression in the brain (Figure 4.9). Nevertheless, in the case of sugar feeding no significant difference to yeast feeding was observed though a tendency of down regulation upon sugar condition was visible in every experiment (Figure 4.10).

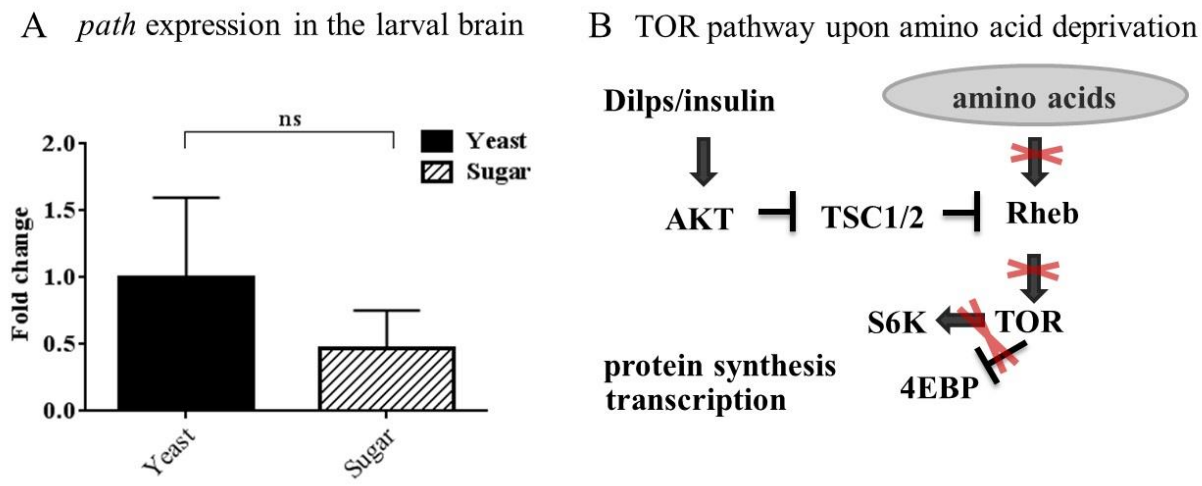


**Figure 4.10 Analysis of *pathetic* expression in the brain of Oregon R-S third instar larvae upon sugar and yeast feeding.**
Early third instar larvae were fed with sugar representing an amino acid deprivation condition for 24 hours. The control larvae were fed with yeast. Expression was analysed in the larval brain. Data was normalized to the yeast condition. *Pathetic* (*path*) transcript level upon yeast feeding was compared to the expression upon feeding on sugar (A). (B) Scheme of amino acid influence on Target of rapamycin (TOR) pathway. Tuberous sclerosis complex 1 (TSC1).Tuberous sclerosis complex 2 (TSC2). Ras homolog enriched in brain (Rheb). (S6K) S6 kinase. (4EBP) 4E binding protein. (Dilps) Drosophila insulin like peptides. (Akt) Homologue of the retroviral oncogene v-Akt. Unpaired 2-tailed Student's t-test with Welch correction was used to analyse the data for significant differences. N=6. p= 0.4956. Not significant (ns): p>0.05. Error bars represent the standard error of the mean (SEM).

Apart from TOR signalling other factors might be involved in the regulation of *pathetic* transcription. Those might also act upon amino acid deficit. It is not known yet in which cells *pathetic* is expressed and whether amino acid deprivation affects TOR signalling in all of these cells equally. To identify those cells, the transcription pattern of *pathetic* was analysed in the brain.

### 4.3.2 *Pathetic* mRNA localisation in the larval brain

The expression pattern of *pathetic* in the brain has not been analysed yet. To find out whether *pathetic* can affect the metabolism and provide nutritional information due to TOR signalling in the brain, the cells in which it is expressed needed to be detected. Therefor RNA antisense and sense probes were produced for *in situ* hybridization analysis. The RNA probe was first tested on embryos to compare the efficiency of the staining with already published data.

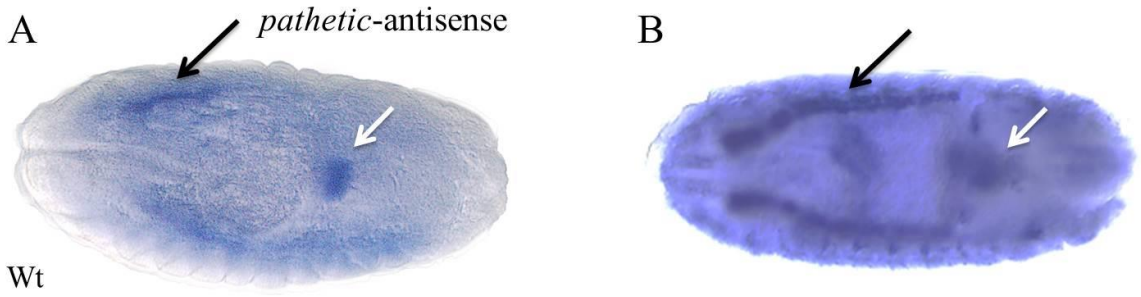


**Figure 4.11. *In situ* hybridisation of the transceptor *pathetic* in embryos.**
(A) *In situ* Hybridisation on a 13-16 stage OregonR-S wildtype (Wt) embryo with a self-generated antisense probe. (B) *In situ* Hybridisation on a 13-16 stage embryo provided by Flyexpress (http://www.flyexpress.net/search.php?type=image&search=FBgn0036007#2) *in situ* hybridization data for *pathetic*. The black arrow marks the salivary gland structure and the white arrow the embryonic midgut. Brightness and contrast were adjusted by Photoshop.

The *in situ* hybridization performed on embryos (Figure 4.11 A) shows the same expression pattern as provided by Flyexpress (Figure 4.11 B). This pattern also matches the *in situ* hybridisation data shown by Goberdhan et al in 2012 (Figure 4.8).

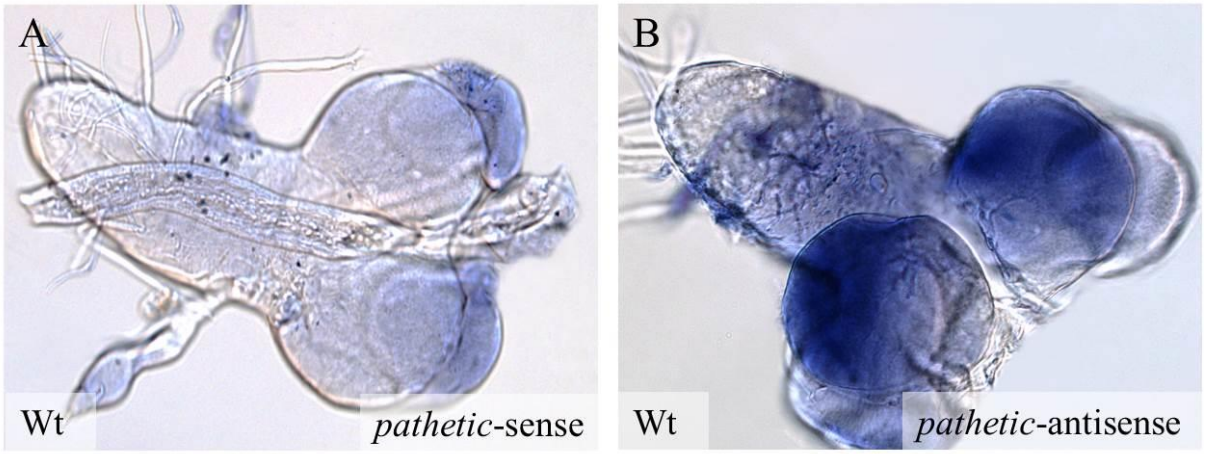


**Figure 4.12. *In situ* hybridization of *pathetic* RNA probes in the larval brain.**
(A) Brain staining with a *pathetic* RNA-sense probe in the wildtype Oregon R-S third instar larva. (B) Brain staining with a *pathetic* RNA-antisense probe in the wildtype Oregon R-S third instar larva. Brightness and contrast were adjusted by Photoshop.

The RNA probe was now used to detect structures of the brain that show a *pathetic* expression. No expression could be visualized in certain neuronal clusters by *in situ* hybridization but a strong expression in the optical lobes was observed.

### 4.3.3 Pathetic-Gal4 expression pattern in the brain

For further analysis of the Pathetic (Path) expression, a Pathetic-Gal4 line was generated. Therefor two different *pathetic* promoter elements were cloned into the pBPGW or the

pBPGUW vector that contains an additional basal promoter. The constructs were used by Bestgene to generate transgenic fruit flies. The flies could express Gal4 under control of a 1.473 kb or 4.818 kb *pathetic* promoter fragment. Transgenic fruit flies containing the larger promoter fragment were not viable. *Drosopila melanogaster* with the pBPGW and the pBPGUW construct showed the same expression pattern. Therefore, a pBPGW line was choosen for further experiments.

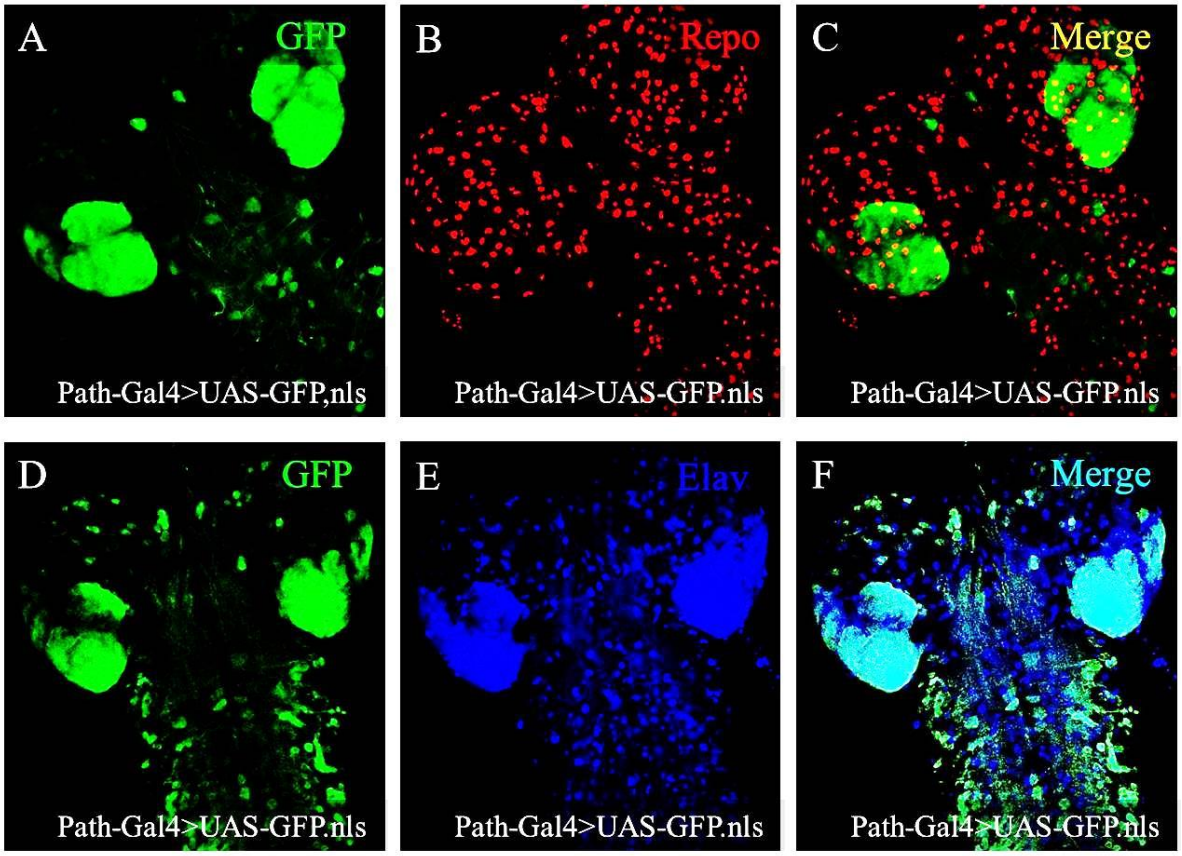


**Figure 4.13 Analysis of the Path-Gal4 expression pattern in the third instar larva brain by antibody staining.**
For expression pattern analysis Path-Gal4 was crossed with the reporter line UAS-GFP.nls. Colocalization with glial cells was analysed using an antibody against the glial cell marker Reversed-polarity (Repo) (A-C) and colocalization with neuronal cells was analysed via an antibody against the neuronal cell marker Embryonic Lethal Abnormal Vision (ELAV) (D-F). Brightness and contrast were adjusted using Fiji.

Homozygous Path-Gal4 flies were used for the analysis of the Pathetic-Gal4 expression pattern. Therefor the Path-Gal4 flies were crossed with the reporter line UAS-GFP.nls. This line expresses GPF under the control of a UAS element. In third instar larvae a strong GFP signal was observed in the salivary glands, the optical lobes and in certain brain cells while a moderate signal in some cells of the gut and in the malphigian tubules could also be detected. These observations match the published data that was described in 4.3.The expression pattern of the brain was analysed further. A GFP signal was observed in the optical lobes as it was

also shown by *in situ* hybridization (Figure 4.12). Besides, in many other cells of the brain a GFP signal was visible (Figure 4.13). To identify the type of cells in which *pathetic* is expressed, marker for different cell types were used during antibody staining. Reversed-polarity (Repo) is explicitly expressed in glial cells and Embryonic Lethal, Abnormal Vision (ELAV) in neurons of the *Drosophila* brain (Xiong et al, 1994; Berger et al, 2007). Therefore, antibodies against Repo and Elav were used as marker for analysis of a colocalisation with the *pathetic* expression pattern. The analysis of the *path* expression in the brain revealed that it is expressed in neurons but not in glial cells (Figure 4.12). Further experiments were performed to identify the neurons in which *pathetic* is expressed.

#### 4.3.3.1 Identification of neurons expressing the transceptor Pathetic

For the identification of Pathetic expressing neurons, Pathetic-Gal4 flies were crossed with the GFP-reporter line UAS-GFP.nls. This way, the cells where Gal4 is expressed under the control of the *pathetic* promoter were marked with a fluorescent signal. The third instar larvae that resulted from these crosses were used for antibody stainings of the brain.

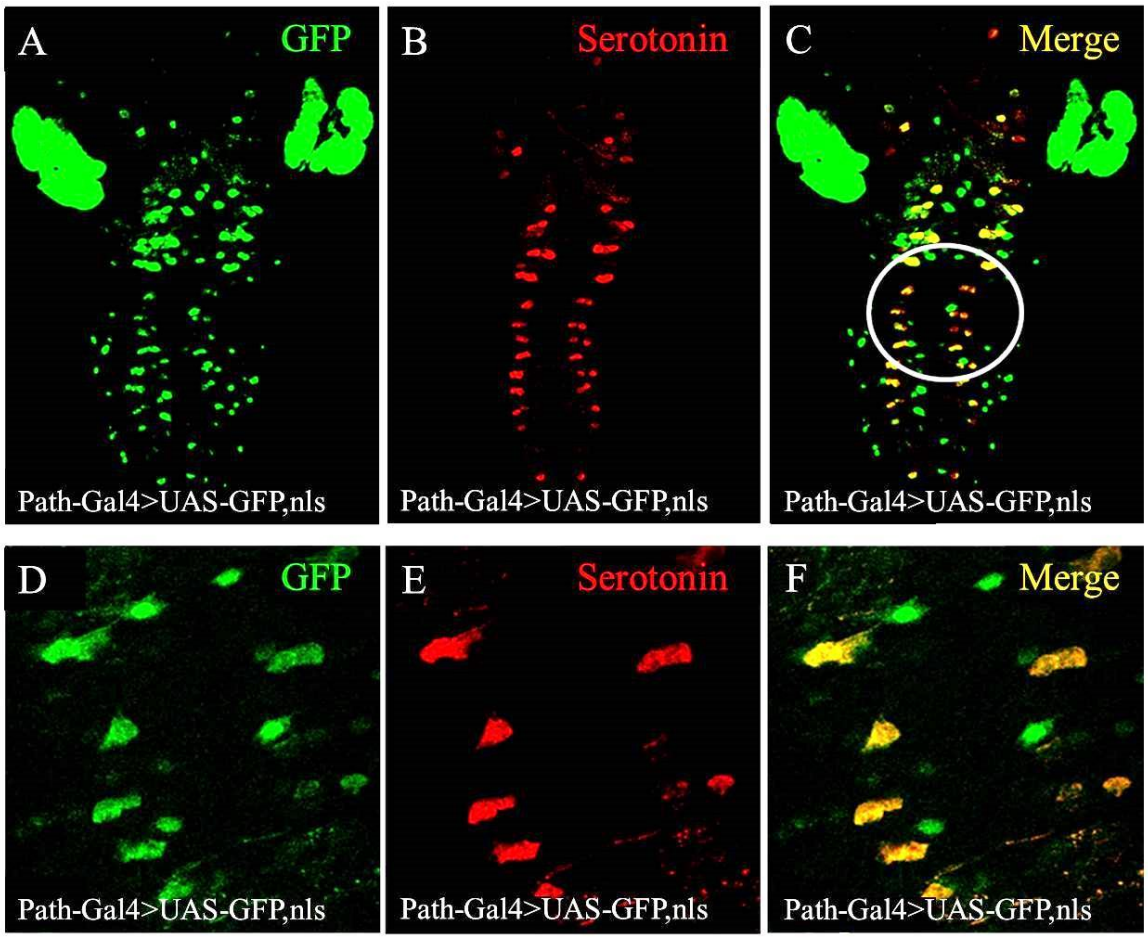


**Figure 4.14 Colocalization of Pathetic-Gal4 with serotonin in the serotonergic clusters.**
For expression pattern analysis Path-Gal4 was crossed with the reporter line UAS-GFP.nls. Colocalization with serotonergic neurons was analysed using an antibody against the neurotransmitter serotonin. (A-C) Staining in the whole third instar larva brain. The further analysed area in (D-F), that

shows the thoracic and abdominal serotonergic clusters, is marked by a white oval (in C). Brighness and contrast were adjusted using Fiji.

For serotonin positive cells, a colocalization with the GFP signal was observed (Figure 4.14). Determined neuronal cells do not grow and proliferate the way other body cells do. Thus, a high expression of an amino acid transceptor like Pathetic with an affinity for glycine and alanine might indicate that TOR signalling has another role in specialized neuronal cells than the promotion of cell growth and proliferation. It was shown that TOR signalling might play a role in neurotransmitter production (Vargas et al, 2010). Then, the pathway is possibly involved in providing the organism with nutritional information in the brain. It was of further interest what kind of function Pathetic and TOR signalling via this transceptor display in serotonergic neurons.

## 4.4 The role of TOR signalling in neurotransmitter production

Vargas et al assumed in 2010 that TOR signalling in the brain might affect the serotonin production. They showed that TOR signalling activation in the brain and the feeding of a serotonin precursor affects food intake in *Drosophila melanogaster* equally. Also in mammals it was observed that the induction of TOR signalling in the hypothalamus or the injection of serotonin into the hypothalamus displays the same effect on food intake (Cota et al, 2006; Leibowitz, 1989; Leibowitz and Alexander, 1998). Therefore, the effect of TOR signalling on transcriptional and translational level of the serotonin producing enzymes was analysed in *Drosophila* larvae. Additionally, the serotonin signal in the brain was analysed upon TOR manipulation in serotonin producing neuronal clusters.

### 4.4.1 Trh expression in the brain upon TOR pathway manipulation

The monoamine neurotransmitter serotonin is derived from the amino acid tryptophan. It is produced via a short metabolic pathway. This pathway consists of two steps catalyzed by two different enzymes. The first reaction is mediated by tryptophan hydroxylase (Trh) that uses the aromatic amino acid tryptophan to produce 5-hydroxy-L-tryptophan (5-HTP). In the second step 5HTP is used by the aromatic-L-amino acid decarboxylase (Ddc) to produce serotonin (Figure 4.15).

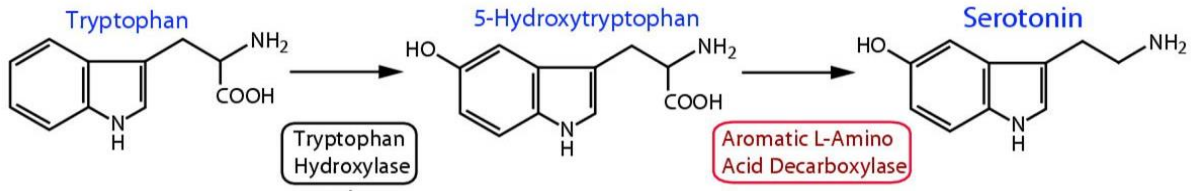


**Figure 4.15 Serotonin production.**
Tryptophan hydroxylase (Trh) uses the amino acid tryptophan to produce 5-hydroxy-L-tryptophan (5-HTP) in a rate limiting step. 5HTP is used by the aromatic-L-amino acid decarboxylase (Ddc) to produce the neurotransmitter serotonin. Modified from Hare and Loer, 2004

TOR pathway manipulation was used to detect a transcriptional or translational regulation of the serotonin producing enzymes. TOR signalling detects amino acid availability and can thereby be modulated via an amino acid rich or amino acid poor nutrition of *Drosophila melanogaster* larvae. Manipulation of TOR pathway is also possible by pharmaceutical components like rapamycin. This inhibitor of TOR pathway binds TOR itself and prevents the kinase function of the enzyme, that way silencing the signalling cascade of the pathway. Another possibility to manipulate the pathway is an ectopic expression of pathway members that regulate the TOR signalling via inhibition or activation of the cascade.

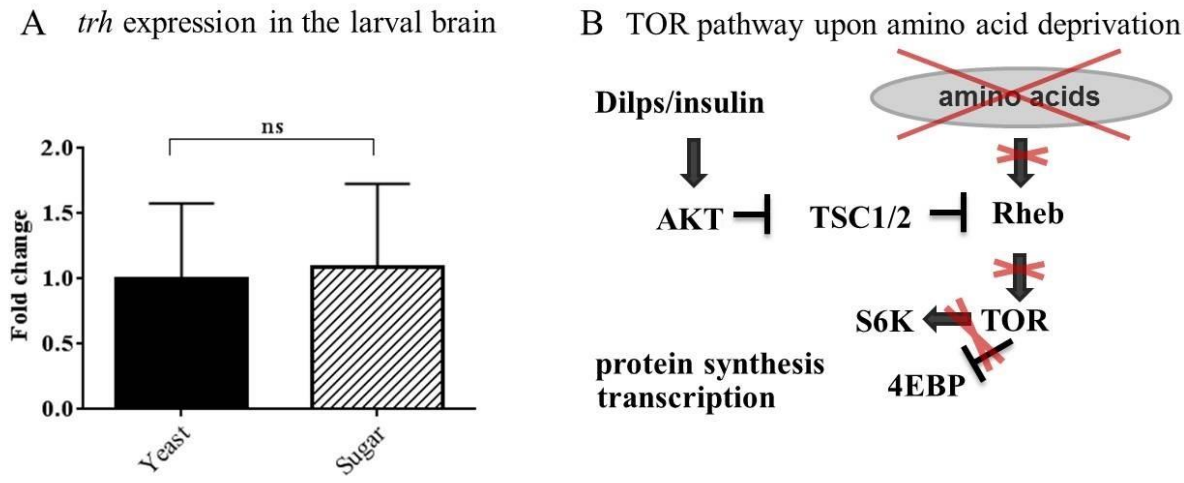


**Figure 4.16 Analysis of *tryptophan hydroxylase* expression in the brain of Oregon R-S third instar larvae upon sugar and yeast feeding.**
Early third instar larvae were fed with sugar for 24 hours. Sugar feeding represents an amino acid deprivation condition. The control larvae were fed with yeast. Expression was analysed in the larval brain. Data was normalized to the yeast condtion. *Tryptophan hydroxylase* (*trh*) transcript level upon yeast feeding was compared to the expression upon feeding on sugar (A). (B) Scheme of Target of rapamycin (TOR) pathway upon amino acid deprivation. Tuberous sclerosis complex 1 (TSC1). Tuberous sclerosis complex 2 (TSC2). Ras homolog enriched in brain (Rheb). (S6K) S6 kinase. (4EBP) 4E binding protein. (Dilps) Drosophila insulin like peptides. (Akt) Homologue of the retroviral oncogene v-Akt. Unpaired 2-tailed Student's t-test with Welch correction was used to analyse the data for a significant difference. N=3. The error bars represent the standard error of the mean (SEM). p= 0.9248; ns: p>0.05.The difference to the control is not significant (ns).

First the transcript level of *trh* was analysed upon sugar and yeast feeding. A higher *trh* expression in larvae fed on yeast was expected if TOR pathway is involved in its regulation. However, no difference between *trh* transcript level in the brain upon sugar and yeast feeding could be distinguished (Figure 4.16). To confirm this result, TOR signalling was downregulated by rapamycin. Therefore, 74+/-2 hours old third instar larvae were fed with yeast containing rapamycin for 24 hours. Control larvae were fed with yeast without rapamycin. The brain transcript level showed that *trh* expression is not affected upon TOR deactivation (Figure 4.17).

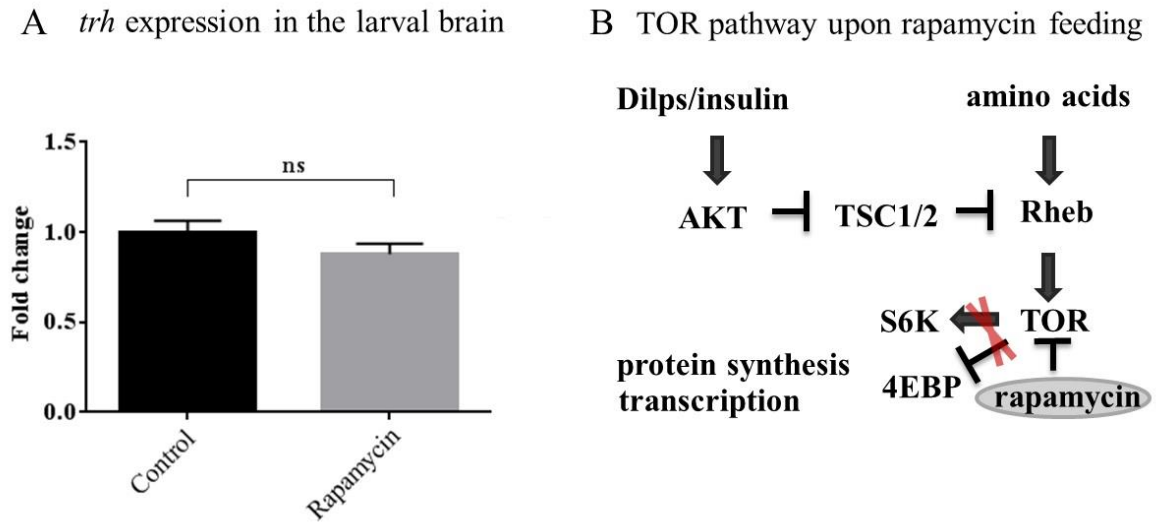


**Figure 4.17 Analysis of *tryptophan hydroxylase* (*trh*) expression in the brain of Oregon R-S third instar larvae upon rapamycin feeding.**
Early third instar larvae were fed with yeast containing rapamycin for 24 hours. The control larvae were fed with yeast without rapamycin. Expression was analysed in the larval brain. *Trh* transcript level upon yeast feeding was compared to the expression upon feeding on yeast with rapamycin (A). (B) Scheme of rapamycin influence on Target of rapamycin (TOR) pathway. Tuberous sclerosis complex 1 (TSC1). Tuberous sclerosis complex 2 (TSC2). Ras homolog enriched in brain (Rheb). (S6K) S6 kinase. (4EBP) 4E binding protein. (Dilps) Drosophila insulin like peptides. (Akt) Homologue of the retroviral oncogene v-Akt. Unpaired 2-tailed Student's t-test with Welch correction was used to analyse the data for significant differences. The error bars represent the standard error of the mean (SEM). N=5; p= 0.1938; not significant (ns): p>0.05

TOR pathway was also manipulated by overexpression of Rheb or TSC1 and TSC2 in Trh positive cells. Therefore, the UAS-Gal4 system was used. Rheb is a GTPase that activates TOR- kinase when GTP bound. TSC1 and TSC2 form a heterodimeric complex that stimulates the GTPase activity of Rheb and the conversion of GTP to GDP. This leads to an inhibition of TOR function. An ectopic overexpression of those pathway components was caused via crosses of Trh-Gal4 and UAS-Rheb or UAS-TSC1; UAS-TSC2 flies. That way, TOR signalling was targeted directly in the Trh producing cells of the offspring. It was expected that larvae of the Trh-Gal4>UAS-Rheb crosses show a higher expression of *trh*

compared to the Trh-Gal4>Wt control larvae if TOR has a direct effect on *trh* regulation. If this would be the case, the Trh-Gal4>UAS-TSC1; UAS-TSC2 larvae should show a lower *trh* expression compared to the control.

A *trh* expression in the larval brain

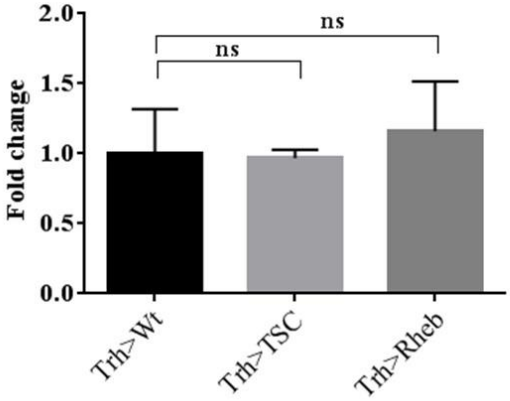


B

t-test

*trh* expression in the larval brain

| Trh-Gal4>Wt vs. | p-value |
|---|---|
| Trh-Gal4>UAS-TSC1/2 | p=0.9332; ns |
| Trh-Gal4>UAS-Rheb | p=0.7523; ns |

**Figure 4.18 Analysis of *tryptophan hydroxylase* expression in the brain of third instar larvae upon manipulation of TOR signalling.**
TOR pathway was manipulated using the Gal4-UAS system. TOR signalling was downregulated in the serotonergic neurons by using the driver line Trh-Gal4 for crosses with UAS-TSC1; UAS-TSC2. An upregulation of TOR signalling was achieved by crossing Trh-Gal4 with UAS-Rheb. As control Trh-Gal4 was crossed with the wildtype strain (Wt) OregonR-S. Expression was analysed in the larval brain. Data was normalized to the control sample. *Trh* transcript level of the control flies was compared to the expression upon TOR signalling activation and deactivation (A). Unpaired 2-tailed Student's t-test with Welch correction was used to analyse the data for significant differences (B). The error bars represent the standard error of the mean (SEM). The differences to the control are not significant (ns). N=3; Not significant (ns): $p>0.05$.

Like the rapamycin and the yeast and sugar feeding, direct TOR activation or deactivation via Rheb or the TSC1 and TSC2 complex in Trh positive cells showed no difference to the control situation (Figure 4.18). Based on these results no direct effect of TOR signalling on *trh* transcript level in the brain could be determined.

### 4.4.2 Trh signal in the brain upon TOR pathway manipulation

TOR signalling is mostly known for its effect on translation by regulation of 4EBP and S6K (Efeyan et al, 2012; Chantranupong et al., 2015). The previous results show no direct effect of TOR on *trh* transcript level but the effect of TOR on translation level still remains unclear. To analyse what kind of effect TOR has on the protein level of Trh, the Gal4-UAS system was used. Upregulation of the pathway was caused by Rheb overexpression and downregulation by TSC1 and TSC2 overexpression in Trh positive cells via Trh-Gal4. A staining with an antibody against Trh was performed and the fluorescence of the fluorophore coupled to the

secondary antibody was measured via Fiji. The fluorescence of the abdominal clusters A1-A9 was not measured as those clusters did not show differences in their signal in previous stainings compared to the controls.

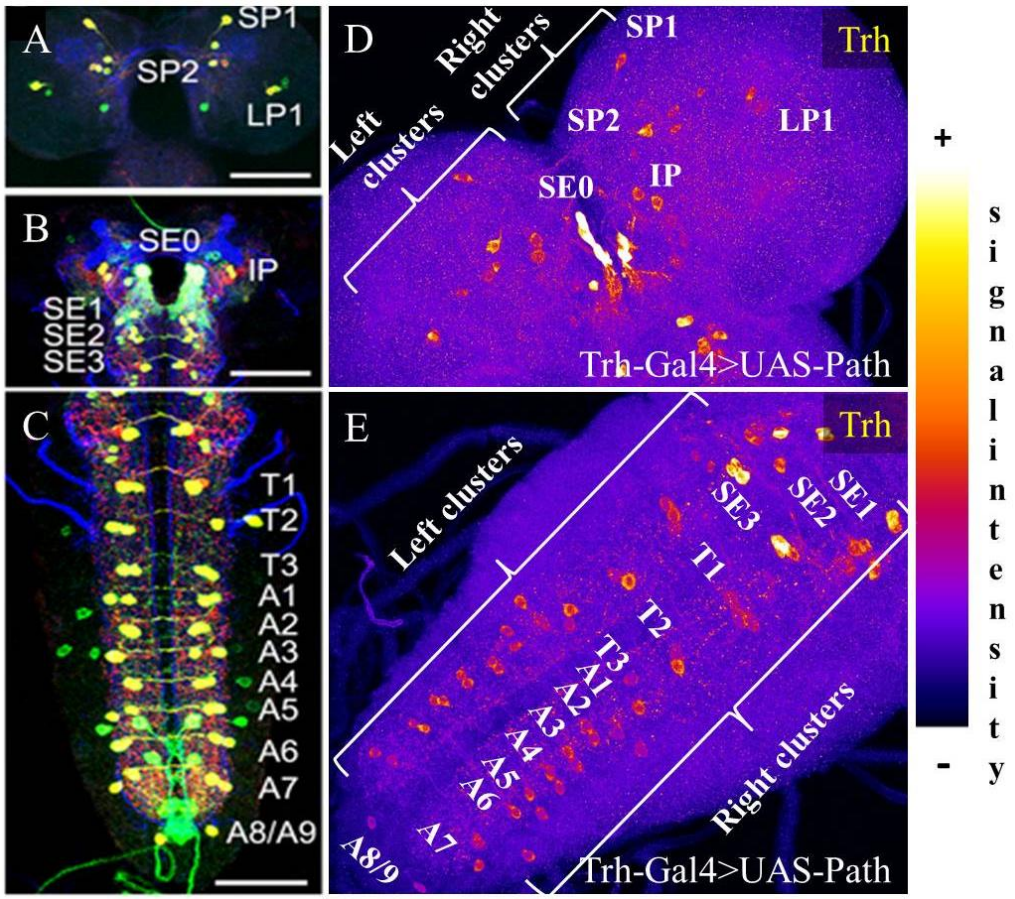


**Figure 4.19 Serotonergic clusters of the larval brain.**
(A), (B) and (C) are modified from Huser et al, 2012. Those images show the serotonergic clusters of the brain in *Drosophila melanogaster* Trh-GAL4/UAS-mCD8::GFP larvae. The anti-FasII/anti-ChAT staining visualizes the neuropil in blue, while the membrane-bound CD8 is labelled in green and the 5HT-immunoactivity in red. The yellow staining shows the merge of the Gal4 expression and the 5HT signal and maps the different serotonergic clusters. (D) and (E) show a staining of a Trh-Gal4>UAS-Path larval brain with a purified Trh antibody, that coincides with the shown serotonergic clusters in the brain in (A)-(C). The increase of signal intensity is visualised from blue to yellow.

The corrected total cell fluorescence of the different serotonergic clusters was determined and data of three brains per three stainings for each of the genotypes Trh-Gal4>UAS-TSC1;UAS-TSC2 and Trh-Gal4>UAS-Rheb and of three brains per two stainings for the genotype Trh-Gal4>UAS-Path were analysed and compared to the corresponding amount of Trh-Gal4>Wt controls. It was assumed that the Trh level changes due to TOR signalling manipulation in all or certain serotonergic clusters.

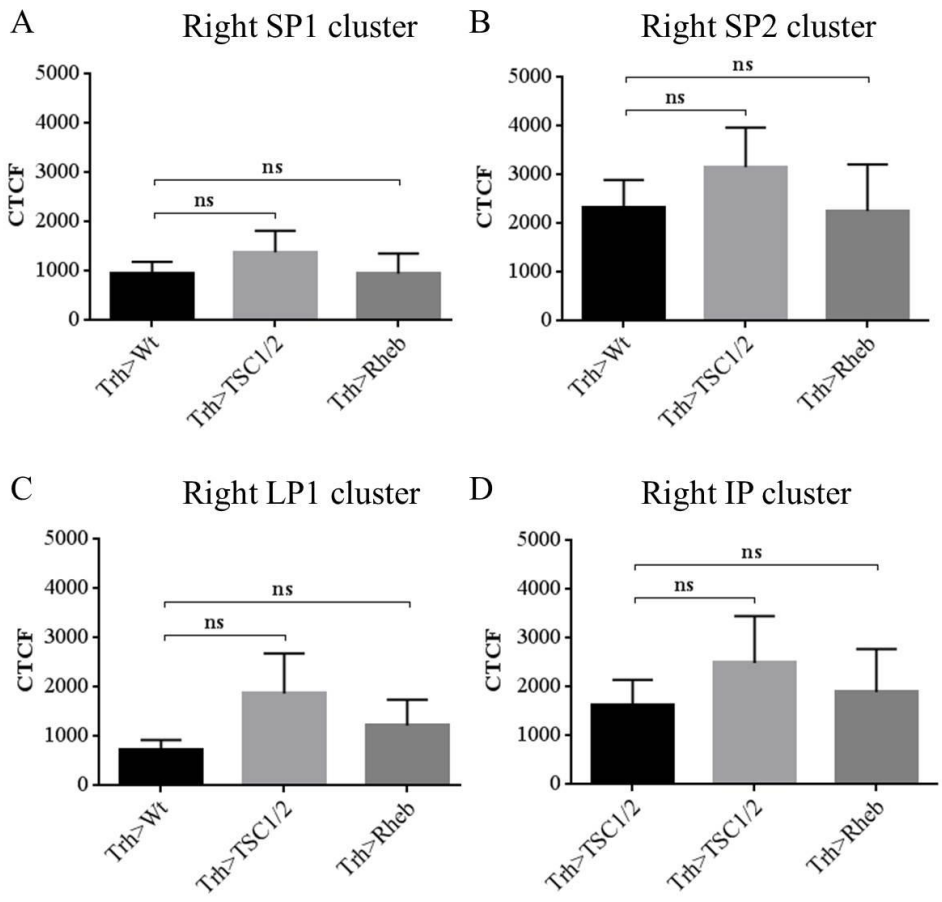


**Figure 4.20 Trh signal in the serotonergic clusters of the right hemisphere.**
(SP1, A; SP2, B; LP1, C; IP, D) Clusters of the right hemisphere. TOR signalling was downregulated in the serotonergic neurons by using the driver line Trh-Gal4 for crosses with UAS-TSC1; UAS-TSC2. An upregulation of TOR signalling was achieved by crossing Trh-Gal4 with UAS-Rheb. As control Trh-Gal4 was crossed with the wildtype strain (Wt) OregonR-S. The Trh signal was measured in the serotonergic clusters of third instar larvae. The figures represent the corrected total cell fluorescence (CTCF) of the clusters in the right hemisphere. N=9. Not significant (ns): $p>0.05$

TOR manipulation using UAS-TSC1; UAS-TSC2 or UAS-Rheb did not show any significant difference or a clear tendency of increase or decrease in Trh level compared to the control (Figure 4.20 and Table 4.1). However, the overexpression of Pathetic resulted in a higher Trh signal of most of the serotonergic clusters compared to the control. Especially, the clusters of the brain hemispheres and of the suboesophageal ganglion show a significant difference in the corrected total cell fluorescence.

Some clusters of the brain show a significant increase of Trh signal upon Pathetic overexpression while the corresponding cluster on the other brain side show no significant difference to the Trh signal of the control (Figure 4.22).

**Table 4.1 Statistical analysis of the Trh signal upon overexpression of the TSC complex or Rheb.**

Unpaired 2-tailed Student's t-test with Welch correction was used to analyse the data for significant differences. The statistical tests were performed with GraphPad Prism. N=9. Ns (not significant): p>0.05

| t-test | | | | |
|---|---|---|---|---|
| **Serotonergic cluster** | **Trh>Wt vs. Trh>TSC** | | **Trh>Wt vs. Trh>Rheb** | |
| | Left cluster | Right cluster | Left cluster | Right cluster |
| SP1 | p=0.3346; ns | p=0.4043; ns | p= 0.9314; ns | p=0.9960; ns |
| SP2 | p=0.5916; ns | p=0.4141; ns | p=0.8467; ns | p=0.9618; ns |
| LP1 | p=0.2765; ns | p=0.2149; ns | p=0.2374; ns | p=0.4280; ns |
| SE0 | p=0.7355; ns | p=0.6454; ns | p=0.2377; ns | p=0.1571; ns |
| IP | p=0.3317; ns | p=0.4459; ns | p=0.5986; ns | p=0.7999; ns |
| SE1 | p=0.5302; ns | p=0.4464; ns | p=0.9266; ns | p=0.5940; ns |
| SE2 | p=0.9489; ns | p=0.3598; ns | p=0.7580; ns | p=0.4661; ns |
| SE3 | p=0.5993; ns | p=0.4740; ns | p=0.7940; ns | p=0.7149; ns |
| T1 | p=0.6409; ns | p=0.6497; ns | p=0.9542; ns | p=0.9050; ns |
| T2 | p=0.2910; ns | p=0.3635; ns | p=0.8407; ns | p=0.6334; ns |
| T3 | p=0.7817; ns | p=0.5935; ns | p=0.7231; ns | p=0.8815; ns |

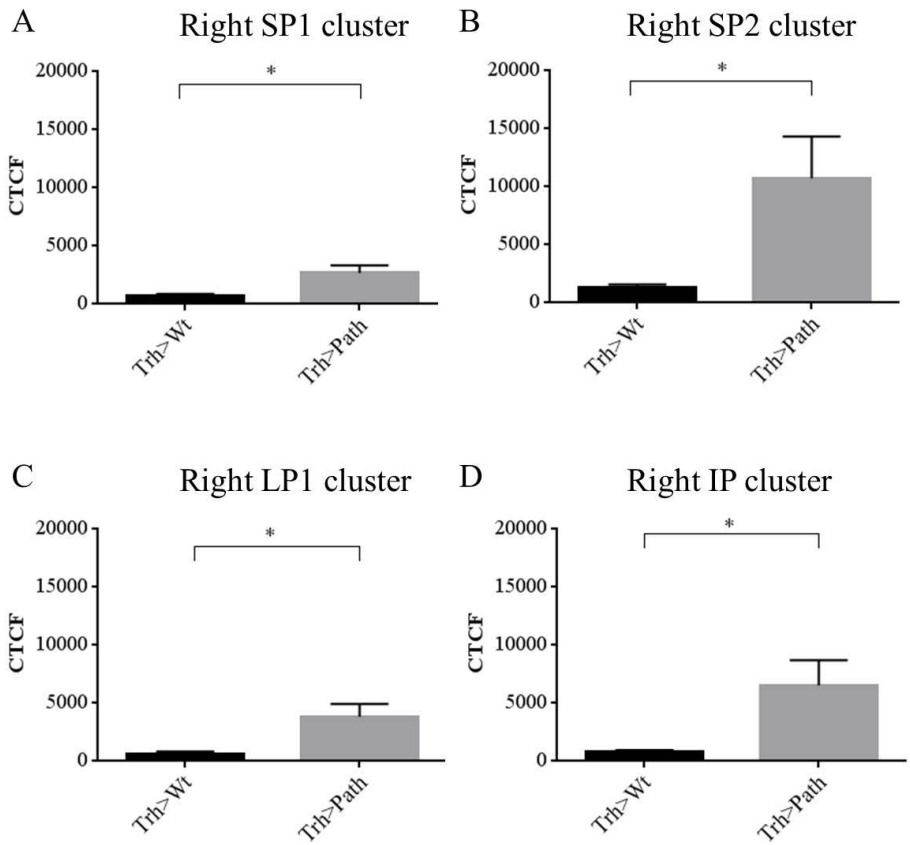


**Figure 4.21 Trh signal in the right hemisphere upon Pathetic overexpression.**

(SP1, A; SP2, B; LP1, C; IP, D) Clusters of the right hemisphere. TOR signalling was upregulated in serotonergic clusters by using the driver line Trh-Gal4 for crosses with UAS-Path. As control Trh-Gal4 was crossed with the wildtype strain (Wt) OregonR-S. The Trh signal was measured in the

serotonergic clusters of third instar larvae. The figures represent the corrected total cell fluorescence (CTCF) of the clusters in the right hemisphere. N=6. Not significant=ns, p>0.05. *: p≤0.05.

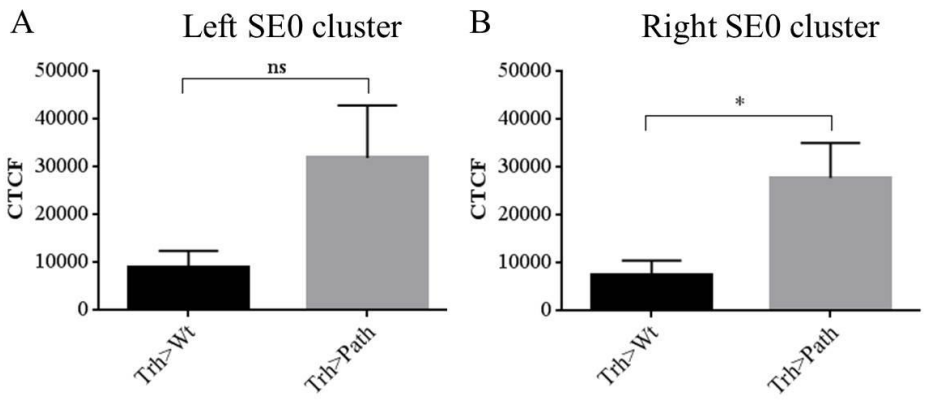


**Figure 4.22 Trh signal in the SE0 cluster upon Pathetic overexpression.**
(A, B) SE0 Clusters of the hemispheres. TOR signalling was upregulated in serotonergic clusters by using the driver line Trh-Gal4 for crosses with UAS-Path. As control Trh-Gal4 was crossed with the wildtype strain (Wt) OregonR-S. The Trh signal was measured in the serotonergic clusters of third instar larvae. The figures represent the corrected total cell fluorescence (CTCF) of the clusters in the brain hemisphere. N=6. Not significant=ns, p>0.05. *: p<0.05.

**Table 4.2 Statistical analysis of the Trh antibody signal upon Pathetic overexpression.**
Unpaired 2-tailed Student's t-test with Welch correction was used to analyse the data for significant differences. The statistical tests were performed with GraphPad Prism. N=6. Ns: p>0.05; *: p≤0.05; **: p≤0,01

| t-test | | |
|---|---|---|
| **Serotonergic cluster** | **Trh>Wt vs. Trh>Path** | |
| | **left cluster** | **right cluster** |
| **SP1** | p=0.0471; * | p=0.0276; * |
| **SP2** | p=0.0225; * | p=0.0467; * |
| **LP1** | p=0.0322; * | p=0.0436; * |
| **IP** | p=0.0390; * | p=0.0448; * |
| **SE0** | p=0.0948; ns | p=0.0393; * |
| **SE1** | p=0.1152; ns | p=0.0807; ns |
| **SE2** | p=0.0708; ns | p=0.0685; ns |
| **SE3** | p=0.0455; * | p=0.0436; * |
| **T1** | p=0.0612; ns | p=0.0458; * |
| **T2** | p=0.0654; ns | p=0.0561; ns |
| **T3** | p=0.0555; ns | p=0.0688; ns |

The SE0, the IP, the SE1 and the T1 were such clusters, in which one of the two corresponding clusters had no significant signal difference to the control while the other did (Table 4.2). Clusters without significant difference still showed a tendency of a higher Trh

signal compared to the control. It could be shown that Pathetic overexpression affects the amount of Trh in serotonin producing neurons.

### 4.4.3 *Ddc* RNA level in the larva upon TOR pathway manipulation

The Dopa decarboxylase (Ddc) catalyzes the second step of the short pathway in which serotonin is produced (Figure 4.15). The enzyme uses the product of the Tryptophan hydroxylase, 5-hydroxythryptophan, to produce 5-hydroxytryptamine or serotonin. It is expressed in serotonergic and dopaminergic cells of the brain where it is involved in neurotransmitter production. Though, it has also different functions in other tissues (Konrad and Marsh, 1987; Walter et al, 1991; Rauschenbach et al, 1997; Wittkopp et al, 2003;).

A *ddc* expression in the larva

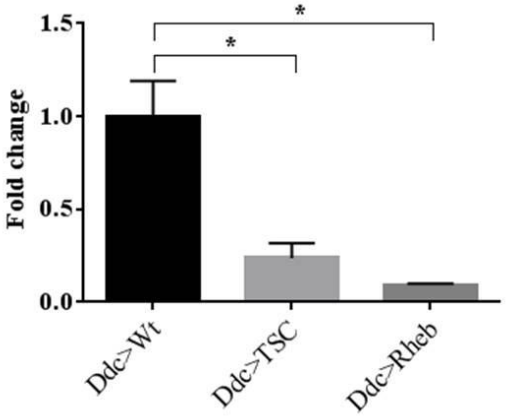


B

t-test

*ddc* expression in the larva

| Ddc-Gal4>Wt vs. | p-value |
|---|---|
| Ddc-Gal4>UAS-TSC1/2 | p=0.0208; * |
| Ddc-Gal4>UAS-Rheb | p=0.0175; * |

**Figure 4.23 Analysis of *dopa decarboxylase* (*ddc*) expression of third instar larvae upon manipulation of TOR signalling in Ddc expressing cells.**
TOR pathway was manipulated using the Gal4-UAS system. TOR signalling was downregulated in the dopaminergic cells by using the driver line Ddc-Gal4 for crosses with UAS-TSC1;UAS-TSC2. An upregulation of TOR signalling was achieved by crossing Ddc-Gal4 with UAS-Rheb. As control Ddc-Gal4 was crossed with the wildtype strain (Wt) OregonR-S. Expression was analysed in the whole larva. Data was normalized to the control sample. *Ddc* transcript level of the control flies was compared to the expression upon TOR signalling activation and deactivation. Unpaired 2-tailed Student's t-test with Welch correction was used to analyse the data for significant differences. N=4. The error bars represent the standard error of the mean (SEM). *: $p \leq 0.05$

In order to find out whether TOR signalling affects serotonin production via regulation of *ddc* expression, the Gal4-UAS system was used. TOR was first manipulated in tissues that are Dopa decarboxylase positive. Therefor the Ddc-Gal4 driver line was used. *Ddc* expression of 96+/-2 hour old third instar larvae with manipulated TOR signaling was determined by Real Time PCR.

A *ddc* expression in the larva

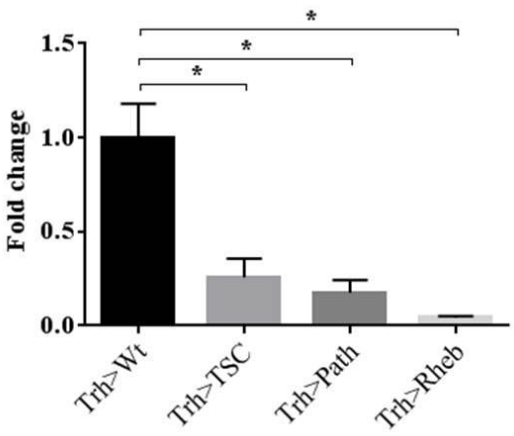


B

t-test

*ddc* expression in the larva

| Trh-Gal4>Wt vs. | p-value |
|---|---|
| Trh-Gal4>UAS-TSC1/2 | p=0.0168; * |
| Trh-Gal4>UAS-Path | p=0.0138; * |
| Trh-Gal4>UAS-Rheb | p=0.0127; * |

**Figure 4.24 Analysis of *dopa decarboxylase* (*ddc*) expression of third instar larvae upon manipulation of TOR signalling in Trh expressing cells.**
TOR pathway was manipulated using the Gal4-UAS system. TOR signalling was downregulated in the serotonergic neurons by using the driver line Trh-Gal4 for crosses with UAS-TSC1;UAS-TSC2. An upregulation of TOR signalling was achieved by crossing Trh-Gal4 with UAS-Rheb or UAS-Path. As control Trh-Gal4 was crossed with the wildtype strain (Wt) OregonR-S. Expression was analysed in the whole larva. Data was normalized to the control sample. *Dopa decarboxylase (ddc)* transcript level of the control flies was compared to the expression upon TOR signalling activation and deactivation. Unpaired 2-tailed Student's t-test with Welch correction was used to analyse the data for significant differences. N=4. The error bars represent the standard error of the mean (SEM). *=p≤0.05

Figure 4.23 shows that TOR activation via Rheb and TOR downregulation via the TSC complex in Ddc positive cells had a negative effect on *ddc* expression. Thereby, TOR activation showed a stronger repression of *ddc* transcription. To confirm that TOR signalling in the serotonin producing cells and not in other *ddc* positive tissues is responsible for this effect, the experiment was repeated using Trh-Gal4. Also in this case, a negative effect of TOR signalling manipulation on *ddc* expression could be observed, indicating that *ddc* expression is affected by a changed TOR signalling in serotonergic neurons (Figure 4.24). The regulation of *ddc* expression needed to be analysed further to confirm a direct effect of TOR on *ddc* expression in the brain.

### 4.4.4 *Ddc* expression in the brain

To determine whether TOR directly affects the *ddc* expression in the central nervous system, the experiment was repeated. Thirty larval brains were used for analysis of TOR pathway manipulation in Trh positive cells. A difference in brain *ddc* expression upon TOR manipulation was expected if TOR is directly involved in the regulation of *ddc* transcript level.

A *ddc* expression in the larval brain

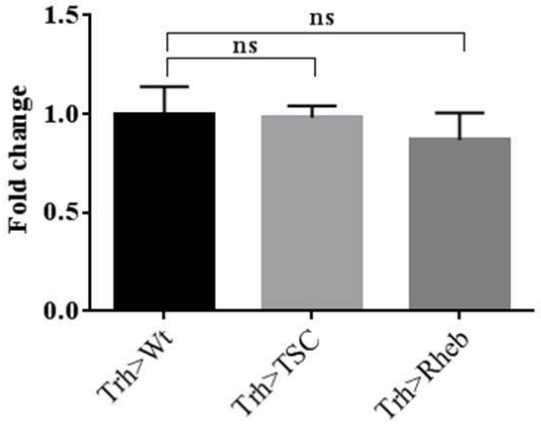


B

t-test

*ddc* expression in the larval brain

| Trh-Gal4>Wt vs. | p-value |
|---|---|
| Trh-Gal4>UAS-TSC1/2 | p=0.9094; * |
| Trh-Gal4>UAS-Rheb | p=0.5363; * |

**Figure 4.25 Analysis of *dopa decarboxylase* (*ddc*) expression in the brain of third instar larvae upon manipulation of TOR signalling.**
TOR pathway was manipulated using the Gal4-UAS system. TOR signalling was downregulated in the serotonergic neurons by using the driver line Trh-Gal4 for crosses with UAS-TSC1;UAS-TSC2. An upregulation of TOR signalling was achieved by crossing Trh-Gal4 with UAS-Rheb. As control Trh-Gal4 was crossed with the wildtype strain (Wt) OregonR-S. Expression was analysed in the larval brain. *Ddc* transcript level of the control flies was compared to the expression upon TOR signalling activation and deactivation. Data was normalized to the control. Unpaired 2-tailed Student's t-test with Welch correction was used to analyse the data for significant differences. N=3. The error bars represent the standard error of the mean (SEM). The differences to the control are not significant (ns). Ns: p>0.05.

Figure 4.25 shows that TOR manipulation in serotonergic neurons does not affect the *ddc* expression in the brain. To analyse that TOR manipulation in the whole organism can affect *ddc* expression in the brain, 74 hour old larvae were deprived of amino acids by feeding them with sugar agar for 24 hours. Controls were fed with yeast. Additionally, the effect on the brain expression upon feeding yeast with rapamycin was analysed. Controls were fed with yeast without rapamycin for twenty-four hours. Again 30 larval brains were used for analysis. The amino acid deprivation, which diminishes the TOR signalling in the whole organism, did not reduce the *ddc* expression in the brain (Figure 4.26). Also rapamycin feeding that inhibits TOR pathway could not induce a decrease of *ddc* transcript level (Figure 4.27). It could be shown that TOR signalling does not affect *ddc* expression in the brain. Though, the expression in the whole larva is decreased upon TOR pathway manipulation in serotonin producing neurons.

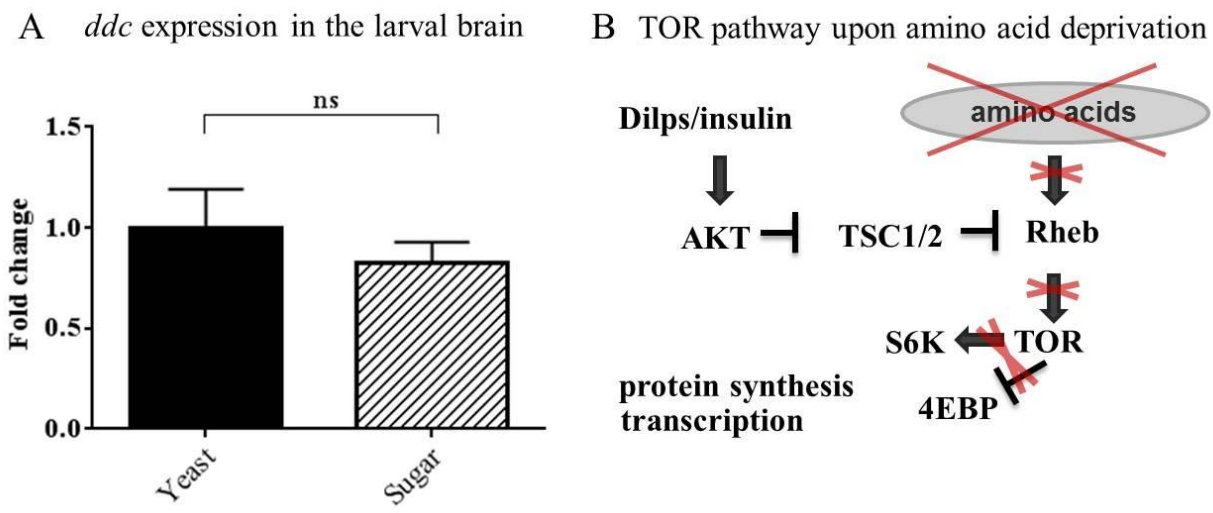


**Figure 4.26 Analysis of *dopa decarboxylase* (*ddc*) expression in the brain of Oregon R-S third instar larvae upon amino acid deprivation.**

Expression was analysed in the larval brain. *Ddc* transcript level upon yeast feeding was compared to the expression upon feeding on sugar. Data was normalised to the yeast condition (A). (B) Effect of amino acid deprivation on Target of rapamycin (TOR) pathway. Tuberous sclerosis complex 1 (TSC1). Tuberous sclerosis complex 2 (TSC2). Ras homolog enriched in brain (Rheb). (S6K) S6 kinase. (4EBP) 4E binding protein. (Dilps) Drosophila insulin like peptides. (Akt) Homologue of the retroviral oncogene v-Akt. Unpaired 2-tailed Student's t-test with Welch correction was used to analyse the data for significant differences. N=3. Error bars represent the standard error of the mean (SEM). There is no significant difference to the control (ns). Ns: p>0.05. p= 0.4793

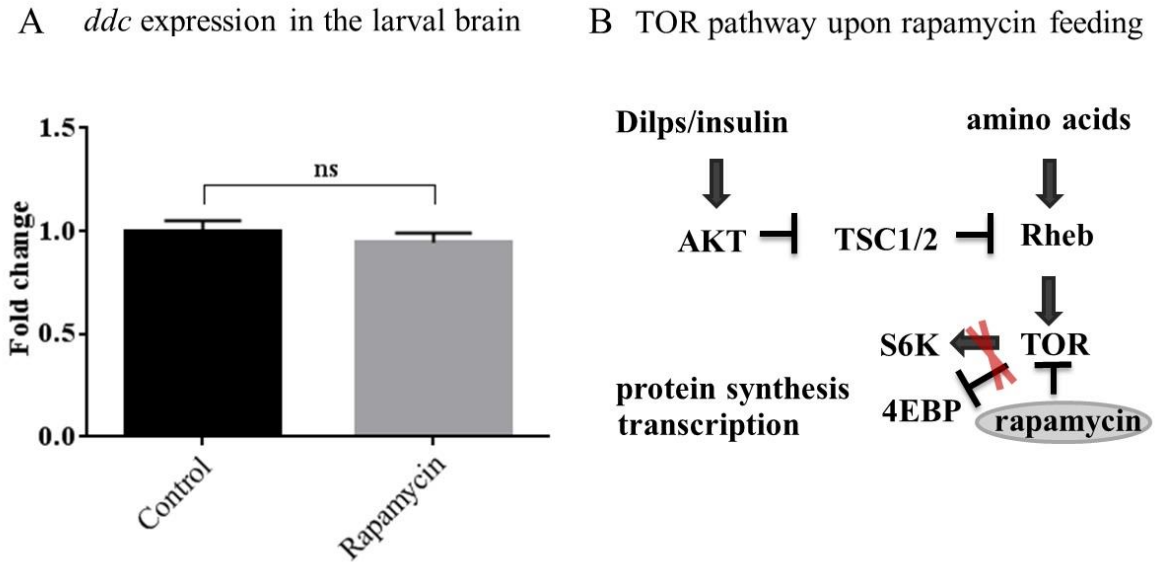


**Figure 4.27 Analysis of *dopa decarboxylase* (*ddc*) expression in the brain of Oregon R-S third instar larvae upon rapamycin feeding.**

Expression was analysed in the larval brain. *Ddc* transcript level upon yeast feeding was compared to the expression upon feeding on yeast with rapamycin. Data was normalised to the yeast control condition (A). (B) Scheme of rapamycin function on Target of rapamycin (TOR) pathway. Tuberous sclerosis complex 1(TSC1). Tuberous sclerosis complex 2 (TSC2). Ras homolog enriched in brain (Rheb). S6 kinase (S6K). 4E binding protein (4EBP). Drosophila insulin like peptides (Dilps). Homologue of the retroviral oncogene v-Akt (Akt). Unpaired 2-tailed Student's t-test with Welch correction was used to analyse the data for significant differences. N=5. Error bars represent the

standard error of the mean (SEM). There is no significant difference to the control (ns). Ns: p>0.05. p= 0.4318

The brain contains more Ddc positive than Trh positive cells. TOR signalling in the brain was manipulated just in Trh positive cells whereas the Real Time PCR detects the expression change in the whole brain. To exclude that ddc expression still might have been changed in certain serotonergic clusters, a fluorescence in situ hybridization was performed. Therefore, brains with manipulated TOR signalling in Trh positive cells were used. The expression in the whole larva upon TOR manipulation in Ddc (Figure 4.23) and Trh (Figure 4.24) positive cells was highly downregulated. Therefore a strong signal difference in serotonergic neurons was expected.

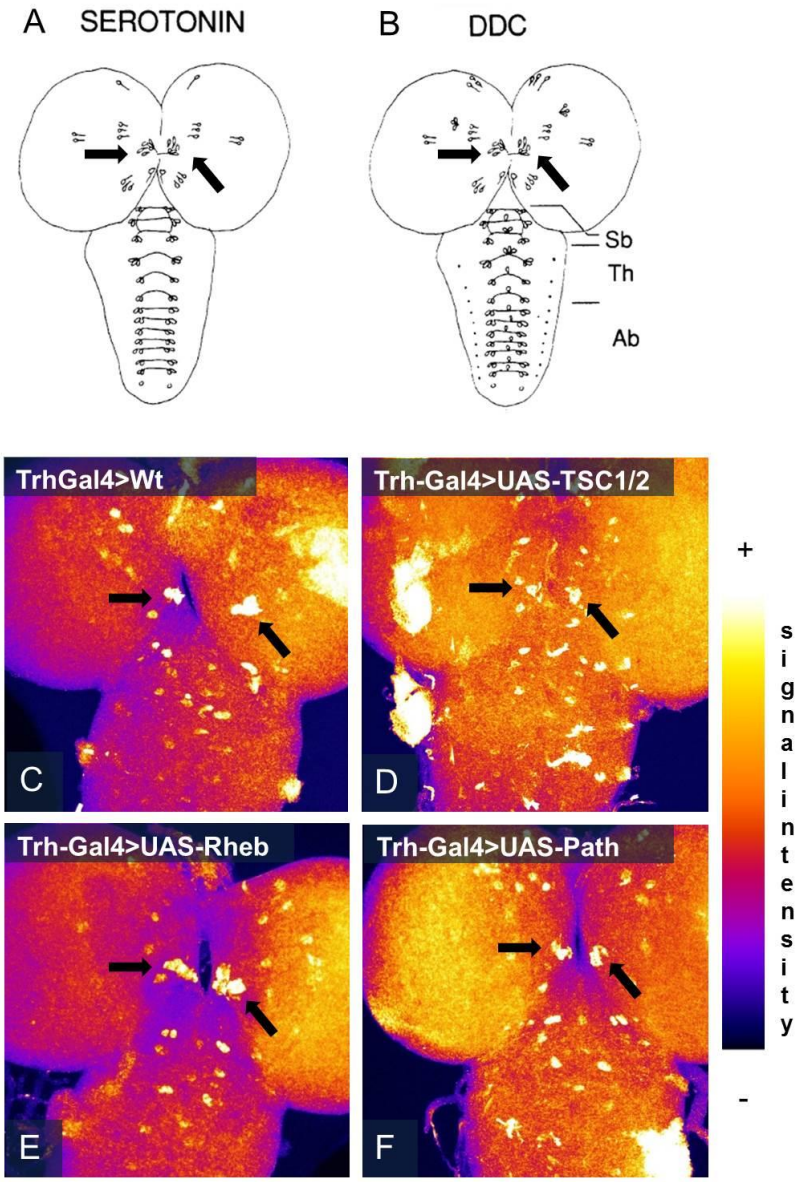


**Figure 4.28 Fluorescence *in situ* hybridization of *dopa decarboxylase* in larvae with manipulated TOR pathway in the brain.**

(A) Serotonergic clusters. (B) Ddc positive clusters. (Sb) Suboesophageal segment. (Th) Thoracic segment. (Ab) Abdominal segment. A-B modified from Beall and Hirsh, 1987. TOR pathway was manipulated using the Gal4-UAS system. As control Trh-Gal4 was crossed with the wildtype strain (Wt) OregonR-S (C). TOR signalling was downregulated in the serotonergic neurons of the offspring by using the driver line Trh-Gal4 for crosses with UAS-TSC1;UAS-TSC2 (D). An upregulation of TOR signalling in the offspring was achieved by crossing Trh-Gal4 with UAS-Rheb (E) or UAS-Path (F). SE0 cluster (Black arrow).

Figure 4.28 shows that also via *in situ* hybridization a difference in *ddc* transcript level, cannot be distinguished. The strong difference in *ddc* expression that was detected in the whole larva upon TOR manipulation could not be observed in the brain. Just the SE0 cluster that is a serotonergic cluster shows a stronger expression in in the control larvae than in the crosses with manipulated TOR signalling in this figure. However, the individual differences of *ddc* expression in the SE0 cluster of other larvae made it difficult to determine an effect with certainty. Thus, the results show that *ddc* expression is not directly regulated by TOR signalling in *ddc* containing neurons. As the total *ddc* expression is not affected in the brain upon TOR manipulation, the change in transcript level of larvae must be due to a regulation of *ddc* transcription in the periphery.

### 4.4.5 *Ddc* expression in the periphery upon TOR manipulation in serotonergic neurons

Besides from serotonin production, Ddc also catalyses the decarboxylation of L-Dopa, a L-Tyrosin derivate. This way it produces dopamine in dopaminergic neurons. Dopamine is a neurotransmitter involved in metabolic regulation, sleep, feeding behavior and learning (Berry et al, 2012; Ueno et al, 2012; Bjordal et al 2014). It is also a precursor of melanin and sclerotin which are important for cuticle pigmentation and formation in the adult flies (Wittkoppet al, 2003). Hence, Dopamine decarboxylase is not only abundant in serotonergic and dopaminergic neurons of the brain but also in the epidermis. According to Flyatlas data presented by flybase.org (http://flybase.org/reports/FBgn0000422.html) *ddc* is also expressed in the gut. There it might be involved in the production of serotonin.

Changes in TOR signalling of the serotonergic neurons showed no direct influence on the expression of serotonin producing enzymes (Figure 4.25 - Figure 4.28). However, the observed changes in the whole organism (Figure 4.24) indicated an influence on *ddc* transcription in the periphery. It was analysed whether the strong downregulation on *ddc* expression in the larva (Figure 4.24) was detected due to a TOR signalling effect in the gut or the epidermis.

A *ddc* expression in the larval gut

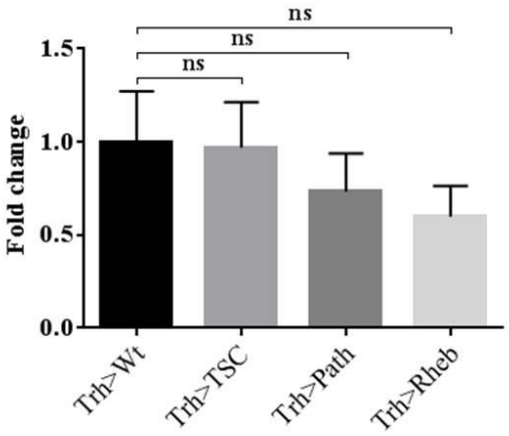


B

t-test

*ddc* expression in the larval gut

| Trh-Gal4>Wt vs. | p-value |
|---|---|
| Trh-Gal4>UAS-TSC1/2 | p=0.9372; ns |
| Trh-Gal4>UAS-Path | p=0.4806; ns |
| Trh-Gal4>UAS-Rheb | p=0.2890; ns |

**Figure 4.29 Analysis of *dopa decarboxylase* (*ddc*) expression in the gut of third instar larvae upon manipulation of TOR signalling.**
TOR pathway was manipulated using the Gal4-UAS system. TOR signalling was downregulated in the serotonergic neurons of the offspring by using the driver line Trh-Gal4 for crosses with UAS-TSC1;UAS-TSC2. An upregulation of TOR signalling in the offspring was achieved by crossing Trh-Gal4 with UAS-Rheb or UAS-Path. As control Trh-Gal4 was crossed with the wildtype strain (Wt) OregonR-S. Expression was analysed in the larval gut. Data was normalized to the control sample. *Ddc* transcript level of the control flies was compared to the expression upon TOR signalling activation and deactivation. Unpaired 2-tailed Student's t-test with Welch correction was used to analyse the data for significant differences. N=3. The error bars represent the standard error of the mean (SEM). The differences to the control are not significant (ns.). Ns: $p>0.05$

Therefore five guts and five cuticulae with attached epidermis of control larvae and larvae with manipulated TOR signalling were dissected. Again, the *ddc* expression was analysed by Real Time PCR. Figure 4.29 shows no difference of *ddc* expression in the gut upon TOR manipulation compared to the control. Therefore, the expression of *ddc* in serotonin producing tissues was not affected by a changed TOR signalling in serotonergic neurons. The repression of *ddc* transcript level of the whole organism might be due to a changed *ddc* expression in the epidermal cells. TOR was not directly manipulated in these tissues.

A *ddc* expression in the epidermis

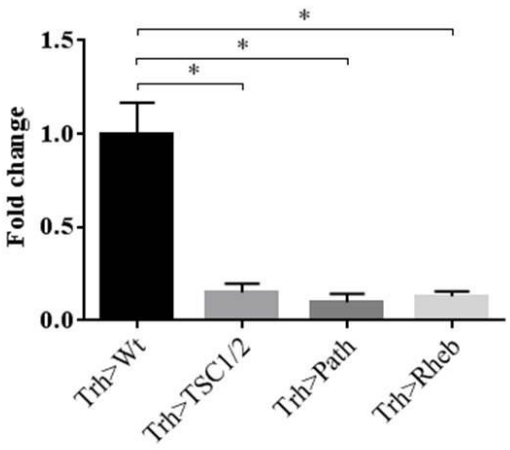


B

t-test

*ddc* expression in the epidermis

| Trh-Gal4>Wt vs. | p-value |
|---|---|
| Trh-Gal4>UAS-TSC1/2 | p=0.0289; * |
| Trh-Gal4>UAS-Path | p=0.0260; * |
| Trh-Gal4>UAS-Rheb | p=0.0319; * |

**Figure 4.30 Analysis of *dopa decarboxylase* (*ddc*) expression in the epidermis of third instar larvae upon manipulation of TOR signalling.**
TOR pathway was manipulated using the Gal4-UAS system. TOR signalling was downregulated in the serotonergic neurons by using the driver line Trh-Gal4 for crosses with UAS-TSC1;UAS-TSC2. An upregulation of TOR signalling was achieved by crossing Trh-Gal4 with UAS-Rheb or UAS-Path. As control Trh-Gal4 was crossed with the wildtype strain (Wt) OregonR-S. Data was normalized to the control sample. Expression was analysed in the larval epidermis. *Ddc* transcript level of the control flies was compared to the expression upon TOR signalling activation and deactivation. Unpaired 2-tailed Student's t-test with Welch correction was used to analyse the data for significant differences. N=3. The error bars represent the standard error of the mean (SEM). *: $p \leq 0.05$.

The expression analysis of *ddc* transcript level in the epidermal tissues (Figure 4.30) shows a strong reduction upon TOR manipulation in serotonergic tissues. The overexpression of the transceptor Pathetic had the same effect as the overexpression of the other regulatory pathway members. It indicates that the decrease of *ddc* transcript level, observed in the whole organism, is due to a changed expression in the epidermis. It was shown that the regulation of epidermal *ddc* expression is affected by TOR signalling in serotonin producing neurons. To identify whether the changed *ddc* level in larvae affects pigmentation in adult flies, the pigmentation phenotype was analysed.

### 4.4.6 Pigmentation of adult males upon manipulation of TOR signalling

The pigmentation of *Drosophila melanogaster* is affected by environmental factors like the nutritional status and temperature. It is mediated by pigment producing enzymes. The melanin pattern in the epidermis was shown to correlate with the spatial expression of *tyrosine hydroxylase (TH)* and *dopa decarboxylase (ddc).* Thus, these two enzymes are involved in the production of dark pigments. Cuticle of flies lacking TH or Ddc showed an albino phenotype in mosaic analysis (True et al, 1999; Gibert et al, 2007). TOR pathway manipulation in

serotonin producing neurons resulted in reduced epidermal *dcc* expression in third instar larvae (Figure 4.30). Therefore, the adult pigmentation pattern was analysed in male flies with manipulated TOR pathway in serotonergic neurons. Adult males were shock frozen with liquid nitrogen eight days after eclosion. The pigmentation pattern of the crosses Trh-Gal4>UAS-TSC1;UAS-TSC2, Trh-Gal4>UAS-Path and Trh-Gal4>UAS-Rheb was compared to the Trh-Gal4>Wt control or to the used driver and effetor lines of these crosses.

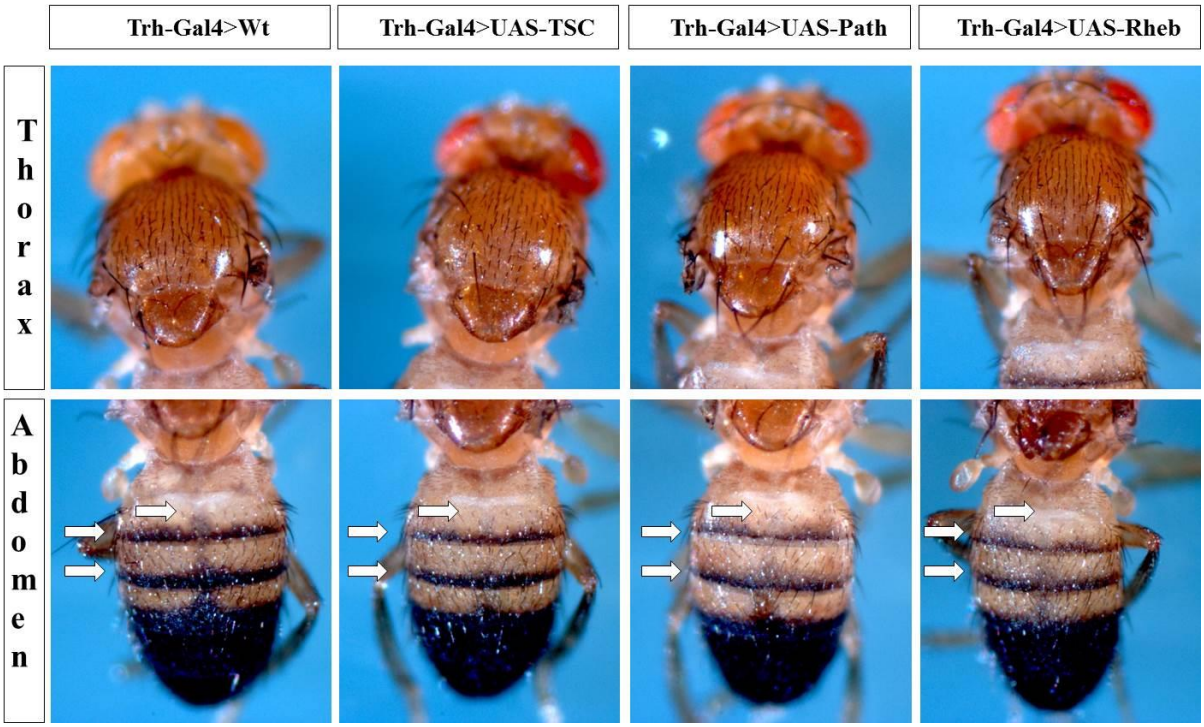


**Figure 4.31 Pigmentation in males upon manipulation of TOR signalling in serotonergic neurons.**
TOR pathway was manipulated using the Gal4-UAS system. TOR signalling was downregulated in the serotonergic neurons of the offspring by using the driver line Trh-Gal4 for crosses with UAS-TSC1;UAS-TSC2. An upregulation of TOR signalling in the offspring was achieved by crossing Trh-Gal4 with UAS-Rheb or UAS-Path. As control Trh-Gal4 was crossed with the wildtype strain (Wt) OregonR-S. Pigmentation was analysed eight days after eclosion in the dorsal thorax and abdomen cuticle of male adult flies. Differences in the pattern are marked by white arrows. N=3

Figure 4.31 shows that the colour pattern in the thorax cuticle did not differ within the different crosses. However, the pigmentation in the abdominal cuticle showed a stronger intensity and spatial dispersal in the control (Trh>Wt). The abdominal stripes in flies with manipulated TOR signalling in serotonergic neurons were thinner and brighter and the midline that united the parallel abdominal stripes in the control flies was almost invisible. Especially for TOR activation via Rheb and Pathetic overexpression a decreased pigmentation was observed.

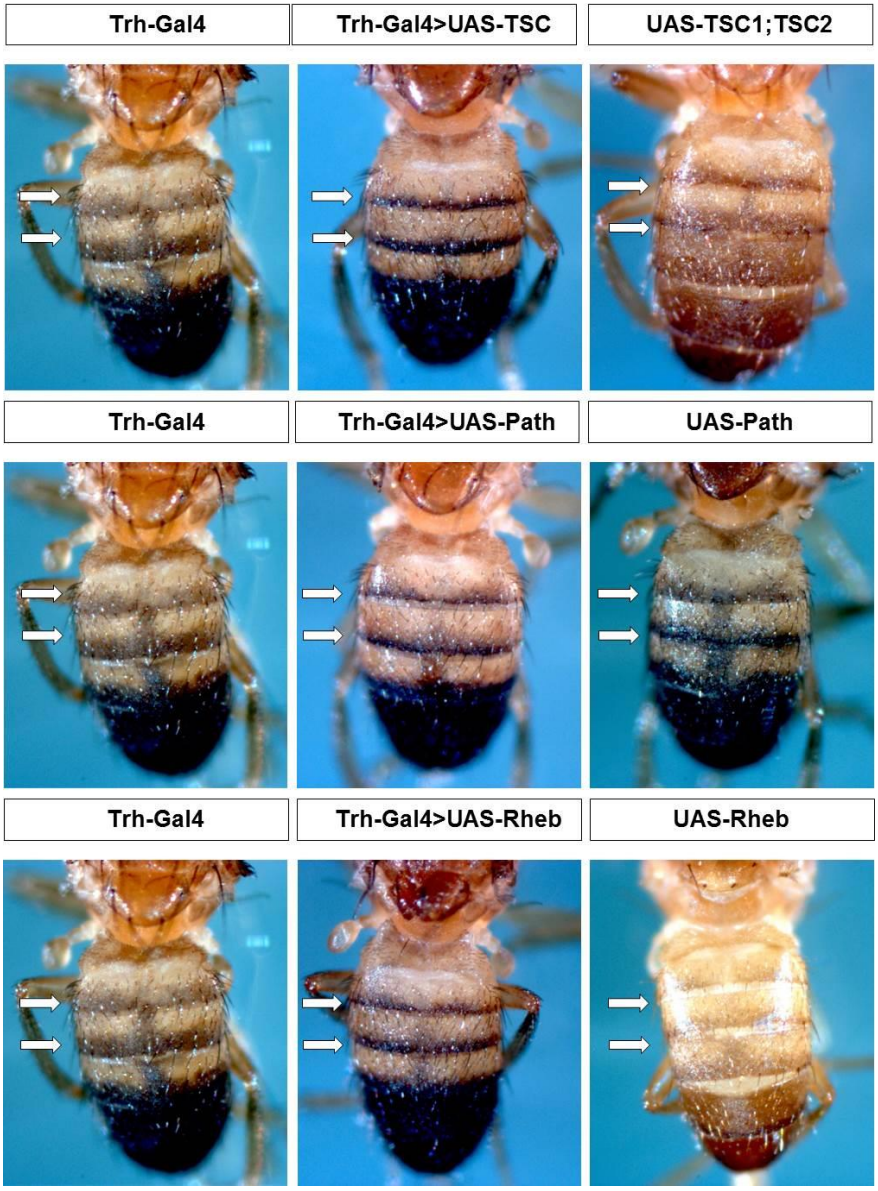


**Figure 4.32 Pigmentation upon TOR manipulation compared to the driver and effector line.**
TOR pathway was manipulated using the Gal4-UAS system. TOR signalling was downregulated in the serotonergic neurons of the offspring by using the driver line Trh-Gal4 for crosses with UAS-TSC1;UAS-TSC2. An upregulation of TOR signalling in the offspring was achieved by crossing Trh-Gal4 with UAS-Rheb or UAS-Path. As control the Gal4 driver line and the UAS effector line were analysed. Pigmentation was analysed eight days after eclosion in the abdomen cuticle of males. Differences in the pattern are marked by white arrows. The driver and effector lines show a stronger pigment distribution than flies with manipulated TOR signalling in serotonergic neurons. N=3

Compared to the driver and effector lines (Figure 4.32), flies with a decreased *ddc* expression during the late larval stage showed a lower pigment distribution. Therefore, changed TOR signalling in serotonergic neurons altered the pigment pattern slightly. Further analysis with a higher quantity of individuals is needed to confirm this result. It was assumed that a change in serotonin production and release might have affected the larval *ddc* expression and adult

pigmentation. Therefore, it was tested whether increased or decreased serotonin release affects *ddc* expression in the larva.

### 4.4.7 *Ddc* expression analysis upon induction and inhibition of serotonin release

Increased and decreased TOR signalling in serotonergic neurons reduced *ddc* expression in the prepupal stage and the pigment distribution of the adult flies. This data suggested that changes in serotonin release or in the release of other factors with influence on the epidermal transcription might have occurred. To analyse whether the release of serotonin affects *dopa decarboxylase* expression, the Gal4-UAS system was used. The serotonin release was manipulated by overexpression of the transient receptor potential channel A (TrpA) or the mutated *shibire* allele shibire$^{ts1}$ in serotonergic neurons. Therefore, the driver line Trh-Gal4 and the effector line UAS-TrpA or UAS-Shibire$^{ts1}$ were used. Both effectors are temperature sensitive and active when shifted to 32°C. Upon temperature shift to 32°C TrpA causes an increased vesicle fusion and serotonin release, while Shibire$^{ts1}$ inhibits serotonin release. For experiments, 72+/-2 hour old Trh-Gal4>UAS-TrpA and Trh-Gal4>UAS-Shibire$^{ts1}$ larvae were transferred to 32°C for twenty-four hours. Controls were kept at 25°C. For Real Time analysis of *dopa decarboxylase* expression whole larvae were used.

The data showed that an increased serotonin release increased *ddc* expression (Figure 4.33 A), while a decrease in serotonin release lead to a down regulation of *ddc* (Figure 4.33 B). To control whether the 24 hour shift to the restrictive temperature of 32° C might have induced the observed effect, the *ddc* expression of the effector line UAS-Shibire$^{ts}$ was examined. The effector line does not overexpress the *shibire$^{ts}$* allele without induction by Gal4. Twenty four hours after a temperature shift *ddc* transcription at 25°C was compared to the *ddc* transcription at 32°C in third instar larvae.

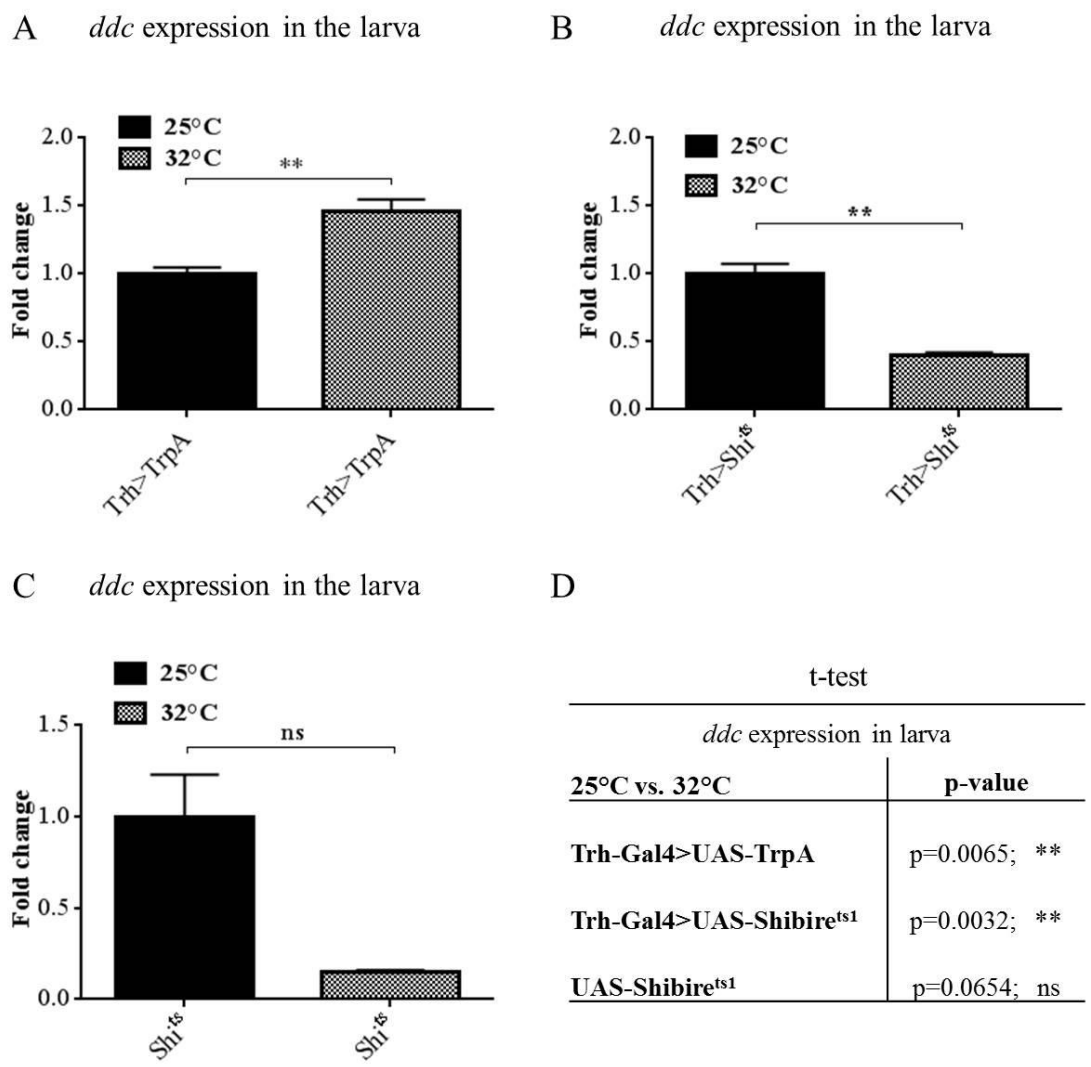


**Figure 4.33 Analysis of *dopa decarboxylase* (*ddc*) expression in third instar larvae upon manipulation of serotonin release.**

Serotonin release was manipulated using the Gal4-UAS system. (A) Thermosensitive depolarization and neurotransmitter release of the serotonergic neurons was increased in Trh-Gal4>UAS-TrpA larvae at 32°C for 24 hours. (B) A thermosensitive decrease of vesicle fusion and neurotransmitter release was achieved in Trh-Gal4>UAS-Shibire$^{ts}$ larvae upon a temperature shift to 32°C for 24 hours. Controls (A-B) were kept at 25°C for 24 hours. (C) As additional control third instar larvae of the effector line UAS-Shibire$^{ts}$ were kept on a restrictive temperature of 32°C or at 25°C for 24 hours. Data was normalized to the temperature condition at 25°C. Expression was analysed by Real Time PCR. (D) Unpaired 2-tailed Student's t-test with Welch correction was used to analyse the data for significant differences. The error bars represent the standard error of the mean (SEM). A: N=4; B: N=4; C: N=3. Ns (not significant): p>0,05 ; **: p≤0.01; ***: p≤0.001

The data for the UAS-Shibire$^{ts}$ control experiments showed a clear downregulation of *ddc* transcript level upon a temperature of 32°C compared to the control temperature condition at 25°C (Figure 4.33 C). The values at 32°C showed a high variance. Due to the Welch correction, which was nessesary because of the variance inhomogeneity of experiment and controls, the difference in the *ddc* expression is rated as not significant. However, due to the observations in the single experiments a temperature effect cannot be excluded. Then, upon

increased serotonin release an even higher upregulating effect than observed in Figure 4.33 A occurs as the temperature effect is compensated.

### 4.4.8 Serotonin signal in the brain upon TOR manipulation

So far, it could be shown that TOR pathway does not affect the serotonin producing enzymes in serotonergic tissues on transcript level. The amount of Tryptophan hydroxylase was increased upon Pathetic overexpression but not upon overexpression of the other pathway members. However, the effect of TOR pathway might be promoted not just due to a regulation of transcriptional or translational level of the serotonin producing enzymes but also due to their phosphorylation level and their activity.

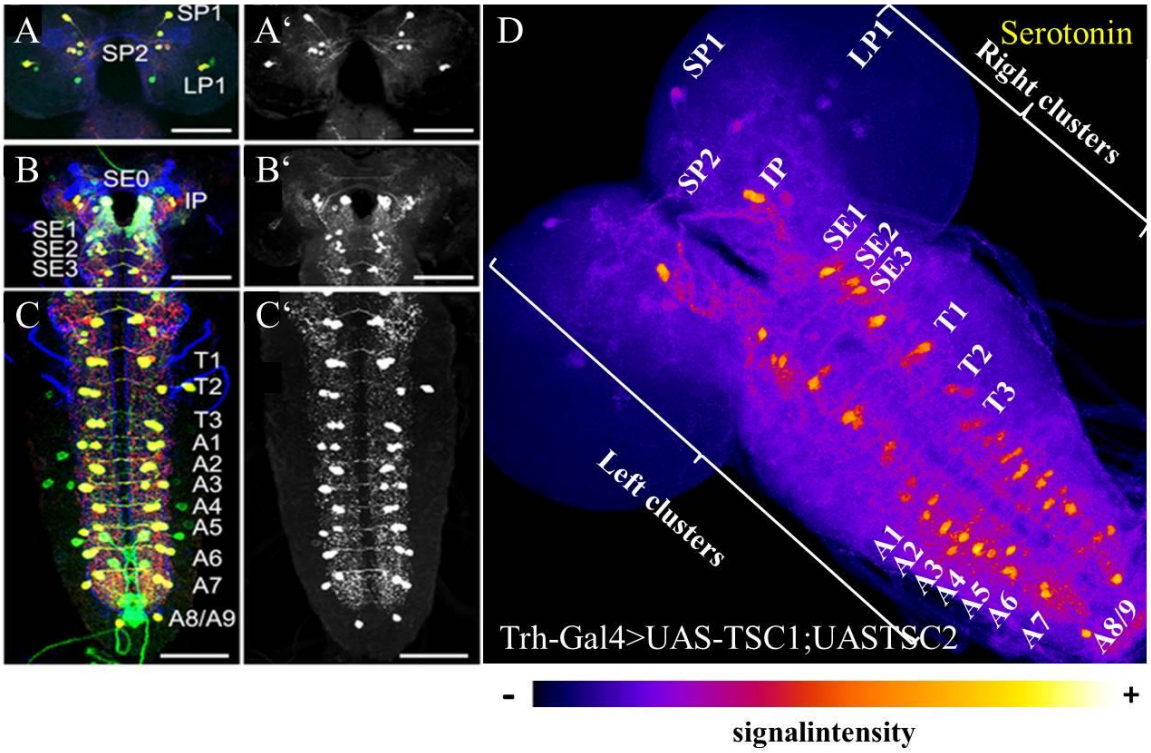


**Figure 4.34 Serotonin staining in the larval brain.**
(A-C) and (A'-C') are modified from Huser et al, 2012. Those images show the serotonergic clusters of the brain in *Drosophila melanogaster* Trh-GAL4/UAS-mCD8::GFP larvae. The anti-FasII/anti-ChAT staining visualizes the neuropil in blue, while the membrane-bound CD8 is labelled in green and the 5HT-immunoactivity in red. The yellow staining shows the merge of the Gal4 expression and the 5HT signal and maps the different serotonergic clusters. (D) Staining of a Trh-Gal4>UAS-TSC1;UAS-TSC2 larval brain with a serotonin antibody, that coincides with the shown serotonergic clusters in the brain in (A)-(C). (D) The increase of signal intensity is visualised from blue to yellow.

To confirm that Pathetic influences the amount of serotonin via TOR, the serotonin production was analysed by measurement of the serotonin level in the serotonergic clusters of the hemispheres, the suboesophageal and thoracic segments. Therefore, antibody stainings were performed and the fluorescence was measured using the program Fiji. SE0 clusters were

not measured because no signal was detected in these clusters during the third larval instar. Also the fluorescence of the abdominal clusters A1-A9 was not measured as those clusters did not show differences in their signal in previous stainings compared to the controls.

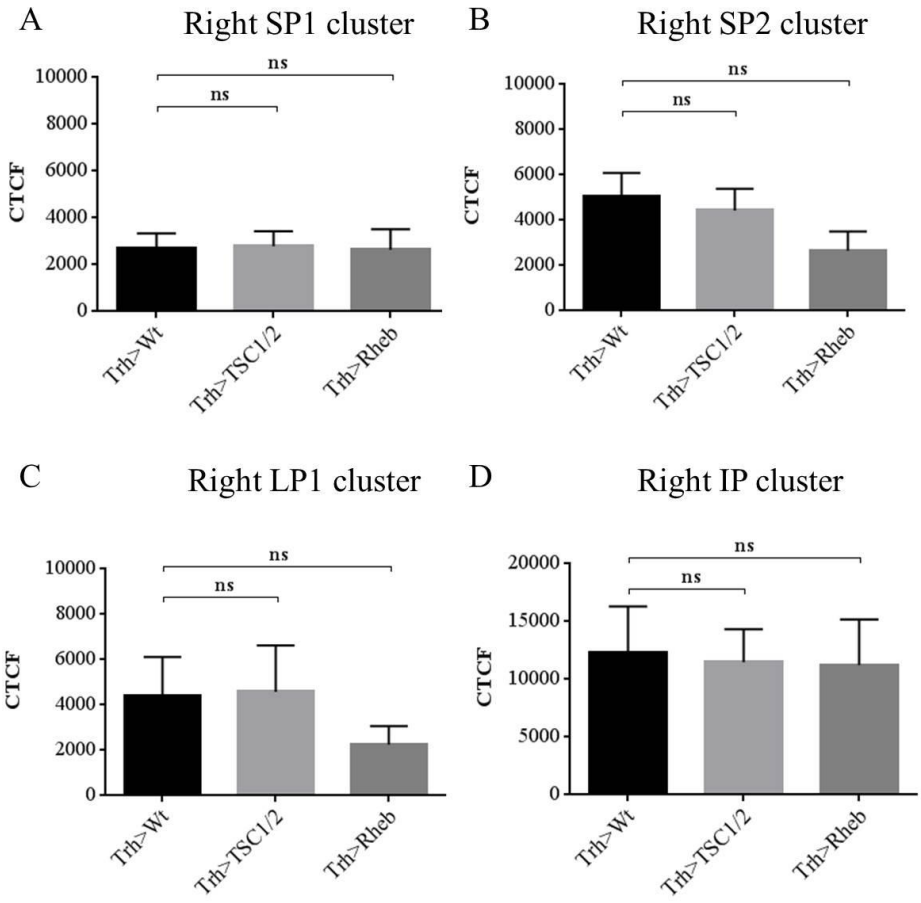


**Figure 4.35 Serotonin signal in the serotonergic clusters of the right hemisphere.**
(SP1, A; SP2, B; LP1, C; IP, D) Clusters of the right hemisphere. TOR signalling was downregulated in the serotonergic neurons by using the driver line Trh-Gal4 for crosses with UAS-TSC1; UAS-TSC2. An upregulation of TOR signalling was achieved by crossing Trh-Gal4 with UAS-Rheb. As control Trh-Gal4 was crossed with the wildtype strain (Wt) OregonR-S. The serotonin signal was measured in the serotonergic clusters of third instar larvae. The figures (A-D) represent the corrected total cell fluorescence (CTCF) of the clusters in the right hemisphere. N=9. Not significant (ns): $p>0.05$

The serotonergic clusters of the brain hemispheres (SP1, SP2, LP1, IP), of the suboesophageal segment (SE1-SE3) and of the thoracic segment (T1-T3) showed no significant difference in serotonin signal upon Rheb and TSC1; TSC2 overexpression (Figure 4.35 and Table 4.3).

**Table 4.3 Statistical analysis of the serotonin signal in the brain upon TOR manipulation.**
Unpaired 2-tailed Student's t-test with Welch correction was used to analyse the data for significant differences. N=9. Ns (not significant): p>0.05; *: p≤0.05; **: p≤0.01

| t-test | | | | |
|---|---|---|---|---|
| **Serotonergic cluster** | **Trh>Wt vs. Trh>TSC** | | **Trhx>Wt vs. Trh>Rheb** | |
| | **left cluster** | **right cluster** | **left cluster** | **right cluster** |
| **SP1** | p=0.6310; ns | p=0.9112; ns | p=0.8447; ns | p=0.9711; ns |
| **SP2** | p=0.6633; ns | p=0.6605; ns | p=0.6307; ns | p=0.0921; ns |
| **LP1** | p=0.7192; ns | p=0.9824; ns | p=0.5181; ns | p=0.2516; ns |
| **IP** | p=0.7292; ns | p=0.8675; ns | p=0.7854; ns | p=0.8503; ns |
| **SE1** | p=0.5827; ns | p=0.9889; ns | p=0.0871; ns | p=0.2289; ns |
| **SE2** | p=0.9247; ns | p=0.8284; ns | p=0.2959; ns | p=0.1642; ns |
| **SE3** | p=0.7358; ns | p=0.9772; ns | p=0.3970; ns | p=0.3876; ns |
| **T1** | p=0.4266; ns | p=0.3343; ns | p=0.3730; ns | p=0.3741; ns |
| **T2** | p=0.3800; ns | p=0.7603; ns | p=0.6476; ns | p=0.5517; ns |
| **T3** | p=0.5101; ns | p=0.5498; ns | p=0.5847; ns | p=0.9099; ns |

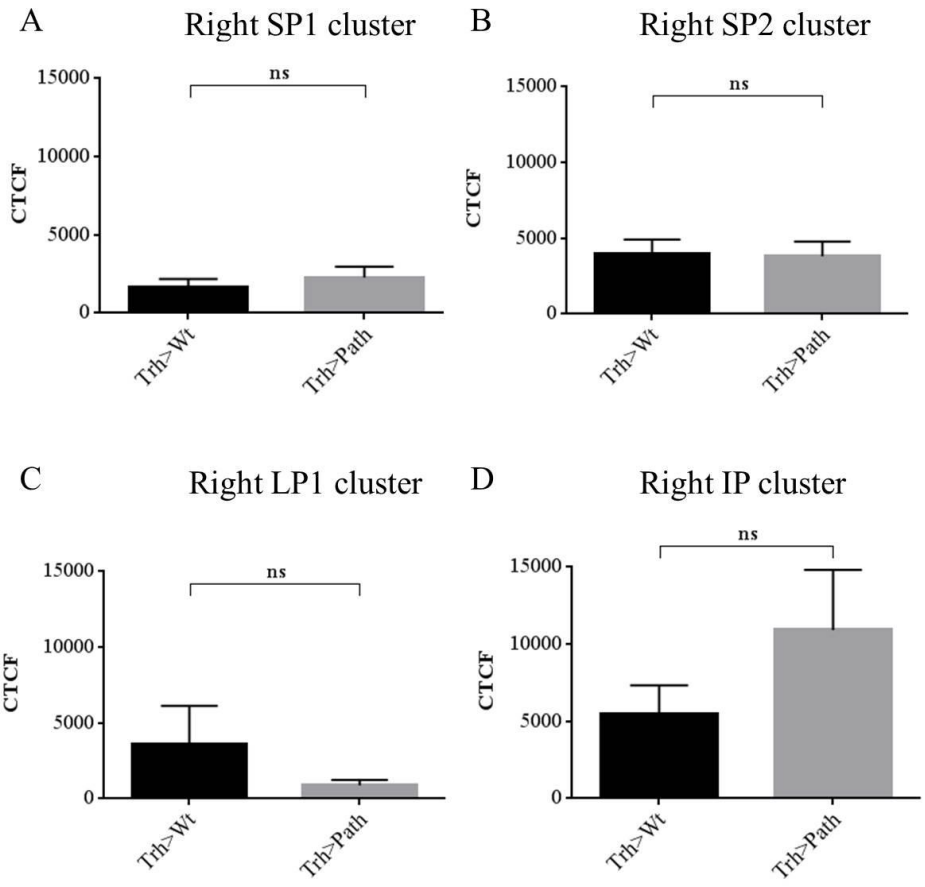


**Figure 4.36 Serotonin signal in the right hemisphere upon Pathetic overexpression.**

(SP1, A; SP2, B; LP1, C; IP, D) Clusters of the right hemisphere. TOR signalling was upregulated in serotonergic clusters by using the driver line Trh-Gal4 for crosses with UAS-Path. As control Trh-Gal4 was crossed with the wildtype strain (Wt) OregonR-S. The serotonin signal was measured in the serotonergic clusters of third instar larvae. The figures (A-D) represent the corrected total cell fluorescence (CTCF) of the clusters in the right hemisphere. N=6. Not significant (ns): p>0.05.

Also the overexpression of Pathetic did not increase the serotonin signal in the larval serotonergic clusters (Figure 4.36 and Table 4.4) although it increased Trh level in those clusters (Figure 4.21).

**Table 4.4 Statistical analysis of the serotonin signal upon Pathetic overexpression.**
Unpaired 2-tailed Student's t-test with Welch correction was used to analyse the data for significant differences. The statistical tests were performed with GraphPad Prism. N=6. Ns (not significant): p>0.05;

| t-test | | |
|---|---|---|
| **Serotonergic cluster** | **Trh-Gal4>Wt vs. Trh-Gal4>UAS-Path** | |
| | **left cluster** | **right cluster** |
| **SP1** | p=0.3850; ns | p=0.4856; ns |
| **SP2** | p=0.2045; ns | p=0.9307; ns |
| **LP1** | p=0.3450; ns | p= 0.2897; ns |
| **IP** | p=0.7693; ns | p=0.2475; ns |
| **SE1** | p=0.1526; ns | p=0.3594; ns |
| **SE2** | p=0.2018; ns | p=0.2519; ns |
| **SE3** | p=0.1374; ns | p=0.4467; ns |
| **T1** | p=0.3976; ns | p=0.3172; ns |
| **T2** | p=0.3017; ns | p=0.2972; ns |
| **T3** | p=0.1769; ns | p=0.2557; ns |

It could be shown that the serotonin signal is not affected by TOR manipulation. However, data indicated that serotonin release is decreased (Figure 4.24, Figure 4.33). It was assumed that the used method was not sensitive enough to reveal low differences in neurotransmitter amount. Therefore, as readout, the effect of TOR signalling in serotonin producing neurons was analysed on fat metabolism and starvation resistance.

## 4.5 Fat metabolism upon TOR manipulation in serotonergic neurons

In mammals and *Caenorhabditis elegans* an effect by TOR and serotonin on fat metabolism was described. Also in *Drosophila melanogaster* an effect of TOR on fat accumulation was shown (Gutierrez et al, 2006).

### 4.5.1 Regulation of the starvation marker *lipase3* upon TOR manipulation in serotonergic clusters

Lipase3 is an acid lipase homolog similar to lysosomal lipases of humans. It was shown to be expressed in the larval fat body and highly induced in the third larval stage of *Drosophila melanogaster* (Pistillo et al., 1998). During third instar, the larval metabolism is preparing for pupation, a long phase without food intake. The enzyme is also highly upregulated upon starvation which indicates that it is needed during a period of food deprivation. Thus, the Lipase3 transcript level is used as a starvation marker (Zinke et al. 1999).

A *lip3* expression in the larva

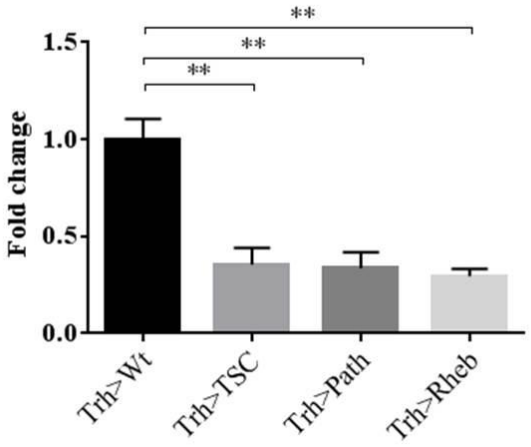


B

t-test

*lip3* expression in the larva

| Trh-Gal4>Wt vs. | p-value |
|---|---|
| Trh-Gal4>UAS-TSC1/2 | p=0.0036; ** |
| Trh-Gal4>UAS-Path | p=0.0030; ** |
| Trh-Gal4>UAS-Rheb | p=0.0041; ** |

**Figure 4.37 Analysis of *lipase3* expression in third instar larvae upon manipulation of TOR signalling.**
TOR pathway was manipulated using the Gal4-UAS system. TOR signalling was downregulated in the serotonergic neurons by using the driver line Trh-Gal4 for crosses with UAS-TSC1;UAS-TSC2. An upregulation of TOR signalling was achieved by crossing Trh-Gal4 with UAS-Rheb or UAS-Path. As control Trh-Gal4 was crossed with the wildtype strain (Wt) OregonR-S. Data was normalized to the control sample. Expression was analysed in the whole larva. *Lipase3* (*lip3)* transcript level of the control larvae was compared to the expression upon TOR signalling activation and deactivation. Unpaired 2-tailed Student's t-test with Welch correction was used to analyse the data for significant differences. N=4. The error bars represent the standard error of the mean (SEM). **=p<0.01.

Third instar larvae with manipulated TOR pathway in serotonin producing neurons show a lower *lipase3* transcript level than the control when fed with nutrient-rich yeast. Like *ddc* expression, *lip3* expression is downregulated equally whether TOR is activated or deactivated in Trh positive cells. It was assumed that the lowered *lip3* level might influence the mobilization of storage lipids and reduce the starvation resistance of flies. Therefore, a starvation assay on flies with manipulated TOR signalling in serotonergic neurons was performed

### 4.5.2 Starvation resistance upon TOR manipulation in serotonergic clusters

The previous results for *lipase3* expression suggest that a low Lipase3 level might occur in larvae with manipulated TOR signalling. This could affect the storage fat mobilization in the fat body. Fat mobilization is important during starvation to provide the organism with enough energy to survive. It was examined whether the lowered *lip3* level due to TOR manipulation in serotonergic tissues leads to a lowered starvation resistance. Therefore, third instar larvae were starved in vials containing PBS agar. Each vial contained 20 third instar larvae. Dead larvae were removed every day. The number of pupated and hatched larvae was documented to compare the survival of larvae without and with TOR manipulation in serotonergic tissues. Upon starvation pupation took place five to six days after egg laying. The adult flies eclosed eleven to 13 days after egg laying. Thus, pupae were counted after six and adults after fourteen days.

A

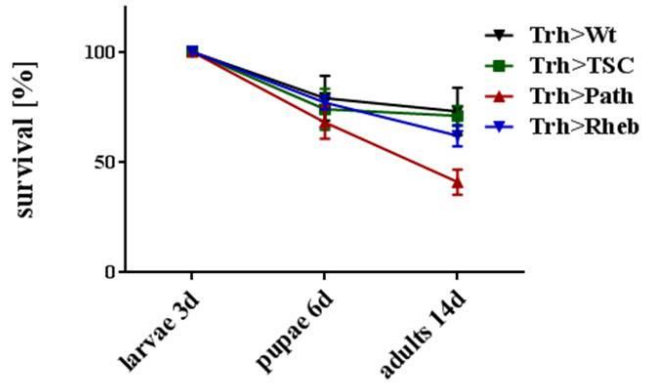


B

Log-rank (Mantel-Cox) test

| Trh-Gal4> Wt vs. | survival |
|---|---|
| Trh-Gal4>UAS-TSC1/2 | p=0.4350; ns |
| Trh-Gal4>UAS-Path | p=0.0108; * |
| Trh-Gal4>UAS-Rheb | p=0.1663; ns |

**Figure 4.38 Survival of third instar larvae with manipulated TOR signalling upon starvation.**
Survival was recorded in 74+/-2 hour (3days) old larvae. TOR signalling was downregulated in the serotonergic neurons by using the driver line Trh-Gal4 for crosses with UAS-TSC1;UAS-TSC2. An upregulation of TOR signalling in the offspring was achieved by crossing Trh-Gal4 with UAS-Rheb or UAS-Path. As control Trh-Gal4 was crossed with the wildtype strain (Wt) OregonR-S. Survival of the control larvae was compared to the survival upon TOR signalling activation and deactivation. Days (d). Log-rank test was used to analyse the data for significant differences. N=5. The error bars represent the standard error of the mean (SEM). *=$p \leq 0.05$.

It was expected, that larvae with manipulated TOR pathway show a lower survival upon food deprivation than the control larvae. The results show that there is no difference in survival to the control whether TOR signalling was upregulated via Rheb overexpression or downregulated via TSC1 and TSC2 overexpression in serotonergic neurons. Just for Pathetic overexpression a significant difference in the amount of eclosed adults was observed (Figure 4.38). Although the larval survival is not affected by UAS-TSC1;UAS-TSC2 or UAS-Rheb

overexpression until the adult stage, a lower survival was observed after eclosion compared to the control. To analyse whether a lowered fat mobilization in the prepupal stage was responsible for this effect, the storage fat level was measured.

### 4.5.3 TOR signalling effect in serotonin producing neurons on fat metabolism of third instar larvae

Although the starvation experiments showed no difference in the survival of larvae with and without manipulated TOR signalling in serotonergic neurons, the lowered survival of the eclosed flies indicated that the fat mobilization might be decreased. Therefore, the triacylglyceride (TAG) content was visualized by thin layer chromatography (TLC).

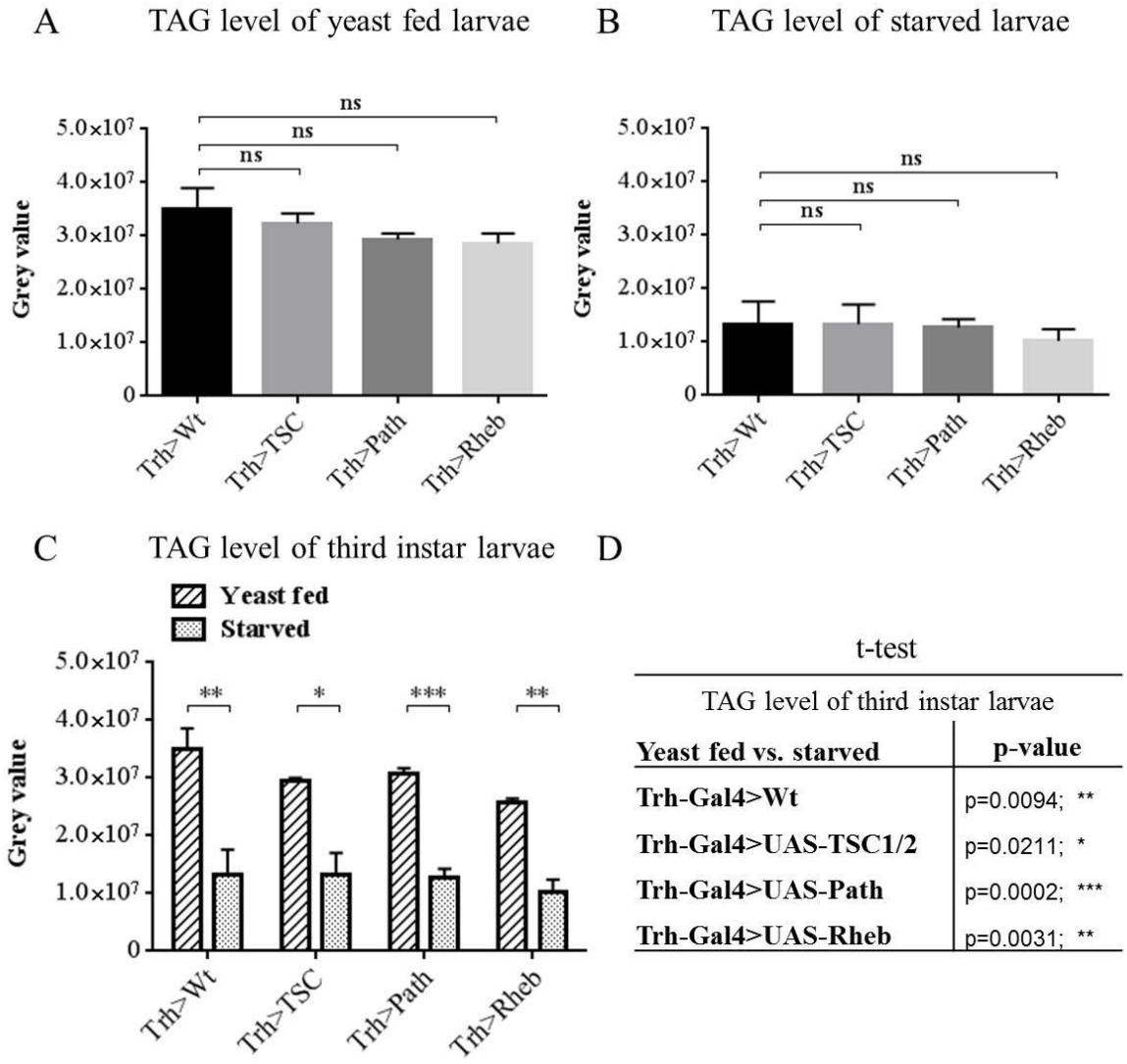


t-test

TAG level of third instar larvae

| Yeast fed vs. starved | p-value |
|---|---|
| Trh-Gal4>Wt | p=0.0094; ** |
| Trh-Gal4>UAS-TSC1/2 | p=0.0211; * |
| Trh-Gal4>UAS-Path | p=0.0002; *** |
| Trh-Gal4>UAS-Rheb | p=0.0031; ** |

**Figure 4.39 Triacylglyceride (TAG) level of third instar larvae with manipulated TOR pathway.**
The TAG level was analysed by thin layer chromatography (TLC) in yeast fed and starved larvae. TOR pathway was manipulated using the Gal4-UAS system. TOR signalling was downregulated in the serotonergic neurons by using the driver line Trh-Gal4 for crosses with UAS-TSC1;UAS-TSC2.

An upregulation of TOR signalling was achieved by crossing Trh-Gal4 with UAS-Rheb or UAS-Path. As control Trh-Gal4 was crossed with the wildtype strain (Wt) OregonR-S. (A) TAG level of yeast fed control larvae was compared to the TAG level upon TOR signalling activation and deactivation in a yeast fed state (N=6). (B) TAG level of starved control larvae was compared to the TAG level upon TOR signalling activation and deactivation in a starved state (N=4). (C) TAG level of fed larvae was compared to the TAG level of the starved state of each cross (N=4). Unpaired 2-tailed Student's t-test with Welch correction was used to analyse the data for significant differences. (D) t-test data of TAG level comparison of the fed and the starved state. N=4. The error bars represent the standard error of the mean. Not significant (ns.)=$p>0.05$; *:$p\leq0.05$; **: $p\leq0.01$; ***: $p\leq0.001$.

The fat level of fed and starved third instar larvae with and without manipulated TOR signalling in serotonergic neurons was examined. The intensity of the TAG signal was measured by Fiji. It was expected that larvae with manipulated TOR pathway and therefore, a reduced *lipase3* transcript level show a higher fat content upon starvation than the control larvae as the fat mobilization in those might be diminished. The results show that the TAG content is equal in larvae with and without manipulated TOR signalling in serotonergic neurons (Figure 4.39 A). Also starved larvae show no difference in the TAG level (Figure 4.39 B). The reduction of fat upon starvation compared to the fed state also shows a similar depletion in all of the crosses (Figure 4.39 C). Consequently, it could be shown that in larvae with activated and deactivated TOR signalling in serotonergic tissues fat storage and mobilization is not diminished. Further experiments were performed on adult flies as the tendency of a lowered starvation resistance was observed after eclosion.

## 4.6 TOR signalling in serotonergic neurons of adult flies

The brain structure and function and also the behavioural repertoire of adult flies are more complex than in larvae. While the larval behaviour is reduced to mostly crawling and feeding, the adult flies are mobile and can choose to find a partner for mating, to show aggression and to move to different food sources. Food preference and also resistance to food deprivation in adult flies was shown to be affected by serotonin (Vargas et al, 2010; Luo et al 2012). Previous results showed that *ddc* and the starvation marker *lipase3* level are decreased upon TOR manipulation in serotonin producing cells in larvae. It was assumed that this effect occurred due to changes in serotonin production and release. Therefore, the *ddc* and *lipase3* transcript levels were analysed in adult flies to identify whether they are regulated the same way after pupation. To identify whether changes in serotonin signalling occur upon TOR manipulation in serotonergic neurons also the resistance to starvation was analysed in adult flies.

### 4.6.1 Transcription level of *ddc* and *lipase3* in adult males upon TOR manipulation

TOR signalling in serotonergic neurons affected the expression of the target genes *ddc* and *lip3* in larvae. It was analysed whether the effect of a manipulated TOR pathway in serotonergic neurons on *ddc* and *lip3* expression is the same in adult flies as in the larval stage. Therefore, the expression of these enzymes in whole adult males was analysed.

A *ddc* expression in adult males

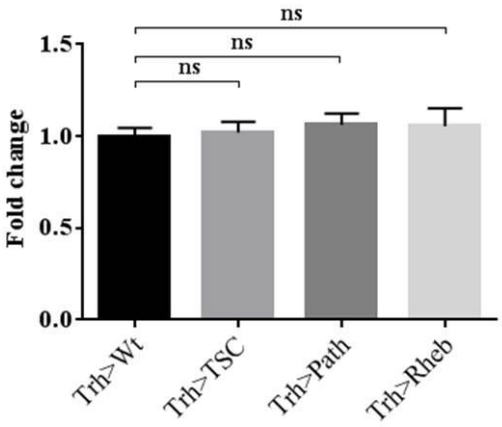


B

t-test

*ddc* expression in adult males

| Trh-Gal4>Wt vs. | p-value |
|---|---|
| Trh-Gal4>UAS-TSC1/2 | p=0.7884; ns |
| Trh-Gal4>UAS-Path | p=0.4344; ns |
| Trh-Gal4>UAS-Rheb | p=0.6299; ns |

**Figure 4.40 Analysis of *dopa decarboxylase* expression in adult males upon manipulation of TOR signalling.**
TOR pathway was manipulated using the Gal4-UAS system. TOR signalling was downregulated in the serotonergic neurons by using the driver line Trh-Gal4 for crosses with UAS-TSC1;UAS-TSC2. An upregulation of TOR signalling was achieved by crossing Trh-Gal4 with UAS-Rheb or UAS-Path. As control Trh-Gal4 was crossed with the wildtype strain (Wt) OregonR-S. Data was normalized to the control sample. Expression was analysed in the adult males. *Dopa decarboxylase* (*ddc*) transcript level of the control fruit flies was compared to the expression upon TOR signalling activation and deactivation. Unpaired 2-tailed Student's t-test with Welch correction was used to analyse the data for significant differences. N=5. The error bars represent the standard error of the mean (SEM). The differences to the control are not significant (ns.). Ns: $p>0.05$

The result for *ddc* expression shows no significant difference between the experiment crosses and the control (Figure 4.40). Therefore, in this case the *ddc* expression in adult males did not resemble the expression in the third instar larvae.

A *lip3* expression in the male fly

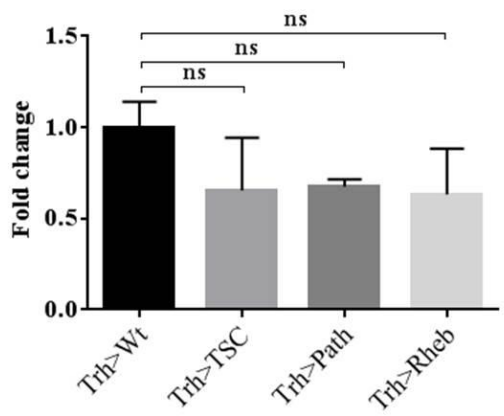


B

t-test

*lip3* expression in the male fly

| Trh-Gal4>Wt vs. | p-value |
|---|---|
| Trh-Gal4>UAS-TSC1/2 | p=0.3391; ns |
| Trh-Gal4>UAS-Path | p=0.1000; ns |
| Trh-Gal4>UAS-Rheb | p=0.2607; ns |

**Figure 4.41 Analysis of *lipase3* (*lip3*) expression in adult males upon manipulation of TOR signalling.**
TOR pathway was manipulated using the Gal4-UAS system. TOR signalling was downregulated in the serotonergic neurons by using the driver line Trh-Gal4 for crosses with UAS-TSC1;UAS-TSC2. An upregulation of TOR signalling was achieved by crossing Trh-Gal4 with UAS-Rheb or UAS-Path. As control Trh-Gal4 was crossed with the wildtype strain (Wt) OregonR-S. Data was normalized to the control sample. Expression was analysed in males. *Lip3* transcript level of the control males was compared to the expression upon TOR signalling activation and deactivation. Unpaired 2-tailed Student's t-test with Welch correction was used to analyse the data for significant differences. N=4. The error bars represent the standard error of the mean (SEM). The differences to the control are not significant (ns.). Ns: p>0.05

Figure 4.41 shows that in adult male fruit flies also the regulation of *lip3* expression in the whole organism is not affected by a changed TOR signalling in serotonergic tissues. Thus, *ddc* and *lip3* transcript level that are affected in the larva are not regulated the same way in the adult males. Although the expression of the starvation marker *lipase3* is not affected in these flies, previous results showed that a tendency of a reduced starvation resistance of adults occurred (Figure 4.38). To determine that starvation resistance is diminished in adults with manipulated TOR pathway in serotonergic neurons, adult males were analysed in a starvation assay.

### 4.6.2 Starvation resistance upon TOR manipulation in adult males

During pupation the larval brain structures and neuronal connections change (Jefferis et al, 2002; Roy et al, 2007). Accordingly, there might be a difference between larvae and adults in the effect of metabolic manipulation in neurons. The previous observation that after eclosion *Drosophila melanogaster* adults with manipulated TOR pathway might be more vulnerable to starvation suggested that starvation resistance could be affected in adults. Therefore, the starvation assay was repeated for adult males with and without manipulated TOR signalling in serotonergic neurons.

A

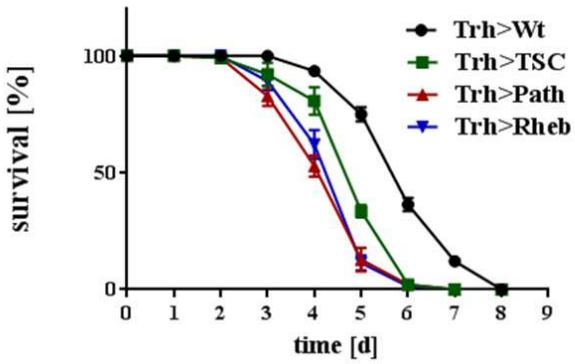


B

Log-rank (Mantel-Cox) test

| Trh-Gal4> Wt vs. | survival |
|---|---|
| Trh-Gal4>UAS-TSC1/2 | p=0.0895; ns |
| Trh-Gal4>UAS-Path | p=0.0003; *** |
| Trh-Gal4>UAS-Rheb | p=0.0018; ** |

**Figure 4.42 Survival of adult males with manipulated TOR signalling upon starvation.** Survival was recorded starting seven days after eclosion. TOR signalling was downregulated in the serotonergic neurons by using the driver line Trh-Gal4 for crosses with UAS-TSC1;UAS-TSC2. An upregulation of TOR signalling was achieved by crossing Trh-Gal4 with UAS-Rheb or UAS-Path. As control Trh-Gal4 was crossed with the wildtype strain (Wt) OregonR-S. Survival of the control flies was compared to the survival upon TOR signalling activation and deactivation. Log-rank test was used to analyse the data for significant differences. N=7. The error bars represent the standard error of the mean (SEM). Not significant (ns): $p>0.05$; **$p\leq0.01$; ***=$p\leq0.001$.

After a period of around 72 hours the fruit flies began to die of food deprivation. However, control flies survived longer than flies with manipulated TOR pathway. Activation of TOR by Rheb or Pathetic overexpression led to a significantly lowered survival upon starvation (Figure 4.42 A and B). The log rank test showed that a downregulation of TOR signalling by TSC complex overexpression did not affect survival significantly although a tendency of a decreased starvation resistance was observed (Figure 4.42 B). The results show that TOR manipulation in serotonergic neurons affects the starvation resistance of adults. The resistance to starvation was also shown to be decreased upon a lowered serotonergic signalling in the IPC's, which increased the insulin signalling in flies (Luo et al, 2012). Therefore, it was analysed whether insulin signalling is increased in flies with manipulated TOR signalling in serotonin producing neurons.

### 4.6.3 TOR signalling manipulation in serotonergic neurons affects insulin signalling in the adult male flies

A diminished starvation resistance was also shown upon a serotonin receptor knockout in the Insulin producing cells. The IPC's in the brain of *Drosophila melanogaster* produce three different types of Drosophila insulin like peptides. Those are Dilp2, Dilp3 and Dilp5. The production and release of these peptides is regulated by different factors and neurotransmitters to adjust the insulin signalling in the body to the organismal needs and to environmental changes. The serotonin receptor *5-HT$_{1A}$* is expressed in the IPC's and was shown to affect

*dilp3* and *dilp5* transcript level and also the level of the neuropeptide Dilp2 (Luo et al, 2012). Upon downregulation of this receptor by RNA interference (RNAi) in the IPC's the starvation resistance of flies was decreased. The ablation of IPC's was shown to increase starvation resistance (Broughton et al, 2005). Hence, a decreased starvation resistance indicates an increased insulin signalling. Due to a negative feedback mechanism on the insulin receptor (InR), transcription of this receptor is reduced when insulin signalling is elevated. Upon low insulin signalling dFOXO is dephosphorylated and can enter the cell nucleus, where it acts as a transcription factor increasing *InR* transcription. Whereas upon elevated insulin signalling FOXO is phosphorylated and inactive which results in a lowered InR transcript level. Therefore the *InR* transcript level is a marker for insulin signalling.

To analyse whether insulin signalling is elevated in flies with manipulated TOR signalling in serotonergic neurons, the transcript level of *InR* was analysed.

A *InR* expression in the male fly

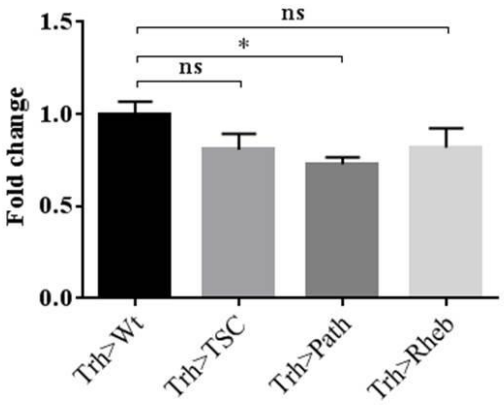


B

t-test

*InR* expression in the male fly

| Trh-Gal4>Wt vs. | p-value |
|---|---|
| Trh-Gal4>UAS-TSC1/2 | p=0.1287; ns |
| Trh-Gal4>UAS-Path | p=0.0181; * |
| Trh-Gal4>UAS-Rheb | p=0.2047; ns |

**Figure 4.43 Analysis of the *insulin receptor* expression in adult males upon manipulation of TOR signalling.**

TOR pathway was manipulated using the Gal4-UAS system. TOR signalling was downregulated in the serotonergic neurons by using the driver line Trh-Gal4 for crosses with UAS-TSC1;UAS-TSC2. An upregulation of TOR signalling was achieved by crossing Trh-Gal4 with UAS-Rheb or UAS-Path. As control Trh-Gal4 was crossed with the wildtype strain (Wt) OregonR-S. Data was normalized to the control sample. Expression was analysed in males. *Insulin receptor* (*InR*) transcript level of the control males was compared to the expression upon TOR signalling activation and deactivation. Unpaired 2-tailed Student's t-test with Welch correction was used to analyse the data for significant differences. N=4. The error bars represent the standard error of the mean (SEM). *:$p \leq 0.05$.

Figure 4.43 shows that the insulin receptor is slightly down regulated in flies with manipulated TOR signalling. This indicates an increase in insulin signalling. Though also for the flies with TSC1; TSC2 and Rheb overexpression in serotonergic neurons the tendency of a decreased *InR* transcription could be observed, the effect is not as strong as for Path overexpression and not significant. Taken together the data for Pathetic overexpression in

serotonin producing neurons showed that insulin signalling was slightly increased, which indicated an increase of Dilp release. Data for TSC1; TSC2 and Rheb overexpression was not sufficient to show a significant increase of insulin signalling compared to the control.

# 5 Discussion

Single amino acids were shown to affect the transcription and translation of target genes (Kimball and Jefferson, 2006). In this thesis the regulatory effect of amino acids on metabolic and neuronal target genes was analysed. The regulation of the target gene *tobi* by amino acids was characterized as an example for a metabolic target in the adjustment of the nutritional information. One of the mechanisms that might be important to mediate the information of the internal amino acid status is the TOR signalling pathway. The information about the availability of certain amino acids is passed to the TOR pathway by transceptors which have an affinity to certain amino acids. TOR signalling then mediates the adjustment of metabolic processes and growth to the amino acid availability (Colombani et al, 2003). TOR pathway is not just involved in amino acid signalling. It was also shown to affect the behavioural adjustment to the organismal needs. For example, the activation of TOR signalling in the brain increased the preference of *Drosophila melanogaster* to protein rich food. The same effect was observed upon feeding of 5HTP, a serotonin precursor that increases serotonin production. It was assumed that TOR signalling in the brain might affect serotonin production and release (Vargas et al, 2010). It is suggested that the signalling process is involved in the provisioning of nutritional information. In this thesis, it could be shown that the transceptor Pathetic is expressed in serotonergic neurons (Figure 4.14). It was characterized whether the serotonin producing enzymes are neuronal target genes of the TOR pathway. Additionally, the effect of Pathetic and TOR signalling on serotonin production was analysed.

## 5.1 The amino acid dependent regulation of *tobi* transcript level

The alpha glucosidase *tobi* is a highly conserved enzyme that is also abundant in zebra fish mouse and in human. It is part of the sugar metabolism and was shown to affect the glycogen breakdown. Though it is involved in the sugar metabolism, its transcription was shown to be affected by the protein level of the ingested food (Buch et al, 2008). This regulation was investigated further in this thesis.

### 5.1.1 The single amino acid composition of a food source affects *tobi* transcript level

Yeast is the natural protein source of *Drosophila melanogaster*. During evolution, the organism adjusted its metabolism to the yeast composition to reach an optimal utilization of its components and in this way optimal growth. The adjustment can be observed by the strong effect yeast has on *tobi* transcript level (Figure 4.1). Transcription of *tobi* was very sensitive to the amount and composition of amino acids and peptides in the food. Especially the composition of yeast peptone was shown to affect *tobi* transcript level stronger than every other peptide and amino acid rich food source.

The single amino acid glycine was able to enhance *tobi* transcription in a concentration dependent way (Figure 4.4). Nutritional stress had the opposite effect on *tobi* transcript level (Figure 4.5). Therefore, an increase of *tobi* transcription by nutritional stress due to amino acid imbalance could be excluded. The induction by glycine was stronger in female than in male flies (Figure 4.4). Also yeast peptone, sugar and fish peptone induced *tobi* expression stronger in females than in males, while soy, gelatine, meat and casein extract feeding did not result in such differences (Figure 4.2). However, some amino acid and peptide compositions led to a sexual dimorphism in the induction of the metabolic target gene transcription. The hemolymph amino acid composition is affected not just by nutrition but also by stress, age and sex (Cônsoli and Vinson, 2002; Hrassnigg et al., 2003). Therefore, it was assumed that the dimorphism occurred due to different metabolic needs of the sexes, which led to different hemolymph amino acid compositions.

Amino acid availability activates TOR signalling. This induction was shown to be mediated by transceptors that have different amino acid affinities and whose expression is also in some cases limited to certain tissues (Colombani et al., 2003; Goberdhan et al, 2005). It was assumed that different amino acid compositions could strongly induce TOR signalling when the corresponding transceptors are highly expressed in the tissue of interest. There might also be a different transceptor distribution in male and female adults of *Drosophila melanogaster*.

It was shown that the availability and composition of peptides is important for the strong induction of *tobi* expression by yeast peptone (Figure 4.3). A yeast food mix induced a stronger effect on *tobi* transcript level than the corresponding food mix of the same amino acid composition in the form of single amino aicds. However, it is not clear whether peptides are able to signal and provide nutritional information on their own. Peptides are cleaved into single amino acids or can be transported directly into the hemolymph as di- and tripeptides. It was assumed that transporters which are involved in peptide transport could also have

transceptor function. In addition, peptides can be used by gut bacteria for D-isomer production of certain amino acids (Lemaitre and Miguel-Aliaga, 2013; Miguel-Aliaga, 2012). In this way, the final amino acid composition in the hemolymph might also be affected. Taken together the amino acid and peptide composition of the food is able to regulate the expression of the metabolic target gene *tobi*. The regulation is assumed to be controlled by the TOR signalling pathway and mediated by specialized transceptors in *tobi* expressing tissues. This was shown when overexpression of the transceptor Pathetic affected *tobi* transcription and the transcriptional TOR target *cabut* alike (Figure 4.7). Additional analyses for example by RNA interference (RNAi) are needed to confirm the effect by Pathetic and TOR signalling on *tobi* expression. It needs to be detemined whether also an effect on Tobi protein level occurs upon Pathetic overexpression. Furthermore, effects by other transceptors have to be analysed.

### 5.1.2 *Pathetic* overexpression might disrupt the interaction of TOR with complex components at the nutrisome

The fat body is responsible for the adjustment of growth in respect to the nutritional situation. Thus, it is an organ that functions as a nutritional sensor. The sensor function was shown to be regulated by the transceptor Slimfast which transports cationic amino acids like arginine and signals the transport to the TOR pathway. In this way, growth in the whole organism is affected (Columbani et al, 2003). Like Slimfast also Pathetic serves as a transceptor that signals the amino acid availability and uptake via TOR. During transport, it shows a high affinity for small neutral amino acids like glycine and alanine (Goberdhan et al, 2005).

It could be shown that the transcript level of the alpha glucosidase *tobi* increased in a concentration dependent manner by the single amino acid glycine (Figure 4.4). An increased transport triggers the TOR pathway which in turn might have activated the transcription of *tobi*. It could be shown that *tobi* transcript level is affected by TOR signalling as rapamycin feeding reduces *tobi* expression (Buch, unpublished data; Figure 8.4 and Figure 8.5). Transceptors like Pathetic were assumed to be involved in this process. Therefore, the effect of Pathetic on tobi expression was analysed further. An overexpression of the Pathetic transceptor in the fat body was assumed to increase *tobi* transcript level via an increased TOR signalling. Instead, it turned out that an increased *pathetic* transcription decreased TOR signalling and *tobi* expression (Figure 4.7). Therefore, a negative effect of transceptor overexpression could be demonstrated and a possible correlation of TOR signalling and *tobi* expression could be confirmed.

While *tobi* expression was decreased, an increase of *pathetic* transcription could also be observed upon hydrogen peroxide feeding (Figure 4.5 and Figure 4.6). The increased Pathetic expression might have an effect on the *tobi* transcription. However, a direct effect of Pathetic availability on *tobi* transcription needs to be investigated further as the regulation of TOR pathway by nutritional stress was not examined yet.

The Proton assisted amino acid transporter Pathetic (Path) forms a complex with the components of the TOR pathway on late lysosomal and endosomal compartments (LELs). Those are then termed as nutrisomes. Pathetic signals the transport of amino acids form these compartments into the cell lumen. However, the mechanism how these amino acids are transported into the compartments remains unclear (Ögmundsdóttir et al, 2012). Therefore, an inducing effect of increased Pathetic expression on TOR signalling could be limited by the amino acid availability in the nutrisome. Pathetic was actually shown to activate TOR pathway. In wing tissue it was also shown to decrease growth (Goberdhan et al, 2005). However, Pathetic seems to affect TOR signalling in a tissue specific way. There could also be the contrary effect by amino acid signalling of the transceptor and an exceeding availability of it. The transport of glycine by Pathetic might induce TOR signalling while an increase of the transceptor availability might disrupt it.

Goberdhan et al observed in 2005 that a strong Pathetic ovexpression decreased overall growth and suggested that it disrupts the formation of a TOR multiprotein complex. So far, other transceptors that are involved in the nutrisome formation have not yet been described. Still, other single amino acids, especially the branched chained amino acids, are able to induce TOR signalling (Kimball and Jefferson, 2006; Meijer and Codogno, 2008). Therefore, there might be further transceptors involved in the provisioning of nutritional information at the nutrisome. Though Pathetic is expressed in the fat body its expression in this organ was rated as moderate by Flyatlas Anatomical Expression Data (http://flybase.org/reports/FBgn0036007.html). By overexpressing Pathetic in the fatbody, the interaction of the TOR complex with Pathetic is increased while the interaction with other transceptors could be lowered. Accordingly, their amino acid signalling would be diminished and because glycine and alanine level in yeast is low compared to the amount of other amino acids (Table 8.2), TOR signalling is decreased compared to the controls, although glycine and alanine transport would be increased.

Taken together, the effect of the amino acid and peptide composition on the metabolic target *tobi* indicated that a nutrient dependent regulation occurred. The nutritional information is assumed to be processed via amino acid sensing pathways. The TOR pathway is the major

pathway for amino acid sensing. It adjusts its target gene expression to the nutrient status (Bülow et al, 2010). It could be shown that TOR signalling affects *tobi* expression (Figure 4.7 and Buch unpublished data in Figure 8.4). TOR pathway was also shown to affect feeding behaviour (Ribeiro and Dickson, 2010). It is suggested that it is involved in the adjustment of appetite to the internal nutrient status. Therefore, its effect on neuronal target genes was analysed to identify a possible function in the provisioning of nutritional information for the brain.

## 5.2 The role of TOR signalling in serotonin production

The transceptor Pathetic was shown to be highly expressed in serotonergic clusters of the larval *Drosophila melanogaster* brain (Figure 4.14). It signals the availability of amino acids via the TOR pathway. Increased preference to protein rich food occurs upon increased activation and inhibition of the TOR pathway. TOR signalling in the brain is involved in the regulation of food preference and displays the same effect as an increased serotonin production (Vargas et al, 2010; Ribeiro and Dickson, 2010). The mechanism of this regulation is unclear. Serotonin signalling affects feeding behaviour and food choice (Leibowitz and Alexander, 1998; Vargas et al, 2010; Gasque et al, 2013). Therefore, it was analysed whether TOR signalling might provide the organism with nutritional information by regulating the serotonin production.

### 5.2.1 The effect of TOR signalling on the transcription of serotonin producing enzymes

TOR signalling affects the transcription of several target genes (Bülow et al, 2010). Also *pathetic* transcript level was shown to be slightly regulated by TOR in the brain (Figure 4.9). Thus, an adaptation of transceptor availability in a nutrient rich environment occurs. *Pathetic* transcription pattern analysis in *Drosophila melanogaster* showed that the transceptor is highly expressed in neuronal cells of the brain (Figure 4.13). Some of these neurons were identified as serotonergic clusters (Figure 4.14). Serotonin is a neurotransmitter that affects feeding and food preference (Leibowitz and Alexander, 1998, Gasque et al, 2013). Previous studies revealed that TOR signalling might affect serotonin production in *Drosophila melanogaster* (Vargas et al, 2010). The regulation of serotonin production via TOR signalling might be mediated by Pathetic. It could contribute to the provision of nutritional information and to the adaptation of food preference. To find out whether TOR signalling or Pathetic

overexpression affects the transcription of the serotonin producing enzymes, several experiments were performed. However, no direct effect of TOR signalling could be confirmed for the transcriptional level of *tryptophan hydroxylase* and *dopa decarboxylase* (Figure 4.16- Figure 4.18 and Figure 4.23 – Figure 4.27). Therefore, it could be shown that the serotonin producing enzymes are no transcriptional targets of TOR signalling in the brain.

### 5.2.2 Pathetic overexpression increases the Trh but not the serotonin signal in serotonergic clusters

The Tryptophan hydroxylase catalyses the rate limiting step in the pathway of serotonin production (Coleman and Neckameyer, 2005; Neckameyer et al, 2007). Its transcript level was not affected by manipulating TOR signalling. Though the TOR pathway also affects transcription of target genes, its main function is the regulation of translation (Miron and Sonenberg, 2001; Kim et al, 2008; Nagarajan and Grewal, 2014). To identify whether the protein level of Trh was affected, the fluorescence signal of Trh in the serotonergic clusters in the brain of Drosophila melanogaster was measured following antibody staining. Thereby, brains with manipulated TOR signalling in the serotonin producing neurons were analysed. Downregulation of TOR by overexpression of the TSC complex and upregulation of TOR by overexpression of Rheb in the serotonin producing clusters showed no effect on Trh signal compared to the control (Table 4.1). However, a Pathetic overexpression showed a significantly higher Trh signal in most of these clusters (Table 4.2). Upon Pathetic overexpression in some clusters on one side of the brain a significantly higher Trh signal was observed, while the corresponding cluster on the other side showed no significant difference (Figure 4.22). The clusters still showed a tendency of an increased signal, which might indicate that the used method is not sensitive enough to detect lower signal differences. The increased Trh protein level that was detected upon Pathetic overexpression could increase serotonin production. However, an increased serotonin signal could not be detected for Pathetic, Rheb or TSC1 and TSC2 overexpression (Figure 4.34 - Figure 4.36 and Table 4.3 – Table 4.4). A high signal variance in the individual brains could be observed in all clusters. Due to these results it cannot be determined with certainty that serotonin production is not changed by manipulating TOR signalling. Further experiments like enzyme-linked immunoabsorbant assays (ELISA) are needed to confirm or exclude possible changes in serotonin level.

An increased serotonin release parallel to an increased serotonin production might occur upon Pathetic overexpression. This would explain why the increased Trh level did not increase the

serotonin signal in the serotonergic clusters. Nevertheless, the data indicates that Pathetic overexpression decreased serotonin release (Figure 4.42, Figure 4.43). Possibly Pathetic decreases the reuptake of serotonin into vesicles or the vesicle fusion und thus serotonin release. Further experiments are needed to identify how Pathetic decreases serotonin release and signalling in *Drosophila melanogaster*.

It is probable that changes in serotonin signal could not be detected by antibody staining and fluorescence measurement. Therefore, other readouts were used to determine changes in serotonin release. Serotonin signalling was shown to affect starvation resistance and insulin signalling in *Drosophila melanogaster* (Ruaud and Thummel, 2008; Luo et al, 2012; Luo et al, 2014). Therefore, the effect of TOR manipulation in serotonergic neurons on the starvation marker *lipase3*, on starvation resistance and on insulin signalling was analysed.

### 5.2.3 The effect of TOR pathway manipulation in serotonergic clusters on fat metabolism

Serotonin was shown to affect fat metabolism in *C. elegans*, in humans and also in the fruit fly (Srinivasan et al, 2008; Jones and Ashrafi, 2009; Luo et al, 2012; Donovan and Tecott, 2013). Adults of *Drosophila melanogaster* with a knockdown of the serotonin receptor $5HT_{1A}$ showed a reduced lipid level upon starvation. Serotonin was also shown to affect starvation resistance in *Drosophila melanogaster*. A decrease in serotonin signalling also decreased the survival upon food deprivation (Luo et al, 2012). The starvation marker *lipase3* is upregulated upon food deprivation (Pistillo et al., 1998, Zinke et al. 1999). Upon TOR manipulation in serotonergic neurons of third instar larvae, *lipase3* level was reduced (Figure 4.37). Perhaps manipulation of the TOR pathway in serotonergic neurons signals a nutrient rich state, lowering *lip3* transcription. It was assumed that a change in *lip3* level could affect the TAG level. However, no such effect could be observed for the storage of lipids upon yeast feeding or starvation (Figure 4.39). This result showed that changes in *lip3* have no effect on lipid level and the fat mobilization in the larvae of *Drosophila melanogaster*.

Adults of *Drosophila melanogaster* showed no difference in their *lipase3* transcript level upon TOR manipulation in serotonin producing neurons (Figure 4.41). Nevertheless, those flies had a reduced starvation resistance, especially upon upregulation of TOR signalling (Figure 4.42). This suggested that the reduced *lipase3* level in the larva might be related to the energy level of the adult. To confirm this assumption, TAG measurements in adults upon starvation are necessary. It is also possible that the *lipase3* level had no effect on the adult starvation response as upon TOR downregulation no significant difference to the control in

starvation resistance was observed, although *lipase3* level was downregulated in the larva. Then the lowered starvation resistance in adult flies occurred due to other effects caused by changes in serotonin production and release.

### 5.2.4 Changes in serotonin production might lead to reduced starvation resistance during pupation

The effect of starvation was also explored in third instar *Drosophila melanogaster* larvae until development into adults. Vargas et al showed in 2010 that a lowered serotonergic signalling by $5HT_{1A}$ receptor knockdown in the IPCs leads to a decrease in the starvation resistance. This receptor is expressed in the IPCs during the adult stage. Activation of the TOR pathway via Rheb and Pathetic in serotonergic tissues decreases the survival of adults upon starvation (Figure 4.42). The downregulation via TSC overexpression showed no significant difference compared to the control although a tendency of a reduced starvation resistance could be observed (Figure 4.42). No effect on starvation resistance could be revealed during development of third instar larvae (Figure 4.38). However, it could be shown that the survival of adults as well as of pupae into the adult stage was reduced in larvae with Pathetic overexpression in Trh positive cells (Figure 4.38). Upon Pathetic overexpression in serotonin producing neurons also a significant increase of Trh level in most serotonergic clusters was observed (Table 4.2). Upon Rheb and TSC overexpression no difference in the Trh signal could be distinguished. However, in adults also Rheb overexpression lead to a significantly reduced starvation resistance and TSC complex overexpression showed the same tendency (Figure 4.42). Thus, there might be the same but slighter changes in Trh level than upon Pathetic overexpression that could not be measured so far. These results indicate that Pathetic overexpression induces a stronger effect on serotonin production or release than the overexpression of important TOR pathway regulators. Maybe the changes in serotonergic signalling induce a reduced resistance to starvation. Thereby, the strong effect by Pathetic overexpression causes starvation as soon as the adult structures and expression patterns are established in the pupa. Here, the serotonin receptor $5HT_{1A}$ in the IPC's might be involved as it is expressed in the adult stage and was shown to affect starvation resistance (Luo et al, 2012). Although upon Pathetic overexpression the Trh level is increased, the other results indicate a decrease in serotonin signalling (Figure 4.24, Figure 4.32, Figure 4.33, Figure 4.31). Therefore, signalling via Pathetic might just have increased the translation of Trh but did not activate the enzyme. Kuhn et al showed in 2002 that the brain tryptophan hydroxylase needs to be activated via phosphorylation by the protein kinase A (PKA). Thus, it is assumed

that further factors decrease the serotonin production in spite of an increased enzyme level. A misbalance in TOR signalling might be involved in changes of serotonin production or release.

### 5.2.5 Pigmentation of *Drosophila melanogaster* adults is affected by a changed TOR signalling in serotonergic tissues

The same observation that was shown for *lipase3* expression was also determined for *ddc* expression upon manipulation of the TOR pathway. The expression was reduced in third instar larvae but not in adults (Figure 4.24 and Figure 4.40). The regulation of the metabolism and also the neuronal wiring changes after metamorphosis. Thus, the effect that the manipulation of TOR signalling in serotonin producing neurons had on the expression of these genes was lost after pupation or eclosion. However, the changes in expression that were caused in larvae by a possible change in serotonin production or release affected the phenotype of the adults. This could be observed due to changes in the pigmentation of adults (Figure 4.31 and Figure 4.32). The pigment distribution was decreased in flies with manipulated TOR signalling in serotonergic tissues. This effect might be due to a changed serotonin signalling and a decreased *ddc* expression during the prepupal stage. Whether a decrease or an increase in serotonin production and release resulted in a decreased *ddc* level in larvae, was analysed by Shibire$^{ts1}$ or TrpA overexpression. The induced serotonin release mediated by TrpA had an increasing effect on *ddc* level compared to the control (Figure 4.33 A). In contrast a blockade of serotonin release by Shibire$^{ts1}$ decreased the *ddc* expression (Figure 4.33 B). The UAS-Shibire responder line was used as control regarding *ddc* expression upon different temperatures (Figure 4.33 C). In the UAS-Shibire$^{ts}$ control increased temperature reduced *ddc* transcription but data was not sufficient to show a significant effect for this regulation.

It was shown that *ddc* expression and also pigmentation are decreased by high temperatures (Gibert et al, 2007). Therefore, temperature affects *ddc* transcription the same way as assumed for serotonin deficiency. For the inactivation of the synaptic vesicle formation in serotonergic neurons a temperature shift to 32°C was necessary. The effect of reduced *ddc* transcript level upon inhibition of serotonin release might have been due to changes in temperature (Figure 4.33 B, C). Thereby, a direct correlation of the reduced *ddc* transcript level and an inhibited serotonin release cannot be determined with certainty. Further experiments are needed to identify the mechanism of *ddc* regulation upon temperature increase. Even a promotion of the

temperature effect by serotonin is possible. Tatum et al showed in 2015 that neuronal serotonin release in *Caenorhabditis elegans* is able to induce a heat shock response. Therefore, an effect due to a changed serotonergic signalling also cannot be excluded completely. The temperature shift had no downregulating effect on *ddc* level upon increased serotonin release (Figure 4.33 A). Increased serotonin release increased *ddc* level and abolished the downregulating effect on *ddc* transcription by a restrictive temperature. This indicates that serotonin signalling is needed for an appropriate *ddc* expression in the epidermis. As it was assumed, the data showed that serotonin release affects *ddc* expression in the larva. Further controls are needed to confirm or exclude that setotonin is involved in the regulation of *ddc* expression independant from temperature.

### 5.2.6 TOR manipulation in serotonergic neurons increases insulin signalling in adults of *Drosophila melanogaster*

Insulin producing cells in adults of *Drosophila melanogaster* were shown to express the $5HT_{1A}$ receptor (Luo et al, 2012). When this receptor was knocked down in the IPC's, an increased Dilp2 signal was observed in these neurons indicating changes in Drosophila insulin like peptide (Dilp) production or release. In addition, adult males were less resistant to starvation (Luo et al, 2012). Due to these results it was assumed that serotonergic signalling displays an inhibiting effect on Dilp release. Therefore, upon decreased serotonin signalling, insulin signalling was increased.

By manipulating TOR signalling in serotonergic neurons, a decreased survival rate of adults was observed upon starvation. However, the decrease was only significant for TOR upregulation (Figure 4.42). This result indicated a possible effect on serotonin signalling in the IPC's as described above. Therefore, the effect of such a manipulation on insulin signalling in adult *Drosophila melanogaster* was analysed further in this thesis. Changes in insulin signalling affect the transcription of the insulin receptor (InR). Upon increased insulin signalling the *InR* level is decreased by a negative feedback mechanism (Puig and Tjian, 2005). Thus, the transcript level of the *InR* was analysed to detect changes in insulin signalling upon TOR manipulation in serotonin producing neurons.

Insulin receptor expression in adult males was slightly decreased upon TOR manipulation in Trh positive cells (Figure 4.43). A significant difference compared to the control could be observed upon upregulation of TOR signalling by overexpression of Pathetic. In contrast, data for overexpression of the TSC complex or Rheb was not sufficient to reveal a significant effect. It showed just the tendency of a decreaseed *InR* transcript level (Figure 4.43). The

decrease of *InR* was very low. However, the survival upon starvation of adult males decreased. Again, this effect was strongest in individuals with an upregulation of TOR pathway via overexpression of Pathetic. This result corresponds to the one regarding the changes in insulin receptor expression (Figure 4.42). Therefore, the impairment of a normal TOR signalling in serotonin producing neurons of adults may lead to a reduced serotonin release. This might have affected the serotonin signalling in the IPC's as it was described for the serotonin receptor $5HT_{1A}$ knockdown (Luo et al, 2012). Insulin signalling promotes growth in developing tissues. The weak serotonin effect on insulin signalling and the late expression of the $5HT_{1A}$ receptor might explain why no obvious growth differences were observed in adults with manipulated TOR signalling in serotonergic neurons compared to controls. In addition, Luo et al observed in 2012 that the changed insulin signalling by the $5HT_{1A}$ receptor knockdown in the IPCs was not sufficient to change growth but decreased the starvation resistance in adult males. In summary, the increase of TOR signalling by Pathetic overexpression in Trh positive neurons increases insulin signalling in *Drosophila melanogaster* adults. The data indicates a reduced serotonin signalling in adults upon induction of TOR signalling in serotonin producing neurons.

### 5.2.7 TOR induction and inhibition in serotonergic neurons of *Drosophila melanogaster* larvae and adults

Up- and downregulation of TOR signalling in serotonin producing neurons of the brain led to a decrease of *ddc* level in the epidermis (Figure 4.30) and *lipase3* level of the larva (Figure 4.37). In addition, it also decreased the distribution of pigments in the cuticle of adults (Figure 4.31 and Figure 4.32). It was assumed that a decreased serotonin release is responsible for this effect. The mechanism of this regulation and why TOR up- as well as downreguation displays the same effect is unclear. However, the *ddc* and *lip3* level was not affected by TOR manipulation in adults. Though, TOR up- and downregulation in adults showed the same effect on *InR* level which was decreased. This decrease was significant only for Pathetic overexpression, while for overexpression of Rheb and TSC1;TSC2 data was not sufficient to show a significant effect (Figure 4.43). In this thesis it could be shown that up- and downregulation of TOR signalling displayed the same effects, especially on transcriptional targets in larvae. The preference to protein rich food is also elevated with decreased and increased TOR/S6K signalling in *Drosophila melanogaster* neurons (Ribeiro and Dickson, 2010).

Upon a long phase of starvation, TOR signalling in the whole organism is decreased indicating a lack of amino acids. Thus, the preference to protein rich food would be triggered. This mechanism ensures that the supply of protein is covered after a phase of starvation. As Pathetic is highly expressed in serotonin producing neurons and has a high affinity for alanine and glycine, it signals the transport of these amino acids to the serotonergic neurons. Glycogenic amino acids like alanine and glycine are highly released by muscles upon brief starvation, and their concentration then increases upon deprivation of the other amino acids (Odessey et al, 1974; Pozefsky et al, 1976). Thereby, Pathetic could provide information regarding the nutritional status for the serotonergic neurons via increased alanine and glycine transport and TOR signalling. The nutritional information might then affect pigmentation and starvation resistance in the fruit fly. Upon availability of protein rich food the composition of single amino acids changes and the ratio of alanine and glycine compared to other amino acids in the hemolymph might decrease. It is assumed that TOR signalling is then only moderate in serotonergic neurons due to moderate alanine and glycine signalling via Pathetic. Vargas et al activated TOR signalling in all neurons of the whole brain in 2010 and observed a preference to protein rich food just after a certain period of starvation. In this respect, unbalanced TOR signalling that is highly decreased or increased in serotonergic neurons could lead to a starvation response triggered by these neurons. This response increases the preference for protein as it was shown by Vargas et al in 2010.

For this thesis TOR signalling was manipulated only in serotonergic neurons so, a direct effect of TOR signalling on serotonin production and release could be identified. It could be shown that the enzyme Trh is enriched in larval serotonergic clusters upon Pathetic overexpression (Figure 4.21 and Table 4.2). Trh catalyses the rate limiting step of serotonin production. However, the serotonin signal in the serotoninergic clusters did not increase when Trh level was elevated upon Path overexpression. In contrary, the obtained data suggested that a decrease in serotonin signalling occurred. These results indicate a reduction of serotonin signalling. Maybe changes of TOR signalling in other neurons during a phase of starvation or just a starvation signal is needed for the activation of Trh and for an increased serotonin signalling. In this way, the feeding behaviour could be adjusted to the internal nutrient status and the needs of the organism. Further analysis of serotonin production, release and feeding preference upon manipulation of TOR signalling and starvation are needed to confirm this hypothesis.

### 5.2.8 The nutrient signalling via transceptors of future interest

In the modern society of the western countries the access to food is unlimited. The sufficient supply with nutrients correlates with an increased survival into high age. However, aging is followed by an increased risk to suffer of metabolic and neurodegenerative diseases and also of cancer (de Groot and van Staveren, 2010; Stanfel et al, 2009). This risk was shown to be increased by supernutrition and by consumption of high amounts of meat and milk products. These risk factors lead to an increased metabolic rate and activation of nutrient pathways like TOR (Hafen, 2004; Melnik et al, 2012). Milk and meat products are especially rich in leucine, an amino acid that has the strongest inducing effect on TOR pathway compared to other amino acids (Lynch et al, 2000, Lynch, 2001; Li et al 2011). An impairment in TOR signalling leads to a variety of disorders that can be compensated by plant based nutrition (Cherniack, 2010; Castillo-Pichardo and Dharmawardhane, 2012; Syed et al, 2013; Hasima and Aggarwal, 2014). Secondary metabolites of plants were shown to inhibit TOR signalling and therefore might be able to protect against certain metabolic disorders (Kuranda et al, 2006; Reinke et al, 2006; Saldanha et al, 2013; Castillo-Pichardo and Dharmawardhane, 2012; Beevers et al, 2013). As amino acid transceptors directly affect TOR signalling regarding their distribution in tissues and their affinities for certain amino acids, they could be of interest to target disorders in certain tissues. Thus, therapy based nutrition could be improved and a beneficial nutrient composition could be adjusted (Taylor, 2014).

The human Proton assisted amino acid transporter 1 (PAT1) is expressed in neurons (Boll et al, 2004). The results gained for Pathetic in *Drosophila melanogaster* could be used as a reference to find out which function the PAT1 transceptor might have in human neurons. It could be shown that Pathetic is involved in the regulation of Trh in serotonergic neurons and also in the serotonin signalling of *Drosophila melanogaster*. The effect of amino acid and TOR signalling on Trh production and on serotonin signalling in *Drosophila melanogaster* needs to be confirmed by further experiments.

An impairment of serotonin signalling in the human brain leads to depression and a decrease in life quality (Vashadze and Sardzhveladze, 2009; Rapaport et al, 2005). If TOR affects the production of neurotransmitters like serotonin via specialised transceptors, it could provide the organism with nutritional information and adjust the behaviour to the organismal requirements. However, it could also be used as a target to systematically manipulate neurotransmitter production and to balance mental illnesses. By this means, diet composition could also help to improve psychological disorders. A targeted manipulation of TOR signalling via specialized transceptors could improve mood, fat metabolism, food choice,

energy expenditure and other health promoting effects. This could possibly be achieved without increasing aging related negative effects like cancer, type 2 diabetes and neurodegenerative diseases.

# 6 Summary

The target of rapamycin (TOR) signalling pathway provides eukaryotes with the information of internal amino acid availability (Hyde et al, 2003). TOR signalling is involved in the regulation of transcription and translation of genes affecting growth, proliferation and metabolism. In this way, the production of metabolic enzymes is adjusted to the internal nutrient status and the needs of the organism. Transceptors like Pathetic are involved in this adjustment. Such an adjustment could be observed for the alpha glucosidase Tobi, which is conserved throughout evolution and is involved in the glycogen breakdown (Buch et al, 2008). The transcript level of this gene is dependent on peptide and amino acid availability and composition. In *Drosophila melanogaster*, the amino acid and peptide composition of its natural food source yeast leads to highest *tobi* expression level. The manipulation of TOR pathway by overexpression of the transceptor Pathetic decreases the transcription of *tobi* and of the TOR target *cabut*. These results indicate that *tobi* level is adjusted to the internal amino acid status via TOR signalling. TOR also affects the behavioural adjustment of *Drosophila melanogaster* (Ribeiro and Dickson, 2010). TOR/S6K signalling in neuronal cells of the brain influences the preference to protein rich food. Thereby, increased as well as decreased TOR/S6K signalling led to an increase of this preference. Serotonin production might be involved in this process (Vargas et al, 2010). It could be shown that the transceptor Pathetic is highly expressed in serotonergic neurons. Overexpression of Pathetic in these neurons leads to an increase of Trh in the larval brain. Trh catalyses the rate limiting step of serotonin production. However, the serotonin signal is not increased. Apparently, other factors or pathways are needed to activate the enzyme. Manipulation of TOR signalling in serotonergic neurons reduces the transcript level of the larval starvation marker *lipase3*, the pigment precursor producing enzyme *ddc* in the larval epidermis and the pigment distribution in adults. Pigmentation is dependent on the nutritional status of *Drosophila melanogaster* and is decreased upon nutrient deprivation. A regulation of *ddc* is also observed upon a decrease or increase of serotonin release in the larva. Insulin signalling as well as starvation resistance in adults was shown to be decreased upon TOR upregulation in serotonergic neurons. An increased insulin signalling and starvation resistance occurs upon inhibition of serotonin signalling in the insulin producing cells (Luo et al, 2012). It could be shown that TOR reduces serotonin release in serotonergic clusters of the *Drosophila melanogaster* brain. It is of further interest whether other neurotransmitters are affected by TOR in the same way.

# 7 References


1. Andrés AM, de Hemptinne C, Bertranpetit J. Heterogeneous rate of protein evolution in serotonin genes. Mol Biol Evol. 2007 Dec;24(12):2707-15.

2. Araki K, Ellebedy AH, Ahmed R. TOR in the immune system. Curr Opin Cell Biol. 2011 Dec;23(6):707-15.

3. Arquier N, Géminard C, Bourouis M, Jarretou G, Honegger B. Drosophila ALS regulates growth and metabolism through functional interaction with insulin-like peptides. Cell Metab. 2008 Apr;7(4):333-8.

4. Arrese EL, Soulages JL. Insect fat body: energy, metabolism, and regulation. Annu Rev Entomol. 2010;55:207-25.

5. Ballou LM, Lin RZ. Rapamycin and mTOR kinase inhibitors. J Chem Biol. 2008 Nov;1(1-4):27-36.

6. Barker GA, Ellory JC. The identification of neutral amino acid transport systems. Exp Physiol. 1990 Jan;75(1):3-26.

7. Beall CJ, Hirsh J. Regulation of the Drosophila dopa decarboxylase gene in neuronal and glial cells. Genes Dev. 1987 Jul;1(5):510-20.

8. Becher PG, Flick G, Rozpędowska E, Schmidt A, Hagman A, Lebreton S, Larsson MC, Hansson BS, Piškur J, Witzgall P, Bengtsson M. Yeast, not fruit volatiles mediate Drosophila melanogaster attraction, oviposition and development. Functional Ecology. 2012 May 18; 26(4):822-828.

9. Beevers CS, Zhou H, Huang S. Hitting the golden TORget: curcumin's effects on mTOR signaling. Anticancer Agents Med Chem. 2013 Sep;13(7):988-94.

10. Begg M, Robertson FW. Nutritional requirements of Drosophila melanogaster. Nature. 1948 May 15;161(4098):769.

11. Berg JM, Tymoczko JL, Sryer L. Stryer Biochemie. München, Elsevier GmbH. 6. überarb. Aufl; 2007.

12. Berger C, Renner S, Lüer K, Technau GM. The commonly used marker ELAV is transiently expressed in neuroblasts and glial cells in the Drosophila embryonic CNS. Dev Dyn. 2007 Dec;236(12):3562-8.

13. Berry JA, Cervantes-Sandoval I, Nicholas EP, Davis RL. Dopamine is required for learning and forgetting in Drosophila. Neuron. 2012 May 10;74(3):530-42.

14. Bettelheim FA, Brown WH, Campbell MK, Farrell SO. Brooks, Introduction to General, Organic and Biochemistry. Cengage Learning Inc. 9. Edition; 2010.

15. Bjordal M, Arquier N, Kniazeff J, Pin JP, Léopold P. Sensing of amino acids in a dopaminergic circuitry promotes rejection of an incomplete diet in Drosophila. Cell. 2014 Jan 30;156(3):510-21.

16. Boll M, Daniel H, Gasnier B. The SLC36 family: proton-coupled transporters for the absorption of selected amino acids from extracellular and intracellular proteolysis. Pflugers Arch. 2004 Feb;447(5):776-9.

17. Broughton SJ, Piper MD, Ikeya T, Bass TM, Jacobson J, et al. Longer lifespan, altered metabolism, and stress resistance in Drosophila from ablation of cells making insulin-like ligands. Proc Natl Acad Sci U S A. 2005 Feb 22;102(8):3105-10.

18. Buch S, Melcher C, Bauer M, Katzenberger J, Pankratz MJ. Opposing effects of dietary protein and sugar regulate a transcriptional target of Drosophila insulin-like peptide signaling. Cell Metab. 2008 Apr;7(4):321-32.

19. Castañeda LE, Figueroa CC, Fuentes-Contreras E, Niemeyer HM, Nespolo RF. Energetic costs of detoxification systems in herbivores feeding on chemically defended host plants: a correlational study in the grain aphid, Sitobion avenae. J Exp Biol. 2009 Apr;212(Pt 8):1185-90.

20. Castillo-Pichardo L, Dharmawardhane SF. Grape polyphenols inhibit Akt/mammalian target of rapamycin signaling and potentiate the effects of gefitinib in breast cancer. Nutr Cancer. 2012;64(7):1058-69.

21. Chang HY, Grygoruk A, Brooks ES, Ackerson LC, Maidment NT, et al. Overexpression of the Drosophila vesicular monoamine transporter increases motor activity and courtship but decreases the behavioral response to cocaine. Mol Psychiatry. 2006 Jan;11(1):99-113.

22. Chantranupong L, Wolfson RL, Sabatini DM. Nutrient-sensing mechanisms across evolution. Cell. 2015 Mar 26;161(1):67-83.

23. Chen JH, Ozanne SE, Hales CN. Methods of cellular senescence induction using oxidative stress. Methods Mol Biol. 2007;371:179-89.

24. Cherniack EP. The potential influence of plant polyphenols on the aging process. Forsch Komplementmed. 2010;17(4):181-7.

25. Christensen HN. Amino acid transport systems in animal cells: interrelations and energization. J Supramol Struct. 1977;6(2):205-13.

26. Coleman CM, Neckameyer WS. Serotonin synthesis by two distinct enzymes in Drosophila melanogaster. Arch Insect Biochem Physiol. 2005 May;59(1):12-31.

27. Coleman CM, Neckameyer WS. Substrate regulation of serotonin and dopamine synthesis in Drosophila. Invert Neurosci. 2004 Oct;5(2):85-96.

28. Colombani J, Raisin S, Pantalacci S, Radimerski T, Montagne J, et al. A nutrient sensor mechanism controls Drosophila growth. Cell. 2003 Sep 19;114(6):739-49.

29. Cônsoli FL, Vinson SB. Hemolymph of reproductives of Solenopsis invicta (Hymenoptera: Formicidae)-amino acids, proteins and sugars. Comp Biochem Physiol B Biochem Mol Biol. 2002 Aug;132(4):711-9.

30. Costa IR, Thompson JD, Ortega JM, Prosdocimi F. Metazoan remaining genes for essential amino acid biosynthesis: sequence conservation and evolutionary analyses. Nutrients. 2014 Dec 24;7(1):1-16.

31. Cota D, Proulx K, Smith KA, Kozma SC, Thomas G, et al. Hypothalamic mTOR signaling regulates food intake. Science. 2006 May 12;312(5775):927-30.

32. Courgeon AM, Rollet E, Becker J, Maisonhaute C, Best-Belpomme M. Hydrogen peroxide (H2O2) induces actin and some heat-shock proteins in Drosophila cells. Eur J Biochem. 1988 Jan 15;171(1-2):163-70.

33. Curran KP, Chalasani SH. Serotonin circuits and anxiety: what can invertebrates teach us?. Invert Neurosci. 2012 Dec;12(2):81-92.

34. Csonka FA. Proteins of yeast (Saccharomyces Cerevisiae). J. Biol. Chem., 1935; 109: 703.

35. de Groot CP, van Staveren WA. Nutritional concerns, health and survival in old age. Biogerontology. 2010 Oct;11(5):597-602.

36. del Valle Rodríguez A, Didiano D, Desplan C. Power tools for gene expression and clonal analysis in Drosophila. Nat Methods. 2011 Dec 28;9(1):47-55.

37. Diallinas G. Understanding transporter specificity and the discrete appearance of channel-like gating domains in transporters. Front Pharmacol. 2014;5:207.

38. Dilger RN, Baker DH. Excess dietary L-cysteine causes lethal metabolic acidosis in chicks. J Nutr. 2008 Sep;138(9):1628-33.

39. Donovan MH, Tecott LH. Serotonin and the regulation of mammalian energy balance. Front Neurosci. 2013;7:36.

40. Duffy JB. GAL4 system in Drosophila: a fly geneticist's Swiss army knife. Genesis. 2002 Sep-Oct;34(1-2):1-15. PubMed PMID: 12324939.

41. Dunlop EA, Tee AR. Mammalian target of rapamycin complex 1: signalling inputs, substrates and feedback mechanisms. Cell Signal. 2009 Jun;21(6):827-35.

42. Efeyan A, Zoncu R, Sabatini DM. Amino acids and mTORC1: from lysosomes to disease. Trends Mol Med. 2012 Sep;18(9):524-33. PubMed PMID: 22749019; NIHMSID: NIHMS390711; PubMed Central PMCID: PMC3432651.

43. Fernstrom JD. Diet-induced changes in plasma amino acid pattern: effects on the brain uptake of large neutral amino acids, and on brain serotonin synthesis. J Neural Transm Suppl. 1979.

44. Gasque G, Conway S, Huang J, Rao Y, Vosshall LB. Small molecule drug screening in Drosophila identifies the 5HT2A receptor as a feeding manipulation target. Sci Rep. 2013;3:srep02120.

45. Géminard C, Rulifson EJ, Léopold P. Remote control of insulin secretion by fat cells in Drosophila. Cell Metab. 2009 Sep;10(3):199-207.

46. Giang T, Ritze Y, Rauchfuss S, Ogueta M, Scholz H. The serotonin transporter expression in Drosophila melanogaster. J Neurogenet. 2011 Mar;25(1-2):17-26.

47. Gibert JM, Peronnet F, Schlötterer C. Phenotypic plasticity in Drosophila pigmentation caused by temperature sensitivity of a chromatin regulator network. PLoS Genet. 2007 Feb 16;3(2):e30.

48. Goberdhan DC, Meredith D, Boyd CA, Wilson C. PAT-related amino acid transporters regulate growth via a novel mechanism that does not require bulk transport of amino acids. Development. 2005 May;132(10):2365-75.

49. Goel MK, Khanna P, Kishore J. Understanding survival analysis: Kaplan-Meier estimate. Int J Ayurveda Res. 2010 Oct;1(4):274-8.

50. Grandison RC, Piper MD, Partridge L. Amino-acid imbalance explains extension of lifespan by dietary restriction in Drosophila. Nature. 2009 Dec 24;462(7276):1061-4.

51. Grosjean Y, Grillet M, Augustin H, Ferveur JF, Featherstone DE. A glial amino-acid transporter controls synapse strength and courtship in Drosophila. Nat Neurosci. 2008 Jan;11(1):54-61.

52. Gutierrez E, Wiggins D, Fielding B, Gould AP. Specialized hepatocyte-like cells regulate Drosophila lipid metabolism. Nature. 2007 Jan 18;445(7125):275-80.

53. Hafen E. Cancer, type 2 diabetes, and ageing: news from flies and worms. Swiss Med Wkly. 2004 Dec 18;134(49-50):711-9.

54. Hare EE, Loer CM. Function and evolution of the serotonin-synthetic bas-1 gene and other aromatic amino acid decarboxylase genes in Caenorhabditis. BMC Evol Biol. 2004 Aug 2;4:24.

55. Hasima N, Aggarwal BB. Targeting proteasomal pathways by dietary curcumin for cancer prevention and treatment. Curr Med Chem. 2014;21(14):1583-94.

56. Heinrichsen ET, Zhang H, Robinson JE, Ngo J, Diop S, et al. Metabolic and transcriptional response to a high-fat diet in Drosophila melanogaster. Mol Metab. 2014 Feb;3(1):42-54.

57. Hrassnigg N, Leonhard B, Crailsheim K. Free amino acids in the haemolymph of honey bee queens (Apis mellifera L). Amino Acids. 2003;24(1-2):205-12.

58. Hübner. Nährstoffabhängige Regulation von α-Glucosidasen in Drosophila melanogaster. Diplomarbeit an der Universität Bonn. 2010

59. Hyde R, Taylor PM, Hundal HS. Amino acid transporters: roles in amino acid sensing and signalling in animal cells. Biochem J. 2003 Jul 1;373(Pt 1):1-18.

60. Ikeya T, Galic M, Belawat P, Nairz K, Hafen E. Nutrient-dependent expression of insulin-like peptides from neuroendocrine cells in the CNS contributes to growth regulation in Drosophila. Curr Biol. 2002 Aug 6;12(15):1293-300.

61. Ivanov DK, Papatheodorou I, Ziehm M, Thornton JM. Transcriptional feedback in the insulin signalling pathway modulates ageing in both Caenorhabditis elegans and Drosophila melanogaster. Mol Biosyst. 2013 Jul;9(7):1756-64.

62. Jefferis GS, Marin EC, Watts RJ, Luo L. Development of neuronal connectivity in Drosophila antennal lobes and mushroom bodies. Curr Opin Neurobiol. 2002 Feb;12(1):80-6.

63. Jones KT, Ashrafi K. Caenorhabditis elegans as an emerging model for studying the basic biology of obesity. Dis Model Mech. 2009 May-Jun;2(5-6):224-9.

64. Kim E, Goraksha-Hicks P, Li L, Neufeld TP, Guan KL. Regulation of TORC1 by Rag GTPases in nutrient response. Nat Cell Biol. 2008 Aug;10(8):935-45.

65. Kimball SR, Jefferson LS. New functions for amino acids: effects on gene transcription and translation. Am J Clin Nutr. 2006 Feb;83(2):500S-507S.

66. Kimball SR, Jefferson LS. Signaling pathways and molecular mechanisms through which branched-chain amino acids mediate translational control of protein synthesis. J Nutr. 2006 Jan;136(1 Suppl):227S-31S.

67. Kitamoto T. Conditional modification of behavior in Drosophila by targeted expression of a temperature-sensitive shibire allele in defined neurons. J Neurobiol. 2001 May;47(2):81-92.

68. Kockel L, Kerr KS, Melnick M, Brückner K, Hebrok M, et al. Dynamic switch of negative feedback regulation in Drosophila Akt-TOR signaling. PLoS Genet. 2010 Jun 17;6(6):e1000990.

69. Kolss M, Vijendravarma RK, Schwaller G, Kawecki TJ. Life-history consequences of adaptation to larval nutritional stress in Drosophila. Evolution. 2009 Sep;63(9):2389-401.

70. Konrad KD, Marsh JL. Developmental expression and spatial distribution of dopa decarboxylase in Drosophila. Dev Biol. 1987 Jul;122(1):172-85.

71. Kuhn DM, Arthur R Jr, States JC. Phosphorylation and activation of brain tryptophan hydroxylase: identification of serine-58 as a substrate site for protein kinase A. J Neurochem. 1997 May;68(5):2220-3.

72. Kumsta C, Thamsen M, Jakob U. Effects of oxidative stress on behavior, physiology, and the redox thiol proteome of Caenorhabditis elegans. Antioxid Redox Signal. 2011 Mar 15;14(6):1023-37.

73. Kuranda K, Leberre V, Sokol S, Palamarczyk G, François J. Investigating the caffeine effects in the yeast Saccharomyces cerevisiae brings new insights into the connection between TOR, PKC and Ras/cAMP signalling pathways. Mol Microbiol. 2006 Sep;61(5):1147-66.

74. Kwak SJ, Hong SH, Bajracharya R, Yang SY, Lee KS, et al. Drosophila adiponectin receptor in insulin producing cells regulates glucose and lipid metabolism by controlling insulin secretion. PLoS One. 2013;8(7):e68641.

75. Layalle S, Arquier N, Léopold P. The TOR pathway couples nutrition and developmental timing in Drosophila. Dev Cell. 2008 Oct;15(4):568-77.

76. Leibowitz SF, Alexander JT. Hypothalamic serotonin in control of eating behavior, meal size, and body weight. Biol Psychiatry. 1998 Nov 1;44(9):851-64.

77. Leibowitz SF, Weiss GF, Walsh UA, Viswanath D. Medial hypothalamic serotonin: role in circadian patterns of feeding and macronutrient selection. Brain Res. 1989 Nov 27;503(1):132-40.

78. Lemaitre B, Miguel-Aliaga I. The digestive tract of Drosophila melanogaster. Annu Rev Genet. 2013;47:377-404.

79. Li F, Yin Y, Tan B, Kong X, Wu G. Leucine nutrition in animals and humans: mTOR signaling and beyond. Amino Acids. 2011 Nov;41(5):1185-93.

80. Li L, Edgar BA, Grewal SS. Nutritional control of gene expression in Drosophila larvae via TOR, Myc and a novel cis-regulatory element. BMC Cell Biol. 2010 Jan 20;11:7.

81. Livingstone MS, Tempel BL. Genetic dissection of monoamine neurotransmitter synthesis in Drosophila. Nature. 1983 May 5-11;303(5912):67-70.

82. Lundell MJ, Hirsh J. Temporal and spatial development of serotonin and dopamine neurons in the Drosophila CNS. Dev Biol. 1994 Oct;165(2):385-96.

83. Luo J, Lushchak OV, Goergen P, Williams MJ, Nässel DR. Drosophila insulin-producing cells are differentially modulated by serotonin and octopamine receptors and affect social behavior. PLoS One. 2014;9(6):e99732.

84. Luo J, Becnel J, Nichols CD, Nässel DR. Insulin-producing cells in the brain of adult Drosophila are regulated by the serotonin 5-HT1A receptor. Cell Mol Life Sci. 2012 Feb;69(3):471-84.

85. Lynch CJ, Fox HL, Vary TC, Jefferson LS, Kimball SR. Regulation of amino acid-sensitive TOR signaling by leucine analogues in adipocytes. J Cell Biochem. 2000 Mar;77(2):234-51.

86. Lynch CJ. Role of leucine in the regulation of mTOR by amino acids: revelations from structure-activity studies. J Nutr. 2001 Mar;131(3):861S-865S.

87. Madeira MH, Elvas F, Boia R, Gonçalves FQ, Cunha RA, et al. Adenosine A2AR blockade prevents neuroinflammation-induced death of retinal ganglion cells caused by elevated pressure. J Neuroinflammation. 2015 Jun 10;12:115.

88. Magwere T, Chapman T, Partridge L. Sex differences in the effect of dietary restriction on life span and mortality rates in female and male Drosophila melanogaster. J Gerontol A Biol Sci Med Sci. 2004 Jan;59(1):3-9.

89. Martin JF, Hersperger E, Simcox A, Shearn A. minidiscs encodes a putative amino acid transporter subunit required non-autonomously for imaginal cell proliferation. Mech Dev. 2000 Apr;92(2):155-67.

90. Matthews DM. Mechanisms of peptide transport. Beitr Infusionther Klin Ernahr. 1987;17:6-53.

91. Meijer AJ, Codogno P. Nutrient sensing: TOR's Ragtime. Nat Cell Biol. 2008 Aug;10(8):881-3.

92. Melnik BC, John SM, Carrera-Bastos P, Cordain L. The impact of cow's milk-mediated mTORC1-signaling in the initiation and progression of prostate cancer. Nutr Metab (Lond). 2012 Aug 14;9(1):74.

93. Miguel-Aliaga I. Nerveless and gutsy: intestinal nutrient sensing from invertebrates to humans. Semin Cell Dev Biol. 2012 Aug;23(6):614-20.

94. Miron M, Lasko P, Sonenberg N. Signaling from Akt to FRAP/TOR targets both 4E-BP and S6K in Drosophila melanogaster. Mol Cell Biol. 2003 Dec;23(24):9117-26.

95. Miron M, Sonenberg N. Regulation of translation via TOR signaling: insights from Drosophila melanogaster. J Nutr. 2001 Nov;131(11):2988S-93S.

96. Mocali A, Caldini R, Chevanne M, Paoletti F. Induction, effects, and quantification of sublethal oxidative stress by hydrogen peroxide on cultured human fibroblasts. Exp Cell Res. 1995 Feb;216(2):388-95.

97. Muta K, Morgan DA, Rahmouni K. The role of hypothalamic mTORC1 signaling in insulin regulation of food intake, body weight, and sympathetic nerve activity in male mice. Endocrinology. 2015 Apr;156(4):1398-407.

98. Nagarajan A, Ning Y, Reisner K, Buraei Z, Larsen JP, et al. Progressive degeneration of dopaminergic neurons through TRP channel-induced cell death. J Neurosci. 2014 Apr 23;34(17):5738-46.

99. Nagarajan S, Grewal SS. An investigation of nutrient-dependent mRNA translation in Drosophila larvae. Biol Open. 2014 Oct 10;3(11):1020-31.

100. Nässel DR, Kubrak OI, Liu Y, Luo J, Lushchak OV. Factors that regulate insulin producing cells and their output in Drosophila. Front Physiol. 2013 Sep 17;4:252.

101. Neckameyer WS, Coleman CM, Eadie S, Goodwin SF. Compartmentalization of neuronal and peripheral serotonin synthesis in Drosophila melanogaster. Genes Brain Behav. 2007 Nov;6(8):756-69.

102. Odessey R, Khairallah EA, Goldberg AL. Origin and possible significance of alanine production by skeletal muscle. J Biol Chem. 1974 Dec 10;249(23):7623-9.

103. Ögmundsdóttir MH, Heublein S, Kazi S, Reynolds B, Visvalingam SM, et al. Proton-assisted amino acid transporter PAT1 complexes with Rag GTPases and activates TORC1 on late endosomal and lysosomal membranes. PLoS One. 2012;7(5):e36616.

104. Orlova KA, Crino PB. The tuberous sclerosis complex. Ann N Y Acad Sci. 2010 Jan;1184:87-105.

105. Pozefsky T, Tancredi RG, Moxley RT, Dupre J, Tobin JD. Effects of brief starvation on muscle amino acid metabolism in nonobese man. J Clin Invest. 1976 Feb;57(2):444-9.

106. Puig O, Tjian R. Transcriptional feedback control of insulin receptor by dFOXO/FOXO1. Genes Dev. 2005 Oct 15;19(20):2435-46.

107. Pulver SR, Pashkovski SL, Hornstein NJ, Garrity PA, Griffith LC. Temporal dynamics of neuronal activation by Channelrhodopsin-2 and TRPA1 determine behavioral output in Drosophila larvae. J Neurophysiol. 2009 Jun;101(6):3075-88.

108. Rapaport MH, Clary C, Fayyad R, Endicott J. Quality-of-life impairment in depressive and anxiety disorders. Am J Psychiatry. 2005 Jun;162(6):1171-8.

109. Rauschenbach IY, Sukhanova MJ, Shumnaya LV, Gruntenko NE, Grenback LG, et al. Role of DOPA decarboxylase and N-acetyl transferase in regulation of dopamine content in Drosophila virilis under normal and heat stress conditions. Insect Biochem Mol Biol. 1997 Aug-Sep;27(8-9):729-34.

110. Reinke A, Chen JC, Aronova S, Powers T. Caffeine targets TOR complex I and provides evidence for a regulatory link between the FRB and kinase domains of Tor1p. J Biol Chem. 2006 Oct 20;281(42):31616-26.

111. Ribeiro C, Dickson BJ. Sex peptide receptor and neuronal TOR/S6K signaling modulate nutrient balancing in Drosophila. Curr Biol. 2010 Jun 8;20(11):1000-5.

112. Roy B, Singh AP, Shetty C, Chaudhary V, North A, et al. Metamorphosis of an identified serotonergic neuron in the Drosophila olfactory system. Neural Dev. 2007 Oct 24;2:20.

113. Ruaud AF, Thummel CS. Serotonin and insulin signaling team up to control growth in Drosophila. Genes Dev. 2008 Jul 15;22(14):1851-5.

114. Rydström J. Mitochondrial NADPH, transhydrogenase and disease. Biochim Biophys Acta. 2006 May-Jun;1757(5-6):721-6.

115. Saldanha JF, Leal Vde O, Stenvinkel P, Carraro-Eduardo JC, Mafra D. Resveratrol: why is it a promising therapy for chronic kidney disease patients?. Oxid Med Cell Longev. 2013;2013:963217.

116. Shakhmantsir I, Massad NL, Kennell JA. Regulation of cuticle pigmentation in drosophila by the nutrient sensing insulin and TOR signaling pathways. Dev Dyn. 2014 Mar;243(3):393-401.

117. Shimada-Niwa Y, Niwa R. Serotonergic neurons respond to nutrients and regulate the timing of steroid hormone biosynthesis in Drosophila. Nat Commun. 2014 Dec 15;5:5778.

118. Shingleton AW. Body-size regulation: combining genetics and physiology. Curr Biol. 2005 Oct 25;15(20):R825-7.

119. Silva B, Goles NI, Varas R, Campusano JM. Serotonin receptors expressed in Drosophila mushroom bodies differentially modulate larval locomotion. PLoS One. 2014;9(2):e89641.

120. Simon AF, Daniels R, Romero-Calderón R, Grygoruk A, Chang HY, et al. Drosophila vesicular monoamine transporter mutants can adapt to reduced or eliminated vesicular stores of dopamine and serotonin. Genetics. 2009 Feb;181(2):525-41.

121. Slack C, Werz C, Wieser D, Alic N, Foley A, et al. Regulation of lifespan, metabolism, and stress responses by the Drosophila SH2B protein, Lnk. PLoS Genet. 2010 Mar 19;6(3):e1000881.

122. Srinivasan S, Sadegh L, Elle IC, Christensen AG, Faergeman NJ, et al. Serotonin regulates C elegans fat and feeding through independent molecular mechanisms. Cell Metab. 2008 Jun;7(6):533-44.

123. St Johnston D. The art and design of genetic screens: Drosophila melanogaster. Nat Rev Genet. 2002 Mar;3(3):176-88.

124. Stanfel MN, Shamieh LS, Kaeberlein M, Kennedy BK. The TOR pathway comes of age. Biochim Biophys Acta. 2009 Oct;1790(10):1067-74.

125. Suraweera A, Münch C, Hanssum A, Bertolotti A. Failure of amino acid homeostasis causes cell death following proteasome inhibition. Mol Cell. 2012 Oct 26;48(2):242-53.

126. Syed DN, Adhami VM, Khan MI, Mukhtar H. Inhibition of Akt/mTOR signaling by the dietary flavonoid fisetin. Anticancer Agents Med Chem. 2013 Sep;13(7):995-1001.

127. Tatum MC, Ooi FK, Chikka MR, Chauve L, Martinez-Velazquez LA, et al. Neuronal serotonin release triggers the heat shock response in C elegans in the absence of temperature increase. Curr Biol. 2015 Jan 19;25(2):163-74.

128. Taylor PM. Role of amino acid transporters in amino acid sensing. Am J Clin Nutr. 2014 Jan;99(1):223S-230S.

129. Toshima N, Tanimura T. Taste preference for amino acids is dependent on internal nutritional state in Drosophila melanogaster. J Exp Biol. 2012 Aug 15;215(Pt 16):2827-32.

130. True JR, Edwards KA, Yamamoto D, Carroll SB. Drosophila wing melanin patterns form by vein-dependent elaboration of enzymatic prepatterns. Curr Biol. 1999 Dec 2;9(23):1382-91.

131. Ueno T, Tomita J, Kume S, Kume K. Dopamine modulates metabolic rate and temperature sensitivity in Drosophila melanogaster. PLoS One. 2012;7(2):e31513.

132. Ueno T, Tomita J, Tanimoto H, Endo K, Ito K, et al. Identification of a dopamine pathway that regulates sleep and arousal in Drosophila. Nat Neurosci. 2012 Nov;15(11):1516-23.

133. Vallés AM, White K. Serotonin-containing neurons in Drosophila melanogaster: development and distribution. J Comp Neurol. 1988 Feb 15;268(3):414-28.

134. van Dam TJ, Zwartkruis FJ, Bos JL, Snel B. Evolution of the TOR pathway. J Mol Evol. 2011 Oct;73(3-4):209-20.

135. Vargas MA, Luo N, Yamaguchi A, Kapahi P. A role for S6 kinase and serotonin in postmating dietary switch and balance of nutrients in D melanogaster. Curr Biol. 2010 Jun 8;20(11):1006-11.

136. Varma D, Bülow MH, Pesch YY, Loch G, Hoch M. Forkhead, a new cross regulator of metabolism and innate immunity downstream of TOR in Drosophila. J Insect Physiol. 2014 Oct;69:80-8.

137. Vashadze ShV, Sardzhveladze NM. Relationship between serum blood serotonin and tension--type headache. Georgian Med News. 2009 Jun.

138. Verlinden H, Vleugels R, Vanden Broeck J. Serotonin, serotonin receptors and their actions in insects. Neurotransmitter. 2015; 9 (8): e314. doi: 10.14800/nt.314

139. Walter MF, Black BC, Afshar G, Kermabon AY, Wright TR, et al. Temporal and spatial expression of the yellow gene in correlation with cuticle formation and dopa decarboxylase activity in Drosophila development. Dev Biol. 1991 Sep;147(1):32-45.

140. Webb KE Jr. Intestinal absorption of protein hydrolysis products: a review. J Anim Sci. 1990 Sep;68(9):3011-22.

141. Wittkopp PJ, Carroll SB, Kopp A. Evolution in black and white: genetic control of pigment patterns in Drosophila. Trends Genet. 2003 Sep;19(9):495-504.

142. Wu G. Amino acids: metabolism, functions, and nutrition. Amino Acids. 2009 May;37(1):1-17.

143. Wullschleger S, Loewith R, Hall MN. TOR signaling in growth and metabolism. Cell. 2006 Feb 10;124(3):471-84.

144. Xiong WC, Okano H, Patel NH, Blendy JA, Montell C. repo encodes a glial-specific homeo domain protein required in the Drosophila nervous system. Genes Dev. 1994 Apr 15;8(8):981-94.

145. Yamamoto K, Niwa A. Amino acid and vitamin requirements in mammalian cultured cells. Amino Acids. 1993 Feb;5(1):1-16.

146. Yuan Q, Song Y, Yang CH, Jan LY, Jan YN. Female contact modulates male aggression via a sexually dimorphic GABAergic circuit in Drosophila. Nat Neurosci. 2014 Jan;17(1):81-8.

147. Zhang H, Stallock JP, Ng JC, Reinhard C, Neufeld TP. Regulation of cellular growth by the Drosophila target of rapamycin dTOR. Genes Dev. 2000 Nov 1;14(21):2712-24.

148. Zhang SD, Odenwald WF. Misexpression of the white (w) gene triggers male-male courtship in Drosophila. Proc Natl Acad Sci U S A. 1995 Jun 6;92(12):5525-9.

149. Zhao XL, Campos AR. Insulin signalling in mushroom body neurons regulates feeding behaviour in Drosophila larvae. J Exp Biol. 2012 Aug 1;215(Pt 15):2696-702.

150. Zitserman D, Gupta S, Kruger WD, Karbowniczek M, Roegiers F. The TSC1/2 complex controls Drosophila pigmentation through TORC1-dependent regulation of catecholamine biosynthesis. PLoS One. 2012;7(11):e48720.

## 7.1 Internet Sources

1. The FlyBase Consortium (2015). FlyBase - A Drosophila database. Gene Dmel\Ddc . FlyAtlas Organ/Tissue Expression, larval vs. adult. June 26, 2015. URL:<flybase.org/reports/FBgn0000422.html>

2. The FlyBase Consortium (2015). FlyBase - A Drosophila database. Gene Dmel\path. FlyAtlas Organ/Tissue Expression, larval vs. adult. June 26, 2015. URL:<flybase.org/reports/FBgn0036007.html>

3. GraphPad Software. GraphPad Statistics Guide. Interpreting results: Unpaired t. May 28, 2015.
URL:<
http://www.graphpad.com/guides/prism/6/statistics/index.htm?how_the_unpaired_t_test_works2.htm >

4. The FlyBase Consortium (2015). FlyBase - A Drosophila database. Gene Dmel\path. FlyExpress - Embryonic expression images (BDGP data). June 26, 2015. URL:< flybase.org/reports/FBgn0036007.html >

# 8 Appendix

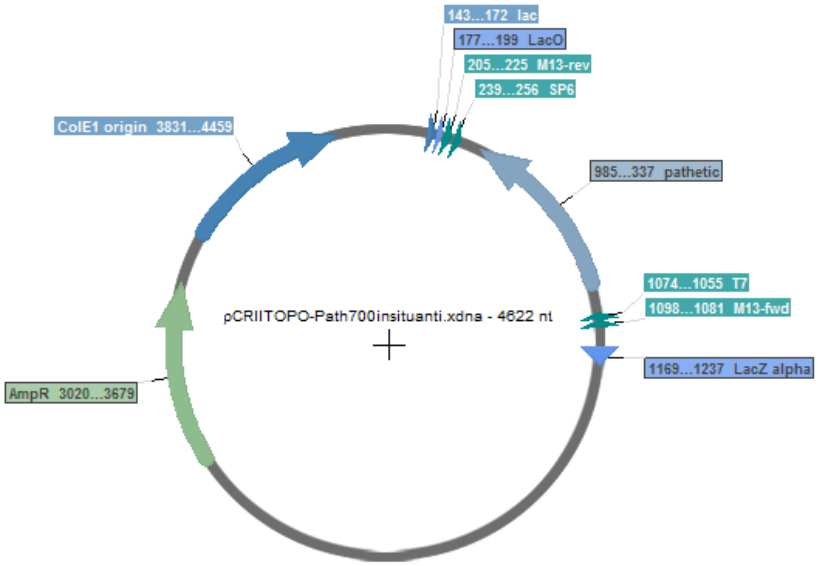


**Figure 8.1 Vector for RNA probe production**
Ampicilin resistance gene (AmpR). Origin of replication (ColE1 origin). Promoter for *in vitro* transcription (T7, SP6). The vector was composed using the Serial Cloner Software

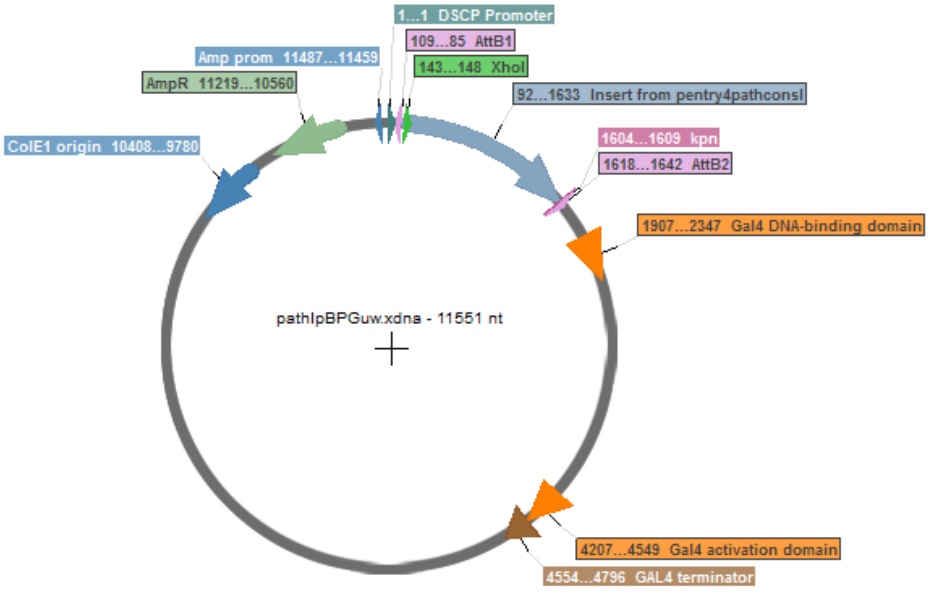


**Figure 8.2 pBPGuw Vector for Gal4 transformant fly line production**
Ampicilin resistance gene (AmpR). Ampicilin resistance gene promoter (Amp prom). Origin of replication (ColE1 origin). Attachment sides (AttB1,AttB2). Restriction sides (XhoI, kpn).

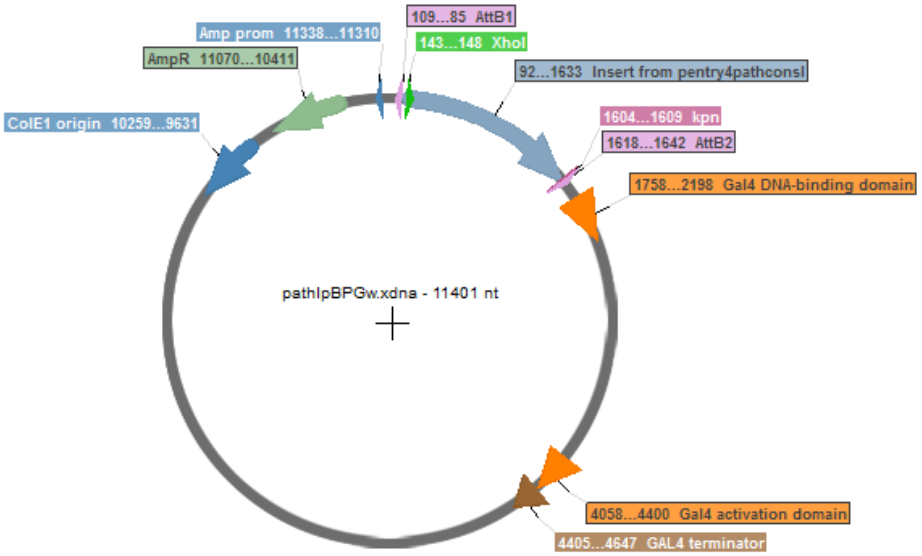


**Figure 8.3 pBPGw Vector for Gal4 transformant fly line production**
Ampicilin resistance gene (AmpR). Ampicilin resistance gene promoter (Amp prom). Origin of replication (ColE1 origin). Attachment sides (AttB1,AttB2). Restriction sides (XhoI, kpn).

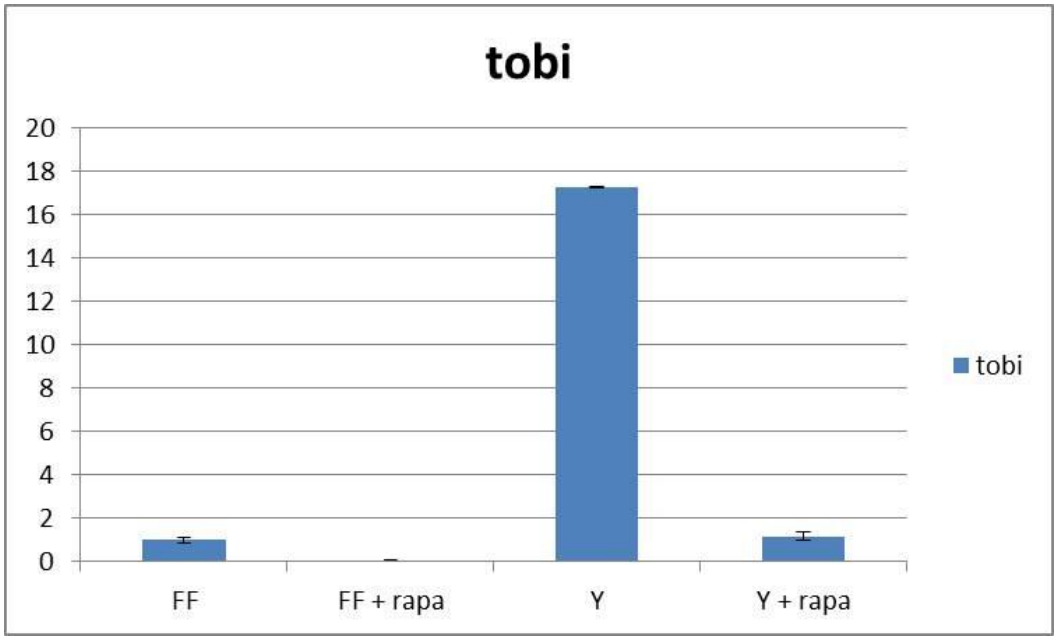


**Figure 8.4 *Tobi* transcript level in the larva upon ramamycin feeding**
The supplemental data was composed and provided by Dr. Susanne Buch. Target of brain insulin (tobi). Standard fly food (FF). Rapamycin (rapa). Yeast (Y). The figure shows a decrease of *tobi* level upon rapamycin feeding in the larva indicating that a high *tobi* expression might be dependent on TOR signalling. N=2.

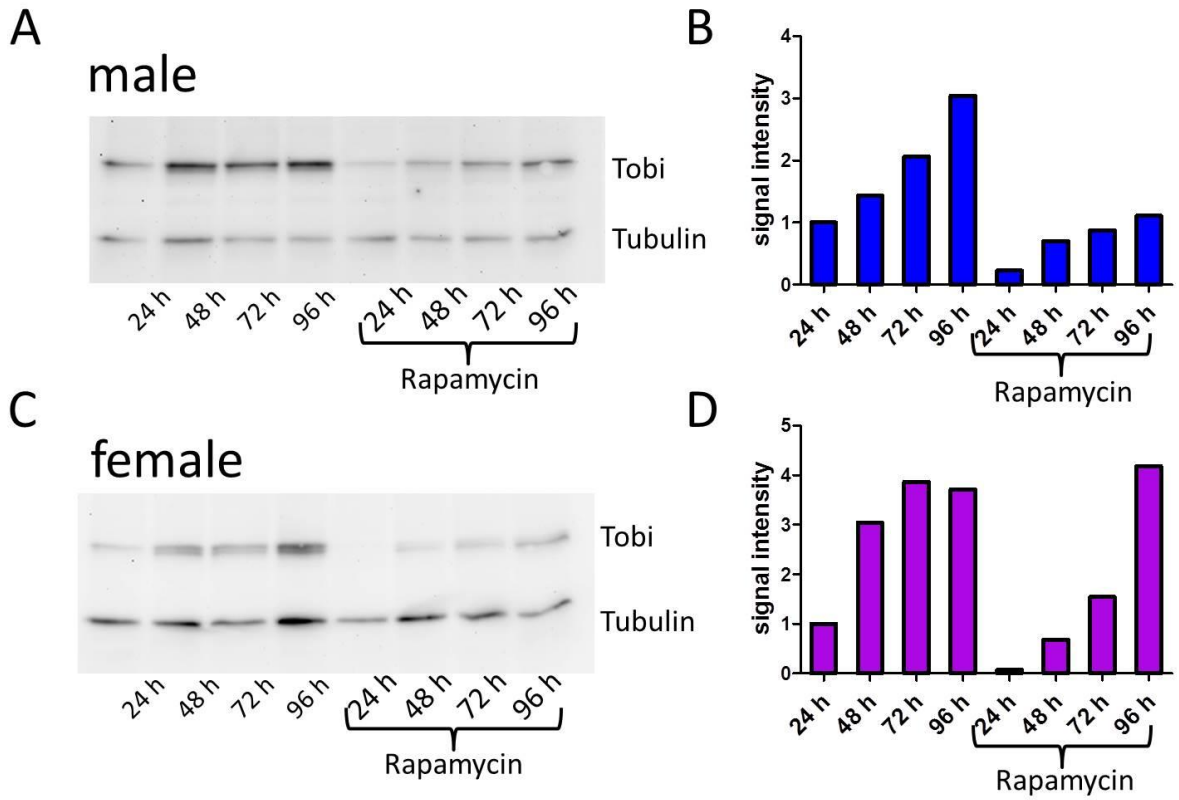


**Figure 8.5 Tobi expression upon rapamycin feeding.**
The supplemental data was composed and provided by Dr. Susanne Buch. The figure shows a decrease of Tobi level upon rapamycin feeding in male (A-B) and female (C-D) adults indicating that a high Tobi expression might be dependent on TOR signalling.

**Table 8.1 Supplemental data for Figure 4.1**

| ***tobi* expression in the female head** | | | |
|---|---|---|---|
| **Sample** | **Expression** | **Expression SEM** | **N** |
| **Yeast** | 1 | 0.28526 | 5 |
| **Sugar** | 0.01456 | 0.00472 | 5 |
| **Soy** | 0.49087 | 0.22435 | 5 |
| **Casein** | 0.34572 | 0.16903 | 5 |
| **Gelatine** | 0.10037 | 0.02723 | 5 |
| **Fish** | 0.0657 | 0.01744 | 5 |
| **Meat** | 0.08809 | 0.02728 | 5 |

**Table 8.2 Amino acid composition of peptones.**
Supplemental data provided by Roth

| | Yeast | Casein | Meat | Fish | Soy | Gelatine |
|---|---|---|---|---|---|---|
| **Amino acid content mg/g** | | | | | | |
| **Alanine** | 43 | 29 | 65 | 70 | 33 | 79 |
| **Arginine** | 32 | 33 | 50 | 51 | 43 | 72 |
| **Aspartic acid** | 64 | 65 | 71 | 58 | 64 | 63 |
| **Cysteic acid** | 70 | 4 | 4 | 96 | 12 | 13 |
| **Glutamic acid** | 107 | 187 | 105 | 110 | 100 | 96 |
| **Glycine** | 28 | 18 | 110 | 34 | 71 | 21 |
| **Histidine** | 14 | 23 | 11 | 27 | 13 | 9 |
| **Isoleucine** | 30 | 45 | 30 | 17 | 26 | 14 |
| **Leucine** | 44 | 76 | 70 | 38 | 40 | 28 |
| **Lysine** | 50 | 65 | 41 | 46 | 31 | 36 |
| **Methionine** | 90 | 24 | 10 | 14 | 7 | 9 |
| **Phenylalanine** | 26 | 41 | 41 | 19 | 21 | 19 |
| **Proline** | 22 | 87 | 75 | 50 | 49 | 12 |
| **Serine** | 29 | 51 | 31 | 32 | 28 | 35 |
| **Threonine** | 30 | 39 | 31 | 26 | 22 | 19 |
| **Tryptophan** | 60 | 11 | 5 | 1 | 4 | 1 |
| **Tyrosine** | 23 | 19 | 21 | 10 | 18 | 7 |
| **Valine** | 34 | 55 | 45 | 24 | 26 | 23 |
| **Taurine** | | | | 42 | | |

**Table 8.3 Supplemental data for Figure 4.2**

| ***tobi* expression in the adult head** | | | |
|---|---|---|---|
| **Sample** | **Expression** | **Expression SEM** | **N** |
| **Casein male** | 0.16938 | 0.03539 | 5 |
| **Casein female** | 0.34572 | 0.16903 | 5 |
| **Fish male** | 0.0071 | 0.0034 | 5 |
| **Fish female** | 0.0657 | 0.01744 | 5 |
| **Meat male** | 0.16224 | 0.10527 | 5 |
| **Meat female** | 0.08809 | 0.02728 | 5 |
| **Gelatine male** | 0.09483 | 0.01657 | 5 |
| **Gelatine female** | 0.10037 | 0.02723 | 5 |
| **Soy male** | 0.34815 | 0.07995 | 5 |
| **Soy female** | 0.49087 | 0.22435 | 5 |
| **Sugar male** | 0.00229 | 0.00027 | 5 |
| **Sugar female** | 0.01456 | 0.00472 | 5 |
| **Yeast male** | 0.33171 | 0.1212 | 5 |
| **Yeast female** | 1 | 0.28526 | 5 |

**Table 8.4 Supplemental data for Figure 4.3**

| ***tobi* expression in the adult head** | | | |
|---|---|---|---|
| **Sample** | **Expression** | **Expression SEM** | **N** |
| **Yeast female** | 1 | 0.28526 | 5 |
| **Yeast amino acid composition female** | 0.21874 | 0.08714 | 5 |
| **Fish female** | 0.0657 | 0.01744 | 5 |
| **Fish amino acid composition female** | 0.05494 | 0.01335 | 5 |
| | | | |
| **Yeast male** | 0.36175 | 0.11395 | 4 |
| **Yeast amino acid composition male** | 0.11655 | 0.04231 | 4 |
| **Fish male** | 0.0122 | 0.00498 | 4 |
| **Fish amino acid composition male** | 0.04192 | 0.01076 | 4 |

**Table 8.5 Supplemental data for Figure 4.4**

| ***tobi* expression in the adult head** | | | |
|---|---|---|---|
| **Sample** | **Expression** | **Expression SEM** | **N** |
| **Control male** | 0.38882 | 0.12931 | 6 |
| **20 mM Glycine male** | 0.63045 | 0.13655 | 6 |
| **200 mM Glycine male** | 1.28571 | 0.16513 | 6 |
| **1 Mm Glycine male** | 1.74591 | 0.63757 | 6 |
| **Control female** | 1 | 0.28785 | 6 |
| **20 mM Glycine female** | 2.01213 | 0.4356 | 6 |
| **200 mM Glycine female** | 2.56524 | 0.57387 | 6 |
| **1 M Glycine female** | 4.2393 | 1.14562 | 6 |

**Table 8.6 Supplemental data for Figure 4.5**

| ***tobi* expression in the adult head** | | | |
|---|---|---|---|
| **Sample** | **Expression** | **Expression SEM** | **N** |
| **Control male** | 0.16108 | 0.0321 | 7 |
| **0.1% hydrogen peroxide male** | 0.10215 | 0.02144 | 7 |
| **1% hydrogen peroxide male** | 0.06095 | 0.01345 | 7 |
| **5% hydrogen peroxide male** | 0.02721 | 0.00724 | 7 |
| **Control female** | 1 | 0.20978 | 7 |
| **0.1% hydrogen peroxide female** | 0.88613 | 0.19358 | 7 |
| **1% hydrogen peroxide female** | 0.57586 | 0.14646 | 7 |
| **5% hydrogen peroxide female** | 0.11577 | 0.04177 | 7 |

**Table 8.7 Supplemental data for Figure 4.6**

| ***pathetic* expression in the adult head** | | | |
|---|---|---|---|
| **Sample** | **Expression** | **Expression SEM** | **N** |
| **Control male** | 1.2469 | 0.12964 | 4 |
| **0.1% hydrogen peroxide male** | 1.19035 | 0.4575 | 4 |
| **1% hydrogen peroxide male** | 1.89014 | 0.20114 | 4 |
| **5% hydrogen peroxide male** | 2.59562 | 0.75117 | 4 |
| **Control female** | 1 | 0.07824 | 4 |
| **0.1% hydrogen peroxide female** | 1.08185 | 0.12702 | 4 |
| **1% hydrogen peroxide female** | 1.6467 | 0.12724 | 4 |
| **5% hydrogen peroxide female** | 2.65373 | 0.35379 | 4 |

**Table 8.8 Supplemental data for Figure 4.7**

| **Target** | **Sample** | **Expression** | **N** |
|---|---|---|---|
| ***cabut*** | **Cg-Gal4 > UAS-Path** | 1.82131 | 4 |
| ***cabut*** | **Cg >Wt** | 1.1099 | 4 |
| ***cabut*** | **Wt > UAS-Path** | 1 | 4 |
| ***path*** | **Cg-Gal4 > UAS-Path** | 4.90092 | 4 |
| ***path*** | **Cg >Wt** | 0.71955 | 4 |
| ***path*** | **Wt >UAS-Path** | 1 | 4 |
| ***tobi*** | **Cg-Gal4 >UAS-Path** | 0.61734 | 4 |
| ***tobi*** | **Cg >Wt** | 1.69645 | 4 |
| ***tobi*** | **Wt >UAS-Path** | 1 | 4 |

**Table 8.9 Supplemental data for Figure 4.9**

| ***pathetic* expression in the larval brain** | | | |
|---|---|---|---|
| **Sample** | **Expression** | **Expression SEM** | **N** |
| **Control** | 1 | 0.0477 | 5 |
| **Rapamycin** | 0.57109 | 0.02724 | 5 |

**Table 8.10 Supplemental data for Figure 4.10**

| ***pathetic* expression in the larval brain** | | | |
|---|---|---|---|
| **Sample** | **Expression** | **Expression SEM** | **N** |
| **Yeast** | 1 | 0.70481 | 6 |
| **Sugar** | 0.44524 | 0.31312 | 6 |

**Table 8.11 Supplemental data for Figure 4.16**

| ***tryptophan hydroxylase* expression in the larval brain** | | | |
|---|---|---|---|
| **Sample** | **Expression** | **Expression SEM** | **N** |
| **Sugar** | 1.08681 | 0.64206 | 3 |
| **Yeast** | 1 | 0.57782 | 3 |

**Table 8.12 Supplemental data for Figure 4.17**

| ***tryptophan hydroxylase* expression in the larval brain** | | | |
|---|---|---|---|
| **Sample** | **Expression** | **Expression SEM** | **N** |
| **Control** | 1 | 0.06417 | 5 |
| **Rapamycin** | 0.87864 | 0.05638 | 5 |

**Table 8.13 Supplemental data for Figure 4.18**

| ***tryptophan hydroxylase* expression in the larval brain** | | | |
|---|---|---|---|
| **Sample** | **Expression** | **Expression SEM** | **N** |
| Trh-Gal4>Wt | 1 | 0.319 | 3 |
| Trh-Gal4>UAS-TSC1/2 | 0.96954 | 0.05737 | 3 |
| Trh-Gal4>UAS-Rheb | 1.16135 | 0.35448 | 3 |

**Table 8.14 Supplemental data for Figure 4.20 and Table 4.1**

| **Corrected total cell fluorescence of Tryptophan hydroxylase signal in serotonergic clusters** | | | | | | |
|---|---|---|---|---|---|---|
| | **Trh>wt (N=9)** | | **Trh>TSC (N=9)** | | **Trh>Rheb (N=9)** | |
| **Cluster** | **Mean** | **SEM** | **Mean** | **SEM** | **Mean** | **SEM** |
| **SP1 left** | 820 | 221.92 | 1225.00 | 338.86 | 785.11 | 330.60 |
| **SP1 right** | 948.11 | 242.07 | 1383.11 | 441.79 | 950.56 | 407.69 |
| **SP2 left** | 2447.00 | 647.06 | 3035.00 | 855.31 | 2226.00 | 917.79 |
| **SP2 right** | 2312.67 | 580.82 | 3156.11 | 817.60 | 2258.11 | 956.56 |
| **LP1 left** | 626.56 | 168.71 | 1035.11 | 316.52 | 1420.67 | 605.49 |
| **LP1 right** | 750.67 | 195.36 | 1866.89 | 812.96 | 1217.44 | 530.44 |
| **SE0 left** | 11197.00 | 2477.93 | 9902.67 | 2833.22 | 23531.67 | 9438.61 |
| **SE0 right** | 8050.78 | 2082.77 | 9343.33 | 1803.72 | 21710.22 | 8594.72 |
| **IP left** | 1652.78 | 505.02 | 2708.44 | 915.03 | 2325.11 | 1133.27 |
| **IP right** | 1632.44 | 511.07 | 2490.67 | 962.13 | 1895.89 | 880.58 |
| **SE1 left** | 1708.00 | 428.94 | 1359.00 | 333.38 | 1632.78 | 677.29 |
| **SE1 right** | 1210.89 | 252.09 | 1646.56 | 492.47 | 1632.11 | 722.03 |
| **SE2 left** | 1817.67 | 610.46 | 1767.67 | 465.18 | 2159.56 | 900.88 |
| **SE2 right** | 1507.33 | 295.32 | 2301.11 | 773.71 | 2462.11 | 1218.75 |
| **SE3 left** | 2178.22 | 539.80 | 2691 | 786.79 | 2504.11 | 1094.01 |
| **SE3 right** | 2155.89 | 547.00 | 2893.22 | 839.06 | 2614 | 1094.94 |
| **T1 left** | 1438.67 | 346.88 | 1729.56 | 502.12 | 1481.56 | 645.05 |
| **T1 right** | 1477.11 | 363.16 | 1775.78 | 531.51 | 1574.56 | 712.13 |
| **T2 left** | 997.56 | 260.35 | 1629.44 | 509.15 | 1106.22 | 461.33 |
| **T2 right** | 1191.11 | 367.62 | 1824.00 | 564.10 | 1556.33 | 650.71 |
| **T3 left** | 605.67 | 171.39 | 680.78 | 203.87 | 735.56 | 314.63 |
| **T3 right** | 693.22 | 213.62 | 931.33 | 378.67 | 752.11 | 323.85 |

**Table 8.15 Supplemental data for Figure 4.21-Figure 4.22 and Table 4.2**

| **Corrected total cell fluorescence of Tryptophan hydroxylase signal in serotonergic clusters** | | | | |
|---|---|---|---|---|
| | **Trh-Gal4>Wt (N=6)** | | **Trh-Gal4>UAS-Path (N=6)** | |
| **Cluster** | **Mean** | **SEM** | **Mean** | **SEM** |
| **SP1 left** | 449.1667 | 134.6406 | 3726.833 | 1252.719 |
| **SP1 right** | 677 | 198.759 | 2683.833 | 661.1013 |
| **SP2 left** | 1283.833 | 309.7742 | 10497.33 | 2837.51 |
| **SP2 right** | 1291.333 | 294.4715 | 10743 | 3601.2 |
| **LP1 left** | 586 | 259.1402 | 3833.667 | 1113.128 |
| **LP1 right** | 445 | 107.717 | 3355.5 | 1085.668 |
| **SE0 left** | 8991.333 | 3431.459 | 31887.83 | 11015.89 |
| **SE0 right** | 7519.167 | 3017.725 | 27783.17 | 7322.597 |
| **IP left** | 781.3333 | 306.6763 | 5618.833 | 1748.833 |
| **IP right** | 752.8333 | 207.7218 | 6531.5 | 2173.7 |
| **SE1 left** | 1238.167 | 520.1699 | 4070.5 | 1458.713 |
| **SE1 right** | 895.6667 | 265.6152 | 5227.167 | 1982.719 |
| **SE2 left** | 1238.167 | 520.1699 | 4070.5 | 1458.713 |
| **SE2 right** | 895.6667 | 265.6152 | 5227.167 | 1982.719 |
| **SE3 left** | 1705.833 | 902.2176 | 6010.167 | 1826.427 |
| **SE3 right** | 1336.333 | 419.0607 | 6167.333 | 2086.81 |
| **T1 left** | 1313.667 | 382.0494 | 8155.5 | 2588.912 |
| **T1 right** | 1233.833 | 328.7251 | 8348.833 | 2654.79 |
| **T2 left** | 956.5 | 334.2691 | 3472 | 1042.832 |
| **T2 right** | 911 | 248.0349 | 3579 | 1013.328 |
| **T3 left** | 721.8333 | 262.1135 | 3432.167 | 1152.018 |
| **T3 right** | 682.1667 | 205.8465 | 3685.833 | 1214.37 |

**Table 8.16 Supplemental data for Figure 4.23**

| ***ddc* expression in the larva** | | | |
|---|---|---|---|
| **Sample** | **Expression** | **Expression SEM** | **N** |
| **Ddc-Gal4>Wt** | 1 | 0.19087 | 4 |
| **Ddc-Gal4>UAS-TSC1; UAS-TSC2** | 0.23686 | 0.08062 | 4 |
| **Ddc-Gal4>UAS-Rheb** | 0.09126 | 0.00896 | 4 |

**Table 8.17 Supplemental data for Figure 4.24**

| ***ddc* expression in the larva** | | | |
|---|---|---|---|
| **Sample** | **Expression** | **Expression SEM** | **N** |
| **Trh-Gal4>Wt** | 1 | 0.17907 | 4 |
| **Trh-Gal4>UAS-TSC1;TSC2** | 0.25643 | 0.10027 | 4 |
| **Trh-Gal4>UAS-Path** | 0.17505 | 0.06645 | 4 |
| **Trh-Gal4>UAS-Rheb** | 0.04205 | 0.00887 | 4 |

**Table 8.18 Supplemental data for Figure 4.25**

| ***ddc* expression in the larval brain** | | | |
|---|---|---|---|
| **Sample** | **Expression** | **Expression SEM** | **N** |
| **Trh-Gal4>Wt** | 1 | 0.1387 | 3 |
| **Trh-Gal4>UAS-TSC1;TSC2** | 0.98114 | 0.06037 | 3 |
| **Trh-Gal4>UAS-Rheb** | 0.86805 | 0.13749 | 3 |

**Table 8.19 Supplemental data for Figure 4.26**

| ***ddc* expression in the larval brain** | | | |
|---|---|---|---|
| **Sample** | **Expression** | **Expression SEM** | **N** |
| **Yeast (Wt)** | 1 | 0.19211 | 3 |
| **Sugar (Wt)** | 0.82442 | 0.10468 | 3 |

**Table 8.20 Supplemental data for Figure 4.27**

| ***ddc* expression in the larval brain** | | | |
|---|---|---|---|
| **Sample** | **Expression** | **Expression SEM** | **N** |
| **Control (Wt)** | 1 | 0.05047 | 5 |
| **Rapamycin (Wt)** | 0.94258 | 0.04757 | 5 |

**Table 8.21 Supplemental data for Figure 4.29**

| ***ddc* expression in the larval gut** | | | |
|---|---|---|---|
| **Sample** | **Expression** | **Expression SEM** | **N** |
| **Trh-Gal4>Wt** | 1 | 0.2717 | 3 |
| **Trh-Gal4>UAS-TSC1; UAS-TSC2** | 0.96941 | 0.24318 | 3 |
| **Trh-Gal4>UAS-Path** | 0.73364 | 0.20479 | 3 |
| **Trh-Gal4>UAS-Rheb** | 0.59981 | 0.16283 | 3 |

**Table 8.22 Supplemental data for Figure 4.30**

| ***ddc* expression in the larval epidermis** | | | |
|---|---|---|---|
| **Sample** | **Expression** | **Expression SEM** | **N** |
| **Trh-Gal4>Wt** | 1 | 0.16629 | 3 |
| **Trh-Gal4>UAS-TSC1; UAS-TSC2** | 0.15079 | 0.0465 | 3 |
| **Trh-Gal4>UAS-Path** | 0.09863 | 0.04407 | 3 |
| **Trh-Gal4>UAS-Rheb** | 0.13046 | 0.02694 | 3 |

**Table 8.23 Supplemental data for Figure 4.33**

| ***ddc* expression in the larva** | | | |
|---|---|---|---|
| **Sample** | **Expression** | **Expression SEM** | **N** |
| **Trh-Gal4>UAS-TrpA 25°C** | 1 | 0.09969 | 4 |
| **Trh-Gal4>UAS-TrpA 32°C** | 1.46192 | 0.17425 | 4 |
| **Trh-Gal4>UAS-Shibere 25°C** | 1 | 0.15593 | 4 |
| **Trh-Gal4>UAS-Shibire 32°C** | 0.40056 | 0.04027 | 4 |
| **UAS-Shibire 25°C** | 1 | 0.39878 | 3 |
| **UAS-Shibire 32°C** | 0.14726 | 0.02019 | 3 |

**Table 8.24 Supplemental data for Figure 4.35 and Table 4.3**

| Corrected total cell fluorescence of serotonin signal in serotonergic clusters | | | | | | |
|---|---|---|---|---|---|---|
| | Trh>wt (N=9) | | Trh>TSC (N=9) | | Trh>Rheb (N=9) | |
| **Cluster** | **Mean** | **SEM** | **Mean** | **SEM** | **Mean** | **SEM** |
| **SP1 left** | 1843 | 452.12 | 2160.22 | 463.81 | 2005.22 | 675.80 |
| **SP1 right** | 2685 | 654.09 | 2788.89 | 642.41 | 2644.78 | 876.28 |
| **SP2 left** | 2856.67 | 904.32 | 3409.67 | 857.93 | 2250.00 | 845.23 |
| **SP2 right** | 5061.11 | 1036.32 | 4426.44 | 967.82 | 2656.56 | 847.35 |
| **LP1 left** | 2226.78 | 1197.20 | 2915.33 | 1449.92 | 1350.89 | 537.29 |
| **LP1 right** | 4520.00 | 1691.10 | 4579.44 | 2047.78 | 2253.00 | 817.51 |
| **IP left** | 9563.56 | 2926.31 | 10951.56 | 2637.07 | 11001.22 | 4273.63 |
| **IP right** | 12304.67 | 4001.55 | 11468.67 | 2868.46 | 11223.67 | 3966.45 |
| **SE1 left** | 7531.89 | 1587.36 | 6341.89 | 1406.80 | 3718.44 | 1357.64 |
| **SE1 right** | 7026.67 | 1939.91 | 6993.44 | 1315.85 | 4024.67 | 1396.34 |
| **SE2 left** | 7167.56 | 1609.56 | 7379.89 | 1515.87 | 4663.22 | 1667.37 |
| **SE2 right** | 7732.33 | 1819.37 | 8273.67 | 1651.59 | 4324.00 | 1459.72 |
| **SE3 left** | 12937.89 | 2973.92 | 11674.56 | 2154.90 | 9174.89 | 3138.48 |
| **SE3 right** | 13452.00 | 3349.41 | 13573.89 | 2525.45 | 9324.44 | 3221.68 |
| **T1 left** | 9811.33 | 2070.85 | 7681.33 | 1582.52 | 6867.89 | 2451.55 |
| **T1 right** | 12370.44 | 2878.21 | 8974.67 | 1792.51 | 8556.78 | 3018.01 |
| **T2 left** | 2144.78 | 559.07 | 1564.56 | 306.23 | 1761.67 | 602.89 |
| **T2 right** | 3035.89 | 711.61 | 3621.67 | 1731.04 | 2395.56 | 776.10 |
| **T3 left** | 1311.67 | 334.92 | 978.56 | 363.63 | 1049.11 | 330.66 |
| **T3 right** | 1693.67 | 493.98 | 1320.11 | 358.17 | 1592.44 | 726.02 |

**Table 8.25 Supplemental data for Figure 4.36 and Table 4.4**

| Corrected total cell fluorescence of serotonin signal in serotonergic clusters | | | | |
|---|---|---|---|---|
| | Trh-Gal4>Wt (N=6) | | Trh-Gal4>UAS-Path (N=6) | |
| **Cluster** | **Mean** | **SEM** | **Mean** | **SEM** |
| **SP1 left** | 1086.333 | 177.8242 | 2153.167 | 1111.993 |
| **SP1 right** | 1636.333 | 540.6913 | 2275.333 | 694.7515 |
| **SP2 left** | 1598.5 | 349.9304 | 4600.5 | 2045.344 |
| **SP2 right** | 3945.5 | 974.5529 | 3822.5 | 976.9892 |
| **LP1 left** | 2513.667 | 1836.736 | 597.3333 | 108.1624 |
| **LP1 right** | 3819.67 | 2463.87 | 886.1667 | 359.0903 |
| **IP left** | 4652.167 | 1981.608 | 5368.833 | 1295.662 |
| **IP right** | 5509.5 | 1819.493 | 10923.67 | 3892.304 |
| **SE1 left** | 5879.833 | 1886.737 | 2555.667 | 850.4833 |
| **SE1 right** | 4986 | 2100.784 | 2723.833 | 949.7702 |
| **SE2 left** | 6111 | 2179.7 | 2695.167 | 1091.003 |
| **SE2 right** | 6705.167 | 2403.09 | 3248 | 1447.054 |
| **SE3 left** | 10113.33 | 3323.705 | 4226.333 | 412.5348 |
| **SE3 right** | 9456.333 | 3006.448 | 6732.833 | 1573.54 |
| **T1 left** | 8216.5 | 2705.25 | 5472.667 | 1432.388 |
| **T1 right** | 10296.5 | 3826.029 | 5804 | 1632.739 |
| **T2 left** | 1996.667 | 831.812 | 1021.667 | 209.0602 |
| **T2 right** | 2598.5 | 923.3619 | 1423.333 | 502.721 |
| **T3 left** | 1354.667 | 515.4993 | 540.5 | 84.13907 |
| **T3 right** | 1471.167 | 605.0526 | 684.1667 | 138.5971 |

**Table 8.26 Supplemental data for Figure 4.37**

| ***lip3* expression in the larva** | | | |
|---|---|---|---|
| **Sample** | **Expression** | **Expression SEM** | **N** |
| **Trh-Gal4>Wt** | 1 | 0.10562 | 4 |
| **Trh-Gal4>UAS-TSC1; UAS-TSC2** | 0.35385 | 0.08847 | 4 |
| **Trh-Gal4>UAS-Path** | 0.3369 | 0.08264 | 4 |
| **Trh-Gal4>UAS-Rheb** | 0.29473 | 0.03687 | 4 |

**Table 8.27 Supplemental data for Figure 4.38 A**

| Survival of third instar larvae upon starvation | | | | | | |
|---|---|---|---|---|---|---|
| **survival [%]** | **3d (larvae)** | | **6d (pupae)** | | **14d (adults)** | |
| **Sample** | **Mean** | **SEM** | **Mean** | **SEM** | **Mean** | **SEM** |
| **Trh-Gal4>Wt** | 100 | 0 | 79 | 10.17 | 73 | 10.79 |
| **Trh-Gal4>UAS-TSC1; UAS-TSC2** | 100 | 0 | 74 | 9.27 | 71 | 4.58 |
| **Trh-Gal4>UAS-Path** | 100 | 0 | 68 | 7.35 | 41 | 5.79 |
| **Trh-Gal4>UAS-Rheb** | 100 | 0 | 77 | 3.00 | 62 | 4.90 |

**Table 8.28 Supplemental data for Figure 4.38 B**

| Survival of third instar larvae upon starvation | | | |
|---|---|---|---|
| **Median of survivors for logrank-test** | **3d (larvae)** | **6d (pupae)** | **14d (adults)** |
| **Sample** | **Median** | **Median** | **Median** |
| **Trh-Gal4>Wt** | 20 | 17 | 17 |
| **Trh-Gal4>UAS-TSC1; UAS-TSC2** | 20 | 15 | 15 |
| **Trh-Gal4>UAS-Path** | 20 | 13 | 9 |
| **Trh-Gal4>UAS-Rheb** | 20 | 16 | 13 |

**Table 8.29 Supplemental data for Figure 4.39 A**

| TAG-level of yeast fed third instar larvae | | | | |
|---|---|---|---|---|
| **Sample** | **Mean** | **SEM** | **N** | **t-test Trh>Wt vs.** |
| **Trh-Gal4>Wt** | 35053395 | 3904467.7 | 6 | - |
| **Trh-Gal4>UAS-TSC1; UAS-TSC2** | 32364901.7 | 1827438.67 | 6 | 0.5524 |
| **Trh-Gal4>UAS-Path** | 29338425 | 1123183.62 | 6 | 0.2106 |
| **Trh-Gal4>UAS-Rheb** | 28575290 | 1880391.82 | 6 | 0.1774 |

**Table 8.30 Supplemental data for Figure 4.39 B**

| TAG-level of starved third instar larvae | | | | |
|---|---|---|---|---|
| **Sample** | **Mean grey value** | **SEM** | **N** | **p-value Trh>Wt vs.** |
| **Trh-Gal4>Wt** | 13182649.8 | 4372541.36 | 4 | - |
| **Trh-Gal4>UAS-TSC1; UAS-TSC2** | 13309615 | 3708430.97 | 4 | 0.9831 |
| **Trh-Gal4>UAS-Path** | 12669775.5 | 1618901.71 | 4 | 0.918 |
| **Trh-Gal4>UAS-Rheb** | 10245028 | 2142736.17 | 4 | 0.5763 |

**Table 8.31 Supplemental data for Figure 4.39 C**

| TAG-level of third instar larvae | | | | | | |
|---|---|---|---|---|---|---|
| | **Yeast fed** | | | **Starved** | | |
| **Sample** | **Mean** | **SEM** | **N** | **Mean** | **SEM** | **N** |
| **Trh-Gal4>Wt** | 34913785 | 3670275.67 | 4 | 13182650 | 4372541.36 | 4 |
| **Trh-Gal4>UAS-TSC1; UAS-TSC2** | 29619700 | 402473.267 | 4 | 13309615 | 3708430.97 | 4 |
| **Trh-Gal4>UAS-Path** | 30652677.5 | 1067043.89 | 4 | 12669776 | 1618901.71 | 4 |
| **Trh-Gal4>UAS-Rheb** | 25718920 | 754133.977 | 4 | 10245028 | 2142736.17 | 4 |

**Table 8.32 Supplemental data for Figure 4.40**

| ***ddc* expression in adult males** | | | |
|---|---|---|---|
| **Sample** | **Expression** | **Expression SEM** | **N** |
| **Trh-Gal4>Wt** | 1 | 0.04461 | 5 |
| **Trh-Gal4>UAS-TSC1; UAS-TSC2** | 1.02022 | 0.05739 | 5 |
| **Trh-Gal4>UAS-Path** | 1.06228 | 0.0607 | 5 |
| **Trh-Gal4>UAS-Rheb** | 1.05464 | 0.09754 | 5 |

**Table 8.33 Supplemental data for Figure 4.41**

| ***lip3* expression in adult males** | | | |
|---|---|---|---|
| **Sample** | **Expression** | **Expression SEM** | **N** |
| **Trh-Gal4>Wt** | 1 | 0.14024 | 4 |
| **Trh-Gal4>UAS-TSC1; UAS-TSC2** | 0.65417 | 0.28992 | 4 |
| **Trh-Gal4>UAS-Path** | 0.67546 | 0.04011 | 4 |
| **Trh-Gal4>UAS-Rheb** | 0.63259 | 0.25104 | 4 |

**Table 8.34 Supplemental data for Figure 4.42 A**

| **Survival of adult males upon starvation** | | | | |
|---|---|---|---|---|
| **survival [%]** | **N=7** | **N=7** | **N=7** | **N=7** |
| **Sample** | **Mean 1day** | **SEM 1day** | **Mean 2days** | **SEM 2days** |
| **Trh-Gal4>Wt** | 100 | 0 | 100 | 0 |
| **Trh-Gal4>UAS-TSC1; UAS-TSC2** | 100 | 0 | 99.29 | 0.71 |
| **Trh-Gal4>UAS-Path** | 100 | 0 | 99.29 | 0.71 |
| **Trh-Gal4>UAS-Rheb** | 100 | 0 | 100 | 0 |
| **Sample** | **Mean 3 days** | **SEM 3 days** | **Mean 4 days** | **SEM 4 days** |
| **Trh-Gal4>Wt** | 100 | 0 | 93.57 | 1.43 |
| **Trh-Gal4>UAS-TSC1; UAS-TSC2** | 92.14 | 4.86 | 80.71 | 5.82 |
| **Trh-Gal4>UAS-Path** | 82.86 | 4.21 | 52.86 | 4.48 |
| **Trh-Gal4>UAS-Rheb** | 89.29 | 3.85 | 62.14 | 6.16 |

| Sample | Mean 5 days | SEM 5 days | Mean 6 days | SEM 6 days |
|---|---|---|---|---|
| **Trh-Gal4>Wt** | 75 | 3.09 | 36.43 | 2.83 |
| **Trh-Gal4>UAS-TSC1; UAS-TSC2** | 33.57 | 2.61 | 2.14 | 1.49 |
| **Trh-Gal4>UAS-Path** | 12.86 | 4.98 | 2.14 | 1.49 |
| **Trh-Gal4>UAS-Rheb** | 11.43 | 3.22 | 1.43 | 0.92 |
| **Sample** | **Mean 7 days** | **SEM 7 days** | **Mean 8 days** | **SEM 8 days** |
| **Trh-Gal4>Wt** | 12.14 | 2.14 | 0 | 0 |
| **Trh-Gal4>UAS-TSC1; UAS-TSC2** | 0 | 0 | 0 | 0 |
| **Trh-Gal4>UAS-Path** | 0 | 0 | 0 | 0 |
| **Trh-Gal4>UAS-Rheb** | 0 | 0 | 0 | 0 |

**Table 8.35 Supplemental data for Figure 4.42 B**

| **Survival of adult males upon starvation** | | | | |
|---|---|---|---|---|
| **Medians for logrank-test (adults)** | | | | |
| | **N=7** | **N=7** | **N=7** | **N=7** |
| **Sample** | **Median 1 day** | **Median 2 days** | **Median 3 days** | **Median 4 days** |
| **Trh-Gal4>Wt** | 20 | 20 | 20 | 19 |
| **Trh-Gal4>UAS-TSC1; UAS-TSC2** | 20 | 20 | 20 | 17 |
| **Trh-Gal4>UAS-Path** | 20 | 20 | 16 | 10 |
| **Trh-Gal4>UAS-Rheb** | 20 | 20 | 18 | 12 |
| **Sample** | **Median 5 days** | **Median 6 days** | **Median 7 days** | **Median 8 days** |
| **Trh-Gal4>Wt** | 15 | 7 | 2 | 0 |
| **Trh-Gal4>UAS-TSC1; UAS-TSC2** | 6 | 0 | 0 | 0 |
| **Trh-Gal4>UAS-Path** | 1 | 0 | 0 | 0 |
| **Trh-Gal4>UAS-Rheb** | 2 | 0 | 0 | 0 |

**Table 8.36 Supplemental data for Figure 4.43**

| ***InR* expression in adult males** | | | |
|---|---|---|---|
| **Sample** | **Expression** | **Expression SEM** | **N** |
| **Trh-Gal4>Wt** | 0.72771 | 0.03741 | 4 |
| **Trh-Gal4>UAS-TSC1; UAS-TSC2** | 0.8182 | 0.10555 | 4 |
| **Trh-Gal4>UAS-Path** | 0.80709 | 0.08544 | 4 |
| **Trh-Gal4>UAS-Rheb** | 1 | 0.06693 | 4 |